Chem Soc Rev

TUTORIAL REVIEW

View Article Online
View Journal | View Issue



Cite this: *Chem. Soc. Rev.*, 2026, **55**, 4960

# Non-isocyanate polyurethane foams: where we stand and what comes next?

Bruno Grignard, *[ab] Maxime Bourguignon, [b] Florent Monie, [bc] Thomas Vidil, [c] Henri Cramail, [c] Gabriel Perli, [d] Haritz Sardon, [d] Jean-Marie Raquez, [e] Sylvain Caillol [f] and Christophe Detrembleur *[bg]

Polyurethane foam stakeholders are currently facing stringent regulatory constraints, such as the REACH regulation restricting the use of isocyanates and increasing environmental pressures calling for more sustainable materials. This dual challenge compels both academia and industry to innovate and redesign conventional PU chemistry and foaming toward non-isocyanate solutions while integrating eco-design principles to enhance recyclability and circularity. This tutorial review summarizes the current advances in synthetic strategies for producing non-isocyanate polyurethanes (NIPUs), with a particular focus on foaming concepts, which have witnessed a significant acceleration in development over the last five years. Emerging end-of-life management solutions *via* chemolysis or physical means – exploiting covalent adaptable network features – and applications of NIPU foams are also discussed. For each aspect, a comparative analysis between conventional PU and NIPU highlights the remaining technological, environmental and economic challenges that must be addressed to achieve competitive, scalable, and sustainable NIPU foams.

Received 4th December 2025

DOI: 10.1039/d5cs00144g

rsc.li/chem-soc-rev

**Key learning points**

(1) Fundamentals and core principles of synthetic methods for non-isocyanate polyurethanes (NIPUs)
(2) Basics of non-isocyanate polyurethane (self-)foaming procedures
(3) Practical approaches to end-of-life strategies for NIPU foams
(4) Performance assessment of emerging applications of NIPU foams
(5) Major differences between non-isocyanate and conventional PU foams; level of competitiveness and remaining challenges

## 1. Introduction to PU foams

In 2023, the polyurethane (PU) foam market was valued at US$ ~49.5 billion, with an expected growth projection up to US$ ~67.8 billion by 2028.[1] The PU foam market dynamic is mainly driven by the increasing demands of end-user industries from the building, automotive/aerospace, furniture, and other sectors.[2–5] These key players are seeking low-cost, energy-efficient, lightweight and durable materials with chemical resistance and adaptable thermo-mechanical properties, particularly in thermal insulation, sealing, structural items of vehicles (seats, soundproofing, interior components, *etc.*), comfort (mattresses, footwear, *etc.*) or personal protective equipment (helmets, filtration, *etc.*) (Fig. 1). Industrially, the popularity of PU foams arises from their versatility and ease of fabrication from low-temperature reactive formulations (generally from room temperature to 40–60 °C) made of polyisocyanates and polyols.[5,6] The PU foaming is achieved by the use of external chemical or physical blowing agents (*i.e.*, exogenous chemical/physical blowing agent) or *via* a

[a] *Federation of Researchers in Innovative Technologies for $CO_2$ Transformation (FRITCO2T), Institutional CCU Technology Platform, 13 allée de la Chimie, 4000, Liège, Belgium. E-mail: bruno.grignard@uliege.be*
[b] *Center for Education and Research on Macromolecules (CERM), Chemistry Department, 13 allée de la Chimie, 4000, Liège, Belgium. E-mail: Christophe.detrembleur@uliege.be*
[c] *Univ. Bordeaux, CNRS, Bordeaux INP, LCPO, UMR562, 16 avenue Pey-Berland,, 33600 Pessac, France*
[d] *POLYMAT and Department of Polymers and Advanced Materials: Physics, Chemistry and Technology, Faculty of Chemistry, University of the Basque Country UPV/EHU, Paseo Manuel de Lardizabal 3, 20018 Donostia-San Sebastián, Spain*
[e] *Laboratory of Polymeric and Composite Materials (LPCM), Center of Innovation and Research in Materials and Polymers (CIRMAP), University of Mons (UMONS), Mons, Belgium*
[f] *Institut Charles Gerhardt Montpellier (ICGM), CNRS, ENSCM, University of Montpellier, 34293 Montpellier, France*
[g] *WEL Research Institute, 1300 Wavre, Belgium*

self-foaming approach,[7] for which the blowing agent ($CO_2$) originates from the isocyanate compound (*i.e.*, endogenous chemical blowing agent).[8] Upon simple addition of water, the hydrolysis of isocyanate releases $CO_2$ *in situ*, causing material expansion during PU network formation.[5,6] Inherently, PU foaming benefits from the high exothermicity of the isocyanate/polyol reaction. The *in situ* heat generation rapidly raises the temperature of the formulation from r.T. to far above 100 °C (generally between 120 and 180 °C), promoting the rapid formation of a polymer network while simultaneously releasing the blowing agent. It also ensures that the polymer architecture is formed at a temperature above its final glass transition or crystallization temperature, as a key element for the preparation of stable rigid PU foams. Leveraging the intrinsic features of the PU chemistry, flexible and rigid foams are easily manufactured through continuous extrusion or slabstock processes, *via* discontinuous reactive injection molding (RIM) or *via* spray foaming.[9] Continuous foam extrusion consists of mixing a pre-formed thermoplastic PU with a chemical or physical foaming agent in an extruder at a temperature high enough to melt the polymer and produce a gas, causing material expansion by a drop in pressure at the exit of the extruder. In the slabstock process, the PU expands and then solidifies within seconds after mixing the reactive ingredients (polyols, polyisocyanates and blowing agent) on a moving conveyor, yet delivering foams in the form of blocks or sandwich panels (*e.g.*, for thermal insulation). In RIM, the reactive formulation is fed under pressure *via* a supply line into a mixing chamber before injection into a (pre-heated) closed mold, where PU expansion and curing occur within a short time. Unlike the continuous processes, RIM is adapted to the design of objects with complex 3D shapes. As an adaptation of RIM, the formed-in-place foam allows for soft foam sealing on location (gasket

**Bruno Grignard**

*Bruno Grignard obtained his PhD from the University of Liège in 2007 in the field of $CO_2$ utilization for macromolecular engineering through controlled polymerization processes. Then, he continued as an associate R&D scientist in charge of the development of the $CO_2$ utilization technologies for polymer processing (foaming, solvent, drying, anti-solvents), polymer synthesis through novel conceptual routes for $CO_2$ conversion and $CO_2$-sourced materials design. He is now a principal research logistician within the "FRITCO$_2$T" R&D platform dedicated to $CO_2$ capture, utilization and recycling at ULiège.*

**Henri Cramail**

*Henri Cramail obtained his PhD from the University of Bordeaux (UB) in 1990 in ring-opening metathesis polymerization. After a post-doctoral stay at the University of Durham, U.K., he became an Assistant Professor of Polymer Chemistry at UB and was appointed as Professor in 1999. In 2004, he was awarded Junior Member of the 'Institut Universitaire de France'. He was Director of the Laboratoire de Chimie des Polymères Organiques (LCPO), CNRS-University of Bordeaux (2007–2016). He is leading the team 'Biopolymers and Bio-based Polymers' focusing on the development of green pathways to bio-based polymers from renewable resources (vegetable oils, polysaccharides, lignin, $CO_2$).*

**Haritz Sardon**

*Dr Haritz Sardon has been a professor at the UPV/EHU since 2018. He graduated from the UPV/EHU in 2011 before joining the group of Dr Hedrick at IBM-Almaden Research Center as a postdoc in 2012. In 2014, he returned to POLYMAT as a group leader. He has received several awards including Excellence of Young Researcher in Chemistry Award by the Spanish Royal Society (2021). His overall research aims to prepare new functional polymeric materials by combining sustainable polymerization based on organocatalysis with biobased monomers or monomers derived from plastic waste*

**Jean-Marie Raquez**

*Jean-Marie Raquez, PhD in Polymer Science, is the head of Laboratory Polymeric and Composite Materials at the University of Mons (Belgium) and Associated Professor at Polytechnique Montreal (canada). His research activities encompass all the general aspects about the realm of "bioplastics", i.e., bio-based and/or biodegradable polymer materials, particularly ranging from their controlled and catalyzed polymerization reactions, production of high performance nanocomposites/nanohybrids via reactive processing (i.e., reactive extrusion and additive manufacturing), to their implementation in diverse applications (packaging, textile, automotive, etc.), including their end-life scenario.*

foaming) by directly applying the two-component formulation onto a substrate *via* a mobile mixing head. Spray foams, particularly suited for insulation applications, utilize a propellant to expel the reactive polyol/isocyanate formulation to surfaces through an application gun/pressurized can. These foaming technologies have been well-managed and exploited for decades. However, the PU foam sector is facing stringent legal regulatory compliance related to health and safety considerations associated with the exposure, handling and use of isocyanates.[10] Further, obligations in creating an industrially viable PU end-of-life scenario to fulfill the sustainable objectives of our modern society, opportunities in exploiting chemicals of bio- and/or $CO_2$ origin,[10–14] and price volatility of raw isocyanates are additional drivers pushing these stakeholders to fundamentally reinvent the fabrication of PU foams without using isocyanates. Routes to isocyanate-free polyurethanes – also named non-isocyanate polyurethanes (NIPUs) – have been extensively described in the past[15–20] and the last months have seen the publication of reviews dedicated to their foaming.[21–24] While these documents provide a good insight into the current state of the technology, they generally lack a tutorial dimension. To bridge this gap, we propose a comprehensive and pedagogical review intended as a *vade-mecum* for newcomers to NIPU synthesis and foaming. This review delves into the underlying mechanisms of each foaming approach with a critical examination of their advantages and limitations compared to conventional PUs as well as their impact on the morpho-structural foam properties. In addition, we explore emerging end-of-life scenarios of NIPU foams and assess the foam utility for key real-world usages.

## 2. How to design non-isocyanate polyurethanes?

Herein, the most relevant NIPU synthetic approaches will be briefly illustrated, explaining only the key features of each concept and positioning them in light of their potential for NIPU foam fabrication. For a more complete and comprehensive overview of the state-of-the-art in NIPU synthesis, we invite the reader to consult previous accounts.[15–20] Ring-opening (co)polymerization (RO(CO)P) methods and step-growth copolymerization are the most relevant tools to fabricate NIPUs.

### 2.1. NIPUs by RO(CO)P

RO(CO)P refers to either the direct copolymerization of aziridines with $CO_2$ or the ionic polymerization of 5- to 7-membered cyclic carbamates.[25] Conceptually similar to the $CO_2$/epoxy polymerization, the $CO_2$/aziridine ROCOP is typically realized within the temperature range of 80 to 150 °C using compressed $CO_2$ ($p_{CO_2}$ = 30–100 bar) with or without a catalyst (Scheme 1, path A).[11,26–32] This synthetic approach produces PU chains containing a significant level of polyamine defects (even > 80%) but also branching. The polyamine defects are significantly minimized by using supercritical $CO_2$ ($100 < p_{CO_2} < 220$ bar) while providing both high molar mass chains ($27\,000 < M_n < 210\,000$ g mol$^{-1}$) and urethane linkage content up to 60%.[28,30] Enrichment of the polymer chains in urethane linkages up to 85% is also observed by using a complex $Y(CCl_3COO)_3$–$ZnEt_2$–glycerine catalytic system[26] and defect-free PUs are even accessible with (binary) organozinc catalysts including $ZnEt_2$, EtZnOMe, $ZnEt_2$/pyrogallol, $ZnEt_2$/resorcinol, $ZnEt_2$/*o*-aminophenol and $ZnEt_2$/*o*-phenylenediamine, but at the expense of the NIPU molar mass being limited to oligomers of 400 to 4500 g mol$^{-1}$, whatever the catalytic system.[27]

5-Membered cyclic carbamates display rather low reactivity, making their ROP challenging.[33–35] Their polymerization is only possible by an anionic pathway with geometrically constrained oxazolidones fused with an alicyclic cyclohexene moiety. Unlike planar "conventional" oxazolidones, the bicyclic structure of the molecule creates a conformational deformation increasing its ring strain, then facilitating its ring-opening (Scheme 1, path B). By using BuLi as the initiator and *N*-acyloxazolidone as the

**Sylvain Caillol**

*Sylvain Caillol is Senior Research Director at CNRS, based at the Charles Gerhardt Institute of Montpellier, and a leading expert in biobased polymers and sustainable polymer design. He is the author of over 300 publications and recipient of multiple awards, and has made major contributions to the development of polyhydroxyurethanes.*

**Christophe Detrembleur**

*Christophe Detrembleur obtained his PhD in 2001 from CERM at the University of Liege (Belgium) in the field of controlled radical polymerization (CRP) techniques. He then moved to Bayer AG (Leverkusen, Germany) to develop polymers from CRP and low-viscous UV-curable polyurethane formulations. After 2.5 years in this company, he joined CERM as a permanent FNRS Researcher (currently working as FNRS Research Director) to create his own research group. His research focuses on the valorization of carbon dioxide as a C1-feedstock for producing low-carbon footprint, circular polymers (e.g., non-isocyanate polyurethanes and polycarbonates) and materials (coatings, adhesives, and foams).*

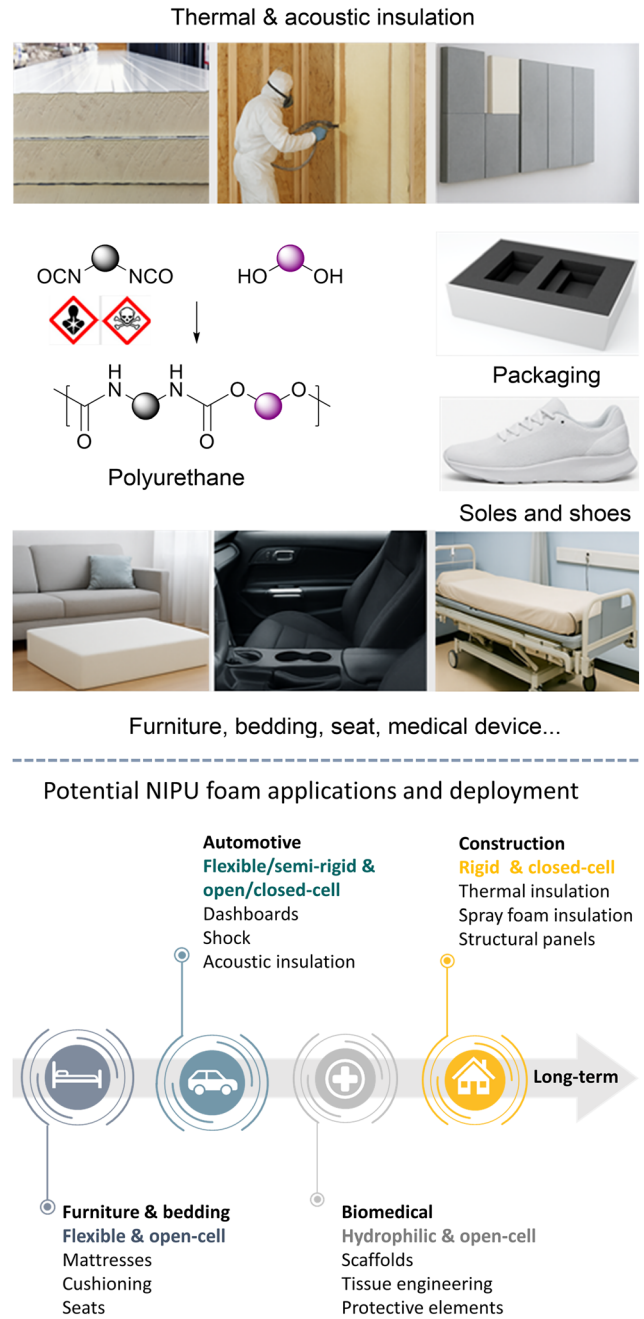


Fig. 1 Polyurethane foam applications and future deployment of NIPU foams.

co-initiator, linear NIPUs with $M_n$ up to 8000 g mol$^{-1}$ have been fabricated.[33] Recently, Rieger designed five-membered cyclic carbamates fused in a *trans* configuration with a limonene unit, which increases the ring strain of the heterocycle and favors its ROP. With Sn(Oct)$_2$ as a catalyst, low dispersity polyurethanes with $M_n$ up to 16 000 g mol$^{-1}$ have been synthesized at 80–100 °C in 15–20 h.[34] Besides, 6- and 7-membered cyclic carbamates undergo (cationic) ROP[36–41] with various catalysts ($Bu_2SnO$, $Bu_2Sn(OCH_3)_2$)[41] or electrophilic initiators (TfOH, TfOMe or $BF_3{\cdot}OEt_2$)[36,40] (Scheme 1, path C). When conducted in bulk at 70–120 °C, PUs with $M_n$ of 14 000–35 000 g mol$^{-1}$ or oligomers with $M_n$ < 5000 g mol$^{-1}$ have been designed from the 6- or 7-membered monomers, respectively.[41] One difficulty in accessing higher molar mass PUs *via* cationic ROP arises from the competition between chain propagation and competitive transfer and termination reactions, creating dead chains.

Limited to rare examples, both RO(CO)P routes yield thermoplastic materials potentially valuable for physical or chemical foaming (*e.g.*, *via* extrusion-foaming or foam molding). However, the challenges associated with $CO_2$/aziridine or cyclic carbamate polymerization (presence of defects, polymerization sensitivity to moisture and air, poor catalyst efficiency) and the immaturity of both methodologies, limited to academic research, make their industrial adoption questionable. Furthermore, NIPUs synthesized using RO(CO)P techniques exhibit low molar masses, resulting in inadequate chain entanglement. This deficiency could potentially adversely affect their mechanical properties, which have not yet been documented. Given the current state of knowledge, large-scale industrial production of these NIPUs remains unlikely in the short term, and the major drawbacks associated with their synthesis severely limit their applicability in foam fabrication.

### 2.2. NIPUs by polycondensation

Polycondensation involves either two monomers (AA + BB monomers), each containing functional groups, or a single molecule bearing both functionalities (AB monomer) (Scheme 2). These monomers react with each other *via* a condensation reaction to form a covalent linkage, together with the concomitant release of a by-product.[42] Repeated condensation reactions with simultaneous removal of the by-product drive chain formation, giving access to polymers of high molar mass. Such a step-growth polymerization generally proceeds in two stages, *i.e.*, oligomerization at low temperature (below 100 °C) followed by chain extension at a higher temperature, typically under vacuum to eliminate the condensate. Melt transurethanization polycondensation has been exploited to fabricate high molar mass NIPUs utilizing either AB monomers (α-hydroxy-ω-O-hydroxyethyl or α-hydroxy-ω-O-hydroxyphenyl urethanes, dihydroxyethyl dicarbamates)[43–47] (Scheme 2, path A) or AA–BB monomer mixtures (dimethyl dicarbamate/diol mixtures) (Scheme 2, path B).[44,48–53] Upon proper elimination of ethylene glycol, the thermally driven self-polycondensation of α-hydroxy-ω-O-hydroxyethyl urethanes catalyzed by tin complexes ($Bu_2SnO$ or $SnCl_2$) at $T$ = 100–150 °C or dihydroxyethyl dicarbamates ($T$ = 170–180 °C) furnishes various NIPUs with decent $M_n$ up to 31 000–64 000 g mol$^{-1}$. However, AB monomers or dihydroxyethyl dicarbamates favor the formation of ethylene carbonate, *via* a back-biting reaction, and amines that can further participate in condensation reactions to create up to 15% of urea defects within the chains. Switching to the polymerization of α-hydroxy-ω-O-hydroxyphenyl urethanes can suppress these back-biting reactions, together with the better leaving group ability of the phenol that allows for creating NIPUs at lower temperatures of 90–120 °C.[46,54] Significant improvements in the NIPU synthesis *via* melt transurethanization polycondensation have been accomplished by combining dimethyl dicarbamate AA monomers with BB diols.[48,51,52] Unlike previous AB monomers, alcoholysis of the AA monomer

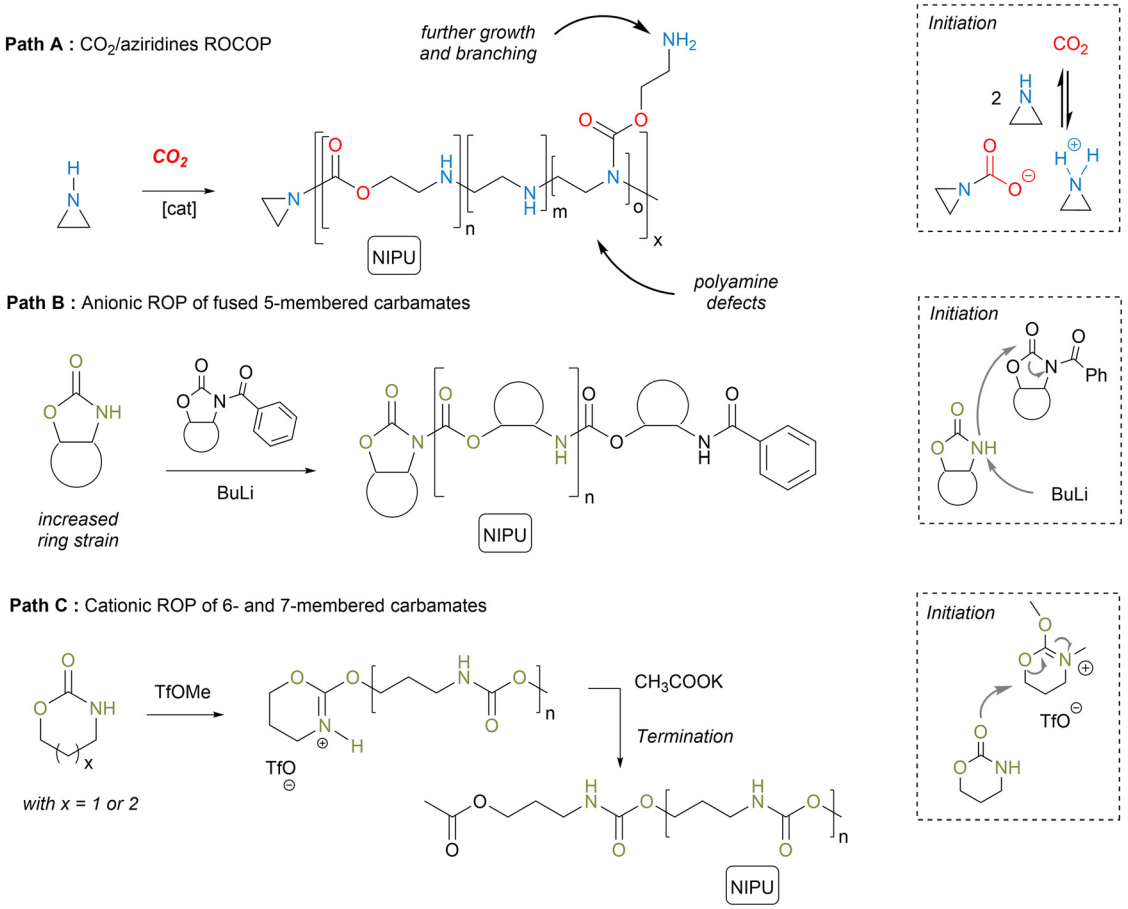


Scheme 1 Non-isocyanate polyurethane synthesis *via* ring-opening (co)polymerization approaches.

by a diol releases MeOH that is easier to eliminate than ethylene glycol or phenol. In addition, upon proper selection of the diol BB monomers, back-biting reactions are suppressed, limiting the formation of urea defects within the chains. Following this methodology, NIPUs with various microstructures and $M_n$ > 50 000 g mol$^{-1}$ have been fabricated. For representative illustrations of these examples, we invite the reader to refer to existing reviews.[42] Polycondensation *via* melt-transurethanization forms thermoplastic NIPUs with decent/high molar masses suitable for foaming processes. Advantageously, the AA or AB monomers are generally accessible from low-cost and commercially available ethylene carbonate or dimethyl carbonate. One has to mention that NIPUs are also accessible *via* a sequential terpolymerization approach involving diamines, $CO_2$, and dihalides.[55–57] The process involves the formation of a dicarbamate salt by the capture of $CO_2$ by a diamine in the presence of a base. This salt further undergoes alkylation *via* an $SN_2$ with alkyl dihalides to create urethane linkages. As this pathway generates equimolar amounts of waste and utilizes undesirable halide chemicals, we have disregarded this synthetic pathway from our survey/analysis.

Polycondensation methods are already deployed at the industrial scale *via* reactive extrusion for the synthesis of other types of polymers (*e.g.*, bisphenol A polycarbonate, polylactic acid, *etc.*). This technique should be adaptable to NIPUs provided that a sufficient supply of monomers is available in the future. Such features should then open perspectives in manufacturing NIPU foams in a single device *via* the reactive extrusion-continuous foaming process.

### 2.3. NIPUs by step-growth polyaddition

Step-growth polyaddition shares similarities with polycondensation except that no by-product is formed during the reaction. Over the last decade, this polymerization manifold has been extensively deployed to synthesize polyhydroxyurethanes (PHUs) (Scheme 3, path A).[15–20] PHUs typically result from the moisture-tolerant polyaddition between 5-membered polycyclic carbonates and polyamines. As the aminolysis of the cyclic carbonate is rather slow even at $T$ > 80 °C, various research teams have developed catalytic solutions to facilitate chain extension by using Lewis acids (Li salts, $MgBr_2$, $Yb(OTf)_3$, *etc.*),[58] organobases (DBU, TBD, phosphazene)[58] or hydrogen bond donors such as (thio)ureas.[59] Recent discoveries have highlighted the multifaceted role of water as a highly efficient accelerator in thermoset PHU fabrication from r.T. reactive formulations.[60] Besides acting as a catalyst for the aminolysis of cyclic carbonates, water also disrupts the multiple intra-/inter-molecular H-bonding interactions within the PHU clusters, enhancing the chains' mobility and delaying the vitrification *via* the hydroplasticization

 

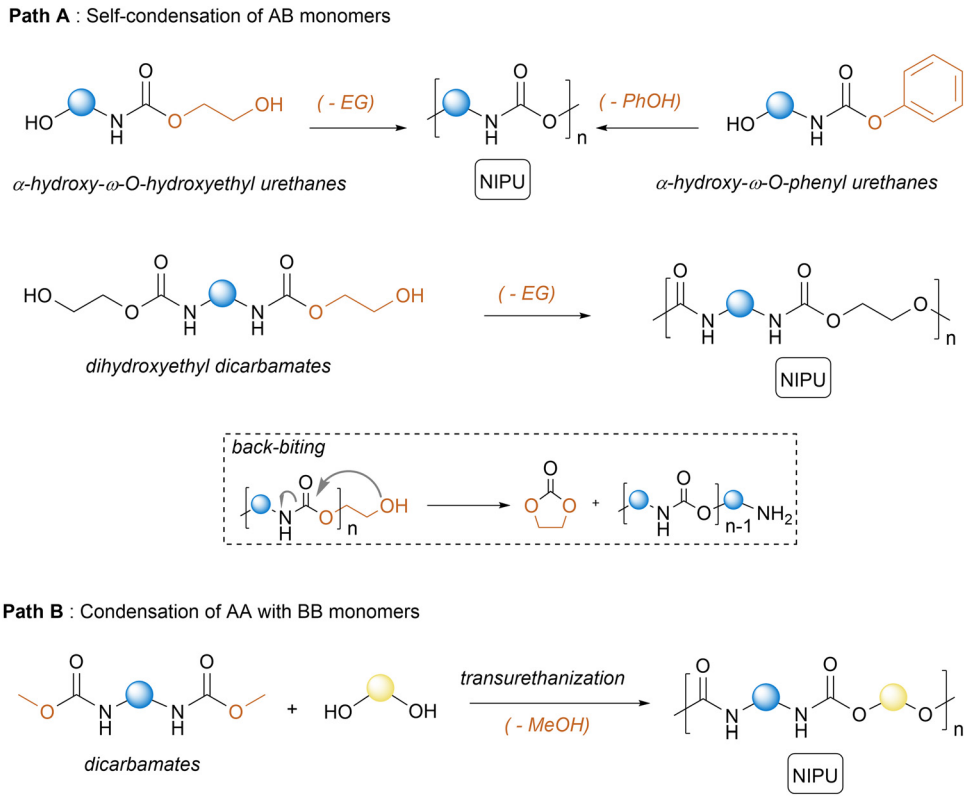


Scheme 2 Non-isocyanate polyurethane synthesis *via* polycondensation methods.

effect.[60,61] Other strategies capitalize on microwave utilization[62–64] or on the smart design of the monomers to facilitate the formation of urethane linkages. Introducing ether, ester or sulfur electron-withdrawing groups in the β-position of the carbonate moiety,[16,65–68] expanding the ring size to 6-membered cyclic carbonates[16,69–71] or inserting *endo*- or *exo*-cyclic vinylene groups within 5-membered cyclic carbonates allows for significant improvement of aminolysis,[72–75] even enabling some r.T. transformations.[16] Playing on the amine structure also shows benefits for the PHU synthesis, especially when using amine scaffolds with β-alcohols.[76] All these reactivity considerations have been detailed and rationalized in a very recent tutorial review, which the reader can refer to.[16] Except for NIPUs synthesized from exovinylene cyclic carbonates and primary amines (furnishing poly(hydroxyoxazolidone)s, a special class of PHUs embedding cyclic urethane linkages) or secondary amines (furnishing poly(oxo-urethane)) (Scheme 2, path B), access to high molar mass PHUs is challenging, with $M_n$ being most often limited to $<15\,000$ g mol$^{-1}$ under bulk or solvent conditions, but reaching up to 35 000 g mol$^{-1}$ by reactive extrusion.[77,78] The cause for the low molar masses partly arises from the reversible nature of the hydroxy-urethane linkages, limiting chain growth to an equilibrium (see Section 4.2). Increasing extents of intermolecular hydrogen bonding over

## Take-home message

**Key differences between conventional PUs and NIPUs**

*Difference 1 – reaction kinetics.* Synthetic routes to NIPUs display insufficient or no exothermicity and proceed more slowly than the fast and exothermic isocyanate/polyol reactions in conventional PUs.

*Difference 2 – microstructure.* NIPUs lack biuret, allophanate, isocyanurate, and uretdione linkages providing rigidity in conventional PUs.[6] The NIPU structures vary significantly from one to another, depending on the chosen synthetic route (*e.g.*, chain-growth *vs.* step-growth polymerization). These structural variations translate into significantly different thermo-mechanical properties.

*Difference 3 – molar mass and architecture.* Achieving high molar mass thermoplastic NIPUs remains difficult; the most mature and efficient methodologies yield thermosetting PHUs.

**Main challenges for NIPU (foam) development**

*Challenge 1 – catalyst and monomer design*. Optimize catalysts, design monomers or hybridize chemistry[85–87] to accelerate urethane formation and offer more flexibility to synchronize polymerization with the release of the blowing agent for adequate foam expansion and curing.

*Challenge 2 – performance matching*. Select monomer combinations that enable the fabrication of NIPUs with thermo-mechanical properties comparable to those of conventional PUs.

*Challenge 3 – synthetic protocols for industrial integration*. Adapt NIPU synthetic methods to align with established PU technologies and processes, ensuring compatibility and smooth retrofitting of existing industrial plants.

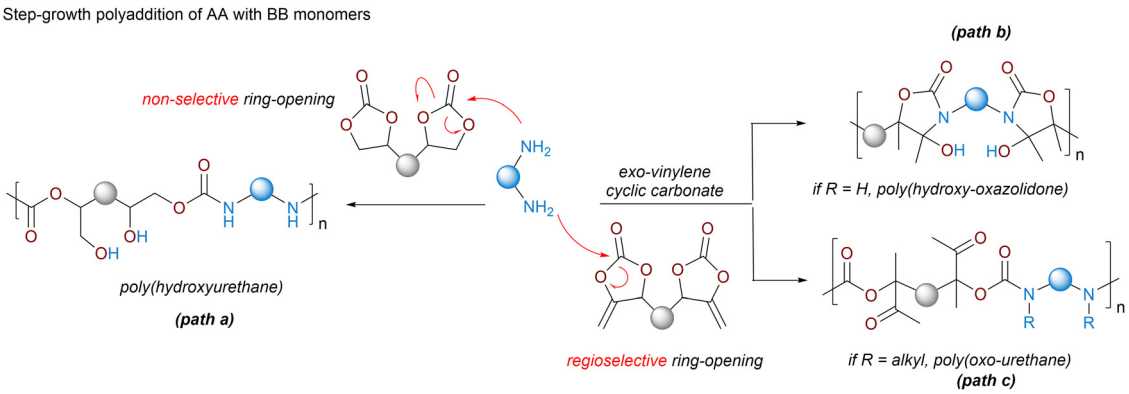


Scheme 3 Non-isocyanate polyurethane synthesis *via* step-growth polyaddition.

the reaction course also hinder chain mobility, ultimately contributing to slowing down the polymerization. While rather limiting for the fabrication of thermoplastic PHUs, this chemistry is, on the contrary, perfectly suited for the synthesis of thermoset PHUs from reactive polyfunctional precursors (with one of the comonomers displaying a functionality greater than 2).[79]

The extensive structural diversity of accessible polyamines and polycyclic carbonate precursors, some of which originate from bio- and/or $CO_2$ sources,[80–84] enables the engineering of PHU thermosets with thermo-mechanical properties that are modular on demand, thereby complying with the specifications of targeted applications. With these assets in our hands, we possess a versatile chemical tool capable of not only supplanting conventional PUs with a non-isocyanate alternative but also adapting to the dominant industrial slabstock, RIM, formed-in-place, or spray foaming technologies of PUs, further allowing for the retrofitting of existing industrial foaming plants.

## 3. How to foam non-isocyanate polyurethanes?

### 3.1. Polymer foaming and underlying mechanism

Understanding and controlling the polymer foaming process is crucial to fabricating materials with adequate properties. Briefly, the foaming mechanism follows three steps, including cell nucleation, growth, and stabilization (Fig. 2).[9,88] Cell nucleation consists of forming a polymer/gas solution by dissolving a blowing agent into a molten polymer/viscous reactive formulation. When reaching supersaturation, the gas dissolved within the polymer causes thermodynamic instability, creating nucleation nodes. This step is followed by cell growth. The increase in gas pressure within the cells and gas diffusion allows the "soft" viscoelastic matrix to expand, creating a porous structure.[89,90] Ensuring proper viscosity control is crucial for uniform bubble growth. Unsuitable polymer viscosity/viscoelastic properties lead to cell drainage and coalescence of the gas bubbles, forming non-homogeneous foams with large cell sizes or even collapsed foams. Too high viscosities limit the polymer expansion. In the last step, cell stabilization prevents the foam from collapsing. This stage is usually controlled by adding stabilizers, by rapid material cooling (most often for thermoplastic foams) or curing (thermosetting foams). Dispersion of bio- (cellulose, lignin, *etc.*),[91] inorganic (silica, fibers, $CaCO_3$, clays, *etc.*)[92–94] or carbon-based (nanotube, black carbon, graphite)[95] fillers within the polymer offers an additional lever to adjust the foam's characteristics. These multi-role additives act as nucleation agents, (melt)viscosity modifiers and/or structural reinforcements. Finally, the proper selection of the blowing agent (physical or chemical, endogenous or exogenous)[8,96] and the foaming process govern the formation of foams with closed- or open-cell structures and controlled cell geometry/size. For example, a physical blowing agent is generally preferred to design low-density foams with closed cells. The decomposition of a chemical blowing agent that releases small gaseous molecules ($CO_2$, $N_2$, or $H_2$) is preferred for one-pot formulations and a simplified setup.[7] The high diffusion rate of these gases within the polymer causes cell rupture, leading to foams with open cells.[7]

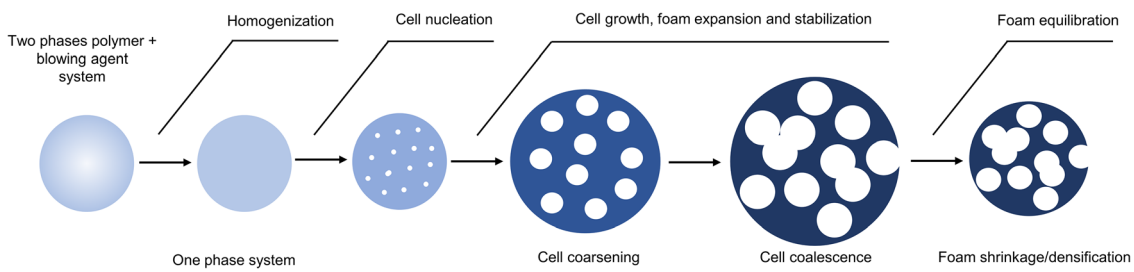


Fig. 2 General polymer foaming mechanism.

 

### 3.2. Physical *vs.* chemical blowing of polymers

Physical foaming leverages the physical change (generally endothermic) of a non-reactive chemical, commonly referred to as a physical blowing agent, blended in a polymer melt/reactive formulation to generate a gas that promotes material expansion.[7] The most prevalent physical changes involve either the volatilization of low-boiling point liquids (endothermic blowing agents) or the release of compressed gas ($CO_2$, $N_2$) to atmospheric pressure. Industrially, the supercritical carbon dioxide-assisted blowing technology is the method of choice to fabricate elastomeric thermoplastic PU foams for high-performance shoe soles (*e.g.*, BASF Infinergy®). Hydrocarbon blowing agents (*e.g.*, pentane) are commonly used for the fabrication of insulation materials (panels, tapes, sealants, *etc.*) from reactive thermosetting formulations.

Chemical foaming leverages the decomposition or chemical reaction of an inorganic salt (*e.g.* carbonate or borohydride salts), or an organic compound (hydrogen peroxide, azocarbodiimides, tetrazoles, semicarbazides, *etc.*), mixed with a polymer melt/reactive formulation, to generate *in situ* volatile compounds (*e.g.* $CO_2$, $N_2$, $H_2$ or water) that promote material expansion.[7] Most chemical blowing agents are classified as "endothermic" as their decomposition is generally triggered by heat and usually leads to foams with open-cell morphology found in items for comfort, protective equipment (shock absorption), acoustic insulators, *etc.*

Self-foaming refers to a particular endogenous chemical blowing process where the blowing agent is generated *in situ* by the (partial) decomposition of a monomer or another reactive foam component (*e.g.*, reactive stabilizer) that is contributing to the polymer structure.[7,8] This methodology is well-adapted to the foaming of conventional PUs from isocyanate/polyol formulations. The partial hydrolysis of the isocyanate releases $CO_2$, causing material expansion simultaneously with PU network construction. Self-foaming methods are predominantly utilized at the industrial scale, occasionally in conjunction with the application of physical blowing agents (*e.g.*, for spray foaming), to generate foams suitable for diverse applications.

Directly adapting a PU foaming process for NIPUs requires substantial adjustments. The limited accessibility of thermoplastic NIPUs confines foam fabrication almost exclusively to thermosetting formulations. Moreover, the inherently low reactivity of NIPU precursors in these formulations poses significant challenges in controlling the viscosity increase, the gelation rate of the NIPU matrix, and the release of the blowing agent (whether endogenous or exogenous). As discussed in the following sections, polyhydroxyurethanes are emerging as the most promising candidate for NIPU foam fabrication.

### 3.3. NIPU foams by physical blowing

**3.3.1. Supercritical $CO_2$-assisted foaming.** Supercritical $CO_2$-assisted foaming ($scCO_2$) is particularly adapted for the foaming of thermoplastics as found industrially in the manufacture of PU soles for athletic shoes. Unlike most of the polymers, which are not soluble in supercritical $CO_2$, $scCO_2$ diffuses rapidly and solubilizes within these matrices owing to specific $CO_2$–polymer interactions (acid–base, van der Waals, dipole–(induced) dipole).[97] These features make $scCO_2$ a particularly well-suited physical blowing agent for batch foaming processes. Conceptually, the foaming is divided into two phases, *i.e.*, a saturation step during which $scCO_2$ diffuses uniformly and saturates the polymer, then cell nucleation and growth triggered by a temperature rise close to the melting/glass transition temperature of the polymer with concomitant $CO_2$ release (Fig. 3).[98,99] Inherent to this process, foams naturally adopt a closed-cell morphology and their morpho-structural properties are easily modifiable by controlling the saturation time, and/or by adjusting the $CO_2$ density *via* simple variation of the impregnation pressure and temperature. This $scCO_2$-assisted foaming method has been adapted by Grignard *et al.* to the fabrication of semi-rigid polyethylene glycol- or plant oil-based PHU foams.[100] Semi-crystalline polymers with a $T_m$ of 87–88 °C have been synthesized from biobased aminotelechelic oligoamides coupled with polyethylene glycol diglycidyl carbonate or partially carbonated soybean oil. Optimization of the foaming sheds light on the necessity to follow a two-step process to obtain homogeneous materials. To maximize $CO_2$ impregnation, the saturation of PHUs is realized at a low temperature of 40 °C and a high pressure of 300 bar. These conditions enable the solubilization of up to 10 wt% of $CO_2$ within PHUs in 3 h. Then, after depressurization, the PHU samples are heated close to the $T_m$ of the polymers (80 °C) for 1 min. This softens the PHU and simultaneously releases trapped $CO_2$, causing material expansion. Well-defined low-density PHU foams ($d$ = 110–176 kg $m^{-3}$), with small pore sizes (diameters from 2.6 to 10.8 μm), narrow pore size distribution and a high cell density ($>1.5 \times 10^{10}$ cells per $cm^3$), are fabricated. Reducing the saturation pressure to 100 bar results in a change of the foam's morphology, with the creation of materials characterized by larger pore sizes and lower cell densities. These changes are correlated with the decrease in $CO_2$ density at low pressure, leading to lower solubilization of $CO_2$ in the matrix during the saturation step.

Efforts to design PHU foams in a single-step foaming process significantly alter the foam characteristics. This strategy involves a saturation step of the PHUs at 90 °C, a temperature close to their $T_m$, followed by a fast vessel depressurization. Due to the low $CO_2$ density even at 300 bar, a long saturation time of 24 h is necessary to dissolve a sufficient amount of $CO_2$ in the matrix. Upon release of the $CO_2$ pressure, poorly defined foams with broad cell size distributions between 4 and 22 μm featuring irregular shapes or even collapsed cells are obtained.[100] A similar trend was reported later by Rwei for the $scCO_2$-assisted one-step foaming of branched PHUs synthesized from bis-phenol A diglycidyl carbonate, a blend of ethylene diamine with 7.5 or 10 mol% of a $C_{36}$ alkylenediamine and ppm amounts of 1,2,4,5-benzenetetracarboxylic acid.[101] Following the saturation of these amorphous polymers at a $p_{CO_2}$ of 150 bar for 6 h at 80 °C – a temperature far exceeding their $T_g$'s estimated at ~30 °C – ill-defined foams with densities of 215 to 432 kg $m^{-3}$ and cell sizes in the 9 to 23 μm range were obtained upon $CO_2$ release. The author correlated the lower foam density of the $C_{36}$ alkylenediamine-rich PHU materials to the higher

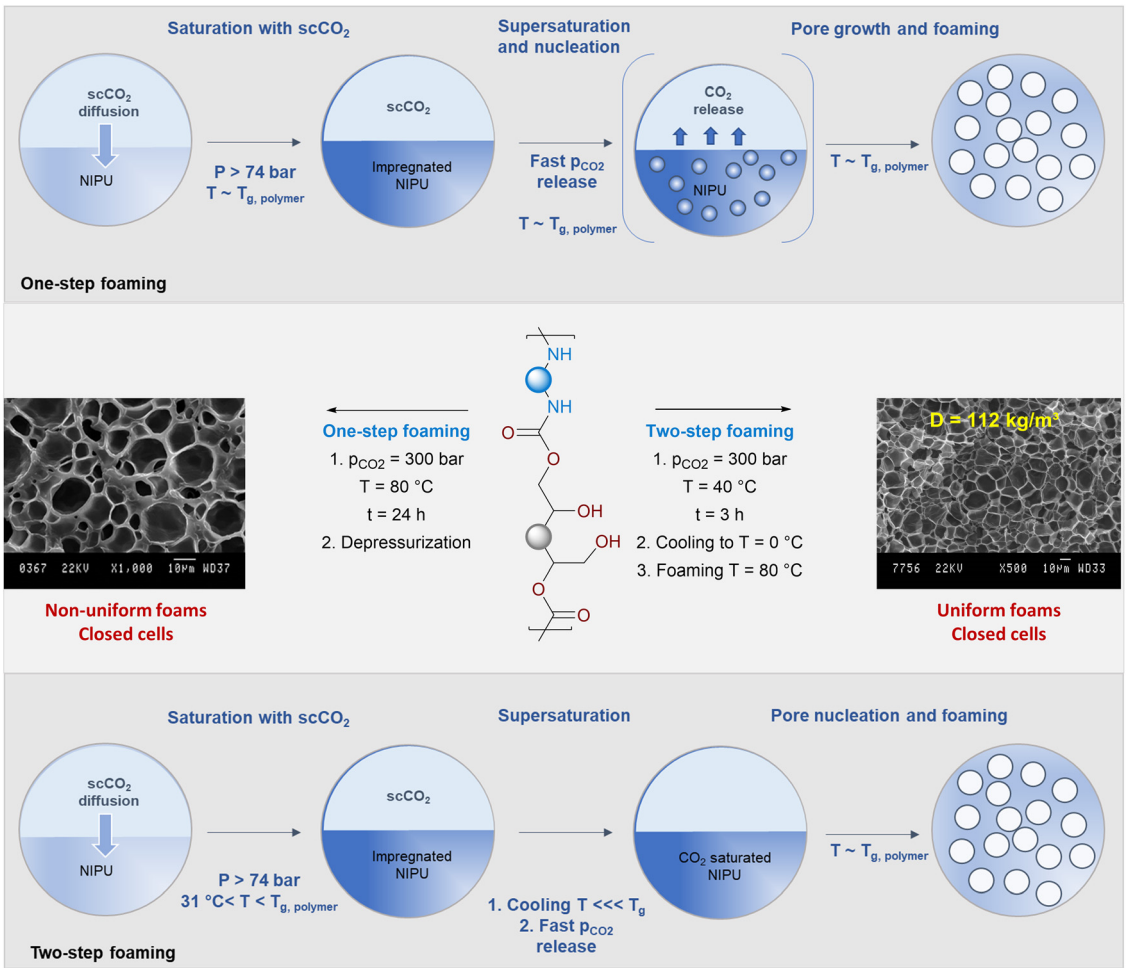


Fig. 3 Supercritical $CO_2$-assisted foaming of thermoplastic PHUs *via* a one-step or two-step procedure. SEM figures reproduced from ref. 100 with permission from the Royal Society of Chemistry. Copyright 2016, Royal Society of Chemistry Publisher.

flexibility of the chain, facilitating the penetration of $CO_2$ within the polymer matrix during the saturation step.

**3.3.2. (Fluoro)hydrocarbons.** The physical blowing of NIPUs by volatile (fluoro)hydrocarbons was first documented in patents related to spray foaming methods.[102,103] Conceptually, the patented reactive thermosetting formulations typically consist of polyamines or aminotelechelic oligohydroxyurethanes mixed with epoxy or acrylic curing agents, along with foaming agents and various additives such as catalysts, rheology modifiers and stabilizers. Pre-heating the foam ingredients to 65 °C before adding the foaming agent (selected from (iso-)pentane, cyclohexane, 1,1,1,3,3-pentafluoropropane (HFC-245fa), *cis*-1,1,1,4,4,4-hexafluoro-2-butene (Opteon™ 1100), 1,1,1,3,3-pentafluorobutane (Solkane®365), *etc.*) or capitalizing on the exothermic heat generated during the network creation by the amine-epoxy or aza-Michael reactions enables the spraying and rapid formation of rigid hybrid NIPU foams within 60 seconds to 2 minutes. The utility of Solkane®365 was revisited later for the fabrication of low-density flexible foams for automotive seats[104]based on PHU reactive formulations composed of an amine (HMDA), blends of trifunctional cyclic carbonates (TMPTC and EO-TMPGC, a carbonated tri-arm oligoPEG) and 1 wt% of DABCO catalyst (Fig. 4A). Through rheology-guided experiments, Blattmann *et al.* correlated gelation rate and pot-life time to the composition of the formulation, both being delayed with increasing contents of EO-TMPGC. Following these outputs, a TMPTC/EO-TMPGC carbonate composition set to 60 wt%/40 wt% offers the best compromise in terms of gelation rate (~14 min) and pot-life time (~8 min). The PHU foam is fabricated using a stepwise approach in aluminum molds pre-heated to 40–50 °C. First, HMDA is mixed with the TMPTC/EO-TMPGC carbonate blend for 4 minutes, followed by the addition of 25 wt% Solkane at r.T. The thermal curing at 80 °C allows for foam expansion within 20 minutes, but a curing of 14 h is required to ensure its dimensional stability. The so-produced flexible foams ($T_g$ = 1 °C) display a density of 142 kg $m^{-3}$, an open-cell morphology and cell diameters of 171 ± 13 μm.

Following a procedure similar to Blattmann, Zhang exploited *trans*-1-chloro-3,3,3-trifluoropropylene (HFO-1233zd, 14 wt%) to foam a reactive NIPU formulation composed of 1,4-cyclohexanedimethanol bis(cyclic carbonate) (CD) and blends of *m*-XDA and PEI (Fig. 4B).[105] Although the morpho-structural properties of the foams are governed by the content of highly reactive PEI, lower-density foams ($d$ = 139 kg $m^{-3}$) with a more uniform pore structure

 

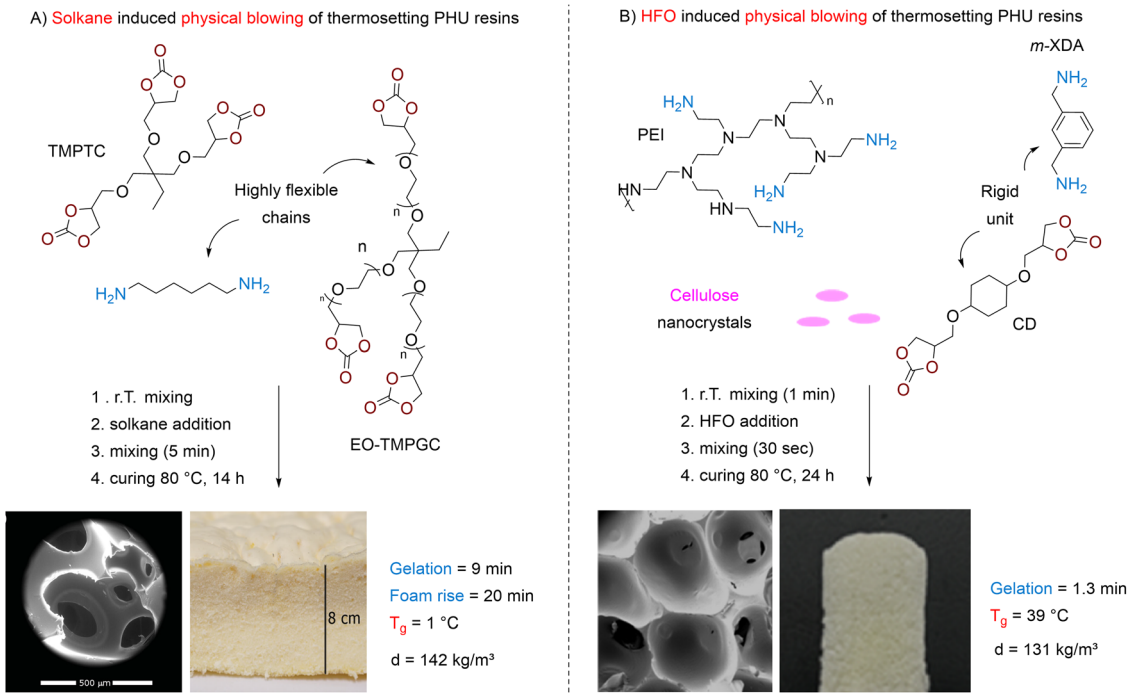


Fig. 4 Foaming of thermosetting PHU resins using Solkane® (A) or HFO-1233zd (B) as a physical blowing agent. SEM picture (A) reproduced from ref. 104 with permission from John Wiley and Sons. Copyright © 2016, Wiley-VCH Verlag GmbH & Co. KGaA, Weinheim. SEM picture (B) reproduced from ref. 105 with permission from Elsevier. Copyright 2025, Elsevier Publisher Ltd.

(cell size of 0.8 mm) are produced at a 40/60 *m*-XDA/PEI blend ratio (by mass). The originality of the work lies in the utilization of cellulose nanocrystals (CNCs) that function as a biosurfactant stabilizing cells and limiting Ostwald ripening. Adding 3.3–9.7 wt% of CNC contributes to the formation of foams with slightly reduced densities (~130 kg $m^{-3}$) and smaller cell diameters (0.6 mm). Furthermore, the presence of the filler enhanced the mechanical properties of the foams, particularly along the foaming direction, with a two- to three-fold increase in the compression modulus, from 0.15 MPa without the additive to 0.35 MPa with 9.7 wt% CNC.

**3.3.3. Miscellaneous solvents.** Acetone has been specifically employed as a physical blowing agent for foaming thermoplastic PHUs of high $T_g$s (80–110 °C), which have been synthesized from aromatic monomers, such as bisphenol-derived cyclic carbonates and *p*-xylylene (*p*-XDA) diamine *via* reactive extrusion.[77] The foaming process involves compression-vacuum molding, where the polymers are dissolved in a minimal volume of acetone to form a homogeneous mixture. The solution is then placed in a closed mold and a dynamic vacuum of 0.5–1 mbar is applied for 4–6 h at a temperature 5 °C below the polymer's $T_g$. With this process, foamability is correlated with the complex viscosity of the PHU. The PHU with the lowest complex viscosity – made from bisphenol A diglycidyl carbonate (BPAdiCC) – produces a foam with a density of only 35 kg $m^{-3}$, which is twice lower than that of other aromatic PHU foams of the series. All foams display an open-cell morphology (85% open porosity) with a pore size of 125–150 ± 20–35 µm and good compression resistance owing to their highly rigid character.

Water, ethanol or binary water/ethanol mixtures have also been used for the fabrication of thermosetting foams.[106] An aminotelechelic hydroxyurethane-*co*-urea oligomer (86% urea linkages) – made by stepwise transurethanization polycondensation of a dicarbamate monomer with a diol (pripol®2033) followed by chain extension with priamine®1074 – is blended with the blowing agent, a bis-aminopropyl-terminated PDMS stabilizer (2 wt%) and a polyepoxy resin as a crosslinker until a homogeneous solution is obtained before curing at 73–120 °C for 2 h. When using water as the blowing agent (content not specified in the original work), the optimal foaming temperature is determined to be 95 °C, yet resulting in a uniform, highly flexible foam with a density of 190 ± 40 kg $m^{-3}$, an open-cell morphology and cells averaging 590 ± 270 µm. Substituting water with ethanol leads to foams with higher density (280 ± 25 kg $m^{-3}$) and smaller cell diameters (280 ± 120 µm). A slight reduction in density (115 ± 40 kg $m^{-3}$) is observed when a 75/25 water/ethanol mixture is used, although the corresponding foam retains a highly heterogeneous cell size distribution (430 ± 150 µm). Changing the stabilizer content (up to 10 wt%), reducing the foaming temperature (from 73 to 85 °C) or changing the water/ethanol composition doesn't improve the morpho-structural characteristics, homogeneity or density of the foams.

### 3.4. NIPU foams by chemical blowing

**3.4.1. Inorganic carbonate salts.** The chemical foaming of NIPUs has been illustrated using $NaHCO_3$, an inorganic salt that decomposes thermally into $Na_2CO_3$, water and $CO_2$ (Fig. 5). By dispersing $NaHCO_3$ at a loading of 5 to 20 wt% in TMPTC/

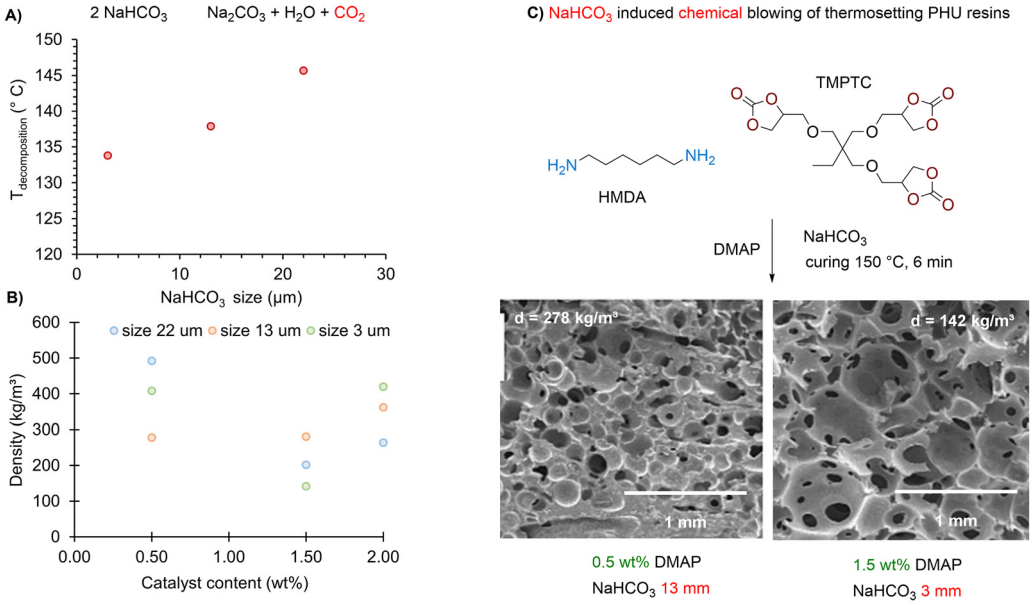


Fig. 5 Chemical blowing of thermosetting PHU foams. (A) Size dependence of the decomposition temperature of $NaHCO_3$ salt; (B) evolution of the foam density with the particle size and catalyst loading; (C) SEM characterization of various thermosetting PHU foams. SEM pictures reproduced from ref. 107 with permission from Elsevier. Copyright © 2023, Elsevier Ltd.

HMDA reactive formulations (with 0.5 to 2 wt% of *N*,*N*-dimethylcyclohexylamine catalyst), Amezúa-Arranz *et al.* have produced a series of PHU foams at 150 °C in 6 min.[107] With this blowing system, the morpho-structural properties of the final materials are governed by the efficiency of the foaming process, which in turn is guided by an adequate balance between PHU viscosity increase, gas release and catalyst loading. Within their investigations, the authors emphasize the complexity of determining the optimal foaming window of a reactive formulation. They found that the decomposition temperature of $NaHCO_3$ depends on its particle size, with a 12 °C difference observed between smaller particles (3 µm, $T_{decomposition}$ = 133.8 °C) and larger particles (22 µm, $T_{decomposition}$ = 145.7 °C) (Fig. 5A). Notably, $NaHCO_3$ with a particle size of 13 µm ($T_{decomposition}$ = 137.9 °C, loading of 10 wt%) allows for the optimal synchronization between viscosity increase, gelation and gas release, delivering slightly anisotropic open-cell foams with the lowest density of 278 kg $m^{-3}$, a mean cell size of 322 ± 32 µm and an open cell content of 83%. Reducing the $NaHCO_3$ particle size to 3 µm produces denser PHU foams (318–482 kg $m^{-3}$) with 77–96% open cells and a smaller cell size (15.2–22.7 µm) due to the rapid gas escape from the too low viscosity matrix. $NaHCO_3$ with a larger size exhibits a decomposition temperature close to 150 °C and leads to insufficient gas production and high-density foams of 321–492 kg $m^{-3}$. Being only valid for a 0.5 wt% catalyst content, these trends change with 1.5 wt% of *N*,*N*-dimethylcyclohexylamine. Higher catalyst concentrations accelerate network gelation, so that 3 µm $NaHCO_3$ is preferred for quicker gas release to promote the expansion of the PHU. This system delivers a uniform foam with a low density of 142 kg $m^{-3}$, an open cell content of 90% and a cell size averaging 329 µm (Fig. 5B).

Other studies, with limited or even no details on the foaming process or foam characteristics, have utilized bicarbonate salts in the production of bio-based PHU foams. Pizzi *et al.* developed glucose-based NIPU oligomers by condensing a dialkylcarbonate monomer derived from glucose with HMDA, followed by curing and foaming at 200 °C for 30 minutes using $NaHCO_3$ (~1 wt%) as the blowing agent and a reactive epoxy-silane coupling agent/compatibilizer (<1 wt%).[108] This formulation produced rigid foams with open cells and densities ranging from 75 to 127 kg $m^{-3}$. However, it seems likely that the role of the silane additive in the foaming process is more significant than initially assumed. We believe that the methoxy-silane groups can participate in (self-)condensation reactions, leading to the formation and release of methanol at 200 °C. Such an assumption is supported by results showing that the absence of $NaHCO_3$ in the reactive NIPU formulation delivered foams with a density of 75 kg $m^{-3}$, which is almost identical to the 88–90 kg $m^{-3}$ density observed under the same conditions in the presence of the salt.

Similarly, some authors reported the dual use of $NH_4HCO_3$ with citric acid to create plant oil-based PHU foams from carbonated linseed oil/HMDA reactive formulations.[109,110] The acid acts as a catalyst, accelerating the decomposition of the bicarbonate salt and releasing gas at 80 °C, while also leading to foam formation within 15 minutes. However, the foam properties evolved over several weeks, transitioning from a stiff material after 24 h to a more rigid structure with a $T_g$ of 42 °C after weeks of equilibration. This gradual change in foam behavior is attributed to the incomplete reaction between the sterically congested internal carbonate moieties and amines within the initial 15 minutes, which slowly progresses over time. Unfortunately, no data on the density, cell size and morphology or mechanical

 

performances of the so-produced expanded materials are provided.

**3.4.2. Azo compound.** Azodicarbonamide, a ubiquitous chemical blowing agent in the foam industry, has been used in the fabrication of PHU foams. Its thermal decomposition proceeds *via* a cascade process which delivers a complex gaseous mixture of $N_2$, CO, $NH_3$ and (iso)cyanic acid and solid by-products (urazole and hydrazodicarbonamide). The decomposition of this blowing agent, which is usually triggered above 200 °C, is facilitated at a lower temperature by the use of the ZnO additive.[111,112] Following a sequential curing of 120 °C for 30 min, followed by a post-treatment at 60 °C for 3 h, flexible PHU foams with $T_g$s of 4.6–6.5 °C have been fabricated from reactive formulations made of carbonated soybean oil (CSBO) and diethylene triamine (DETA) using a 75%/25% azodicarbonamide/ZnO mixture.[113] The foam characteristics were finely tuned by adjusting the loading of the blowing agent, with an optimum value of 10 wt% *vs*. CSBO. This content leads to a material of $d$ = 235 kg m$^{-3}$ with cylindrical open cells of 150–300 μm. Besides, denser ($d$ = 440 kg m$^{-3}$) or non-uniform partly collapsed foams have been obtained by changing the blowing agent content to 6 wt% or 13.5 wt%, respectively. The authors also noted that the catalyst used to synthesize CSBO from $CO_2$ and the corresponding epoxidized bio-oil seems non-innocent in the foaming process. While stable foams have been obtained from CSBO synthesized with ethyl methyl imidazolium bromide ([Emim]Br), they collapse within 20 min when using CSBO produced with $^n$Bu$_4$NBr. Through rheology measurements, the authors highlighted a nearly three-fold acceleration of the PHU gelation when using CSBO made with the imidazolium salt ($t_{gel}$ = ∼9 min) *vs*. the same carbonate precursor produced with the ammonium salt ($t_{gel}$ ∼ 26 min).

### 3.5. How to produce NIPU foams *via* self-blowing methods?

**3.5.1. $H_2$ self-blown foams.** NIPU formulations have been foamed taking advantage of the reaction between a (poly)amine precursor and poly(methylhydrogenosiloxane) (Momentive MH15 or PMH), which generates gaseous dihydrogen as the blowing agent (Fig. 6A).[7] Cornille *et al.* fabricated the first self-foaming PHU by employing TMPTC or a blend of TMPTC and a difunctional polypropylene oxide bis cyclic carbonate (PPODCC – $M_n$ = 725 g mol$^{-1}$) together with Jeffamine EDR148 or Priamine, Momentive MH15 (5 mol% *vs*. amine) and TBD as a catalyst (5 mol% *vs*. 5CC) (Fig. 6B).[114] By adopting a sequential curing at 80 °C for 12 h followed by a post-treatment at 120 °C for 4 h, high-density flexible PHU foams with open-cell morphologies were obtained. The morpho-structural and mechanical characteristics of the foams directly correlate to the crosslinking density of the PHU network, which is governed by the TMPTC content. The denser PHU foam ($d$ = 295 kg m$^{-3}$) with the highest $T_g$ of 19 °C has been elaborated from pure TMPTC and Jeffamine. Substituting part of TMPTC with PPODCC and Jeffamine for Priamine not only allows for a decrease in crosslinking density but also brings flexibility to the network. This is reflected in the reduced density and $T_g$ values, which drop to 195 kg m$^{-3}$ and −18 °C, respectively. In the wake of their seminal works, the same authors improved their foaming process by replacing the TBD catalyst with a more efficient fluorinated thiourea, further opening the doors to the r.T. foaming of PHU.[115] By a slight modification of the TMPTC/PPODCC/Jeffamine composition and $M_n$ variation of the PPOBC (380 or 640 g mol$^{-1}$), flexible foams with densities of 271–303 kg m$^{-3}$, cell size of 140–1300 μm and $T_g$ values of 0–11 °C have been produced at r.T. within 3 days using only 1 mol% of thiourea (*vs*. 5CC).

To tackle the inherent low reactivity of 5CC, Coste *et al.* specifically designed a liquid tetra-functional six-membered cyclic carbonate precursor (T6CC) (Fig. 6C), which has been utilized to prepare PHU foams under catalyst-free conditions.[116] The rapid gelation of the T6CC/cadaverine formulation at 50 °C in ∼5.5 min confirms the higher reactivity of six-membered rings *vs.* five-membered cyclic carbonates, as no gelation is observed in the comparative TMPTC/cadaverine system even after 3 hours. Then, still adopting a shorter sequential curing at 50 °C for 4 h followed by a post-treatment at 120 °C for 2 h, homogeneous high-density PHU foams with diverse material properties have been manufactured from T6CC and various diamines (cadaverine, *m*-XDA or IPDA) using PMH (5 mol% *vs*. amine). The rigid foam made from IPDA ($T_g$ = 27 °C) has the largest pore size of 1.35 ± 0.32 mm and the lowest density of 170 kg m$^{-3}$. The foam density increases with cadaverine (350 kg m$^{-3}$) and *m*-XDA (530 kg m$^{-3}$) while cell sizes reduce to 0.42 ± 0.19 mm and 0.21 ± 0.07 mm, respectively. Both foams display $T_g$ values below r.T. ($T_g$ = 7 and 15 °C), making them flexible. The authors correlated the morpho-structural properties of the foams to the reactivity of the diamines. Unlike the formulation made from IPDA ($T_{gel}$ = 17 min), the fast gelation PHUs based on cadaverine ($T_{gel}$ = 4 min) and *m*-XDA ($T_{gel}$ = 7 min) limit material expansion upon gas release, leading to highly dense foams of smaller cell sizes. PMH has been further utilized for the fabrication of biobased PHU foams by mixing cyclocarbonated lignin with a commercial fatty-acid based dimer diamine (Priamine) as precursors.[117,118] The TBD catalyst and DMSO were to speed up the curing and facilitate the compatibilization of the formulation components, respectively (Fig. 6B). The foaming is initiated by the addition of Momentive (1.5 to 3% in volume) and the curing of the reactive formulation at 150 °C for 12 h. Rigid foams with densities of 241–337 kg m$^{-3}$ and a high $T_g$ of ∼100 °C have been produced. The concept has been recently extended to the preparation of low-density (<100 kg m$^{-3}$) flexible NIPU foams ($T_g$ around −15 °C to −18 °C) containing 17.4 to 35.6% of lignin.[119] A simple adaptation of these works enabled the fabrication of lignin-based nonisocyanate polyurethane/silver nanoparticle composite foams which exhibit antimicrobial properties (cf Section 5).[120]

Slightly different in concept is the utilization of PMH to produce thermosetting foams from (aminotelechelic) NIPU oligomers and polyepoxide crosslinkers (Fig. 6D). This strategy is exemplified by Valette *et al.*, who adapted their previous formulations from physical blowing of NIPUs, by simply replacing water, ethanol or water/ethanol mixtures as a physical blowing agent (*cf.* Section 2.1) with reactive PMH.[121] Foaming was realized at 100 °C for 30 minutes and the authors found

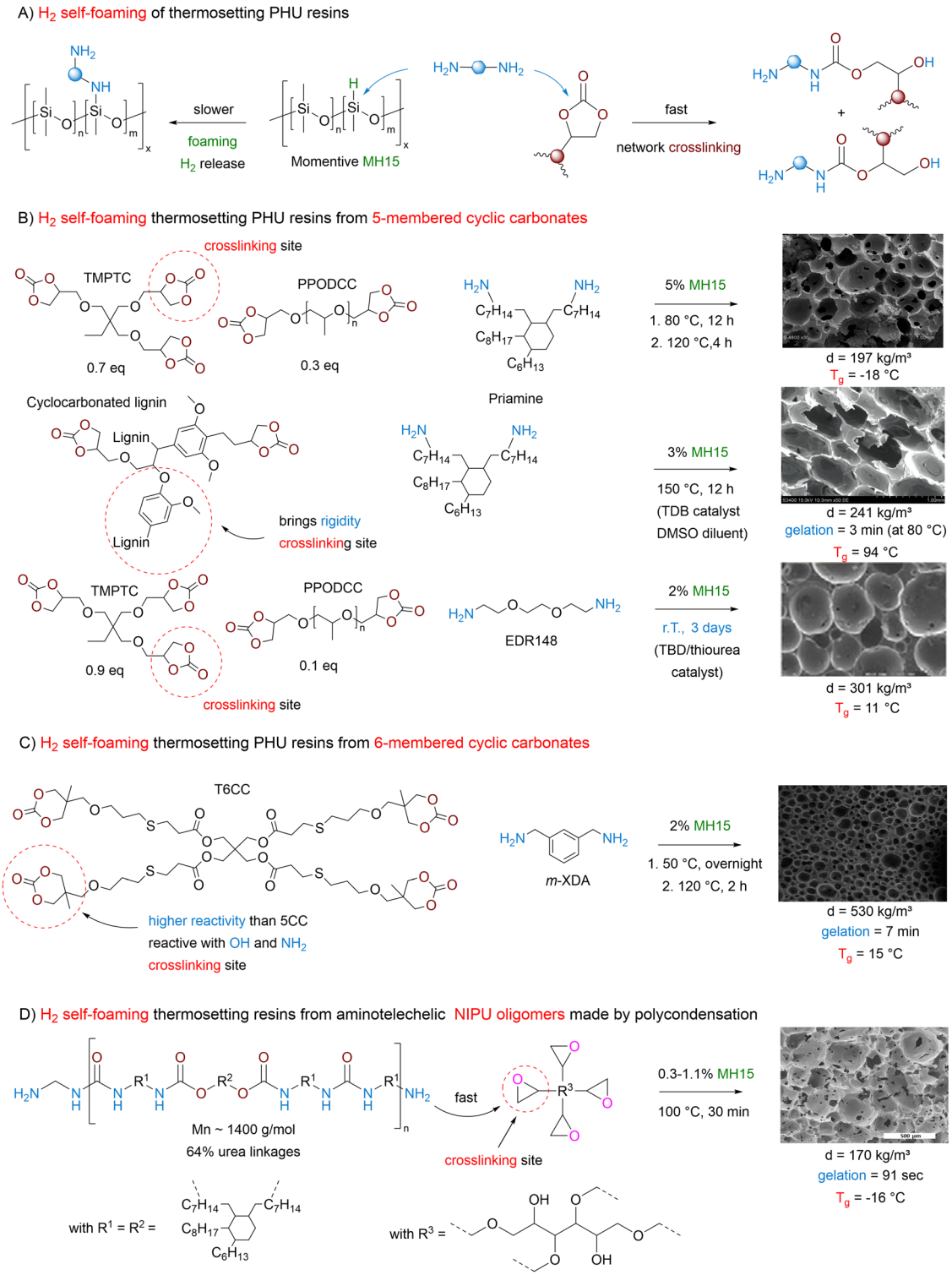


**Fig. 6** $H_2$ self-foaming of NIPUs. (A) Foaming mechanism; (B) thermosetting PHU foams produced from 5-membered cyclic carbonates; (C) thermosetting PHU foams produced from 6-membered cyclic carbonates; (D) thermosetting foams produced from NIPU oligomers synthesized by polycondensation. SEM pictures reproduced (1) from ref. 114 with permission from Elsevier. Copyright © 2015, Elsevier Ltd; (2) from ref. 118 with permission from the Royal Society of Chemistry. Copyright © 2020, Royal Society of Chemistry Publisher; (3) from ref. 115 with permission from Elsevier. Copyright © 2016, Elsevier Ltd; (4) from ref. 116 with permission from Elsevier. Copyright © 2022, Elsevier Ltd; (5) from ref. 121 with permission from Elsevier. Copyright © 2022, Elsevier Ltd.

that a 0.7% loading of PMH is optimal to fabricate foams with the lowest density (160 kg $m^{-3}$), having open cells with a size of 430 ± 210 μm. Based on rheology experiments, the amine/epoxide reaction is fast and allows for gelation in just 1.5 min. Foams can also be produced from r.T. reactive formulations, but curing requires a longer time of 14 h. All foams display a negative $T_g$ value ranging from −28 °C to −10 °C in line with the flexible nature of these materials. Ahmad *et al.* also reported a similar strategy by curing foam formulations made of PMH (5 wt% *vs.* amine), amine-terminated hydroxyurethane oligomers based on castor oil and ethylene diamine, HMDA or diethylene triamine and epoxy resin (structure not specified, EEW ∼190 g $eq^{-1}$). Foams with densities of 155 to 235 kg $m^{-3}$, open-cell morphology with cell sizes of 115 to 142 μm and $T_g$ values of 28–35 °C have been produced at 90 °C in 1 h. As a trend, a rise in the epoxy content within the formulation densifies the NIPU foams, in line with a higher crosslinking density/rate of the network that limits its expansion.

### 3.5.2. $CO_2$ self-blown foams

*3.5.2.1. From five-membered cyclic carbonates.* North has conceptualized the first dual utilization of 5-membered cyclic carbonates (5CC) as both a monomer for the construction of PHUs and a source of $CO_2$ to create pores within the matrix. In his system, the decarboxylation follows in cascade the aminolysis of a specific sorbitol-derived bis-carbonate with a fused ring structure.[122] The ring-opening of the 5CC moieties delivers the two usual β-hydroxyurethane regioisomers. The one with primary alcohols then participates in an intramolecular secondary cyclization with the adjacent unreacted carbonate ring, resulting in the formation of an isosorbide-like structure and the release of $CO_2$ (Scheme 4). When selecting cadaverine or HMDA as comonomers, porous semi-crystalline linear NIPUs ($T_g$ of −31 and −6 °C, $T_m$ of 190 and 180 °C, respectively) were formed in 20 h at 100 °C. Unfortunately, the authors did not evaluate or describe the foam's morphology nor characteristics.

*Thiol-induced foaming.* North's findings highlight the ambident electrophilic character of 5CCs that can be rationalized by the hard and soft acid base (HSBA) theory of Pearson.[123–127] Five-membered cyclic carbonates with a low substitution degree (like ethylene or propylene carbonates) feature two electrophilic sites, *i.e.*, a hard carbonyl and a soft methylene carbon (Scheme 5). By playing with the hard or soft nature of the nucleophiles, it is possible to guide chemo- and regioselective aminolysis and decarboxylation reactions. Hard amine nucleophiles undergo rapid acylation *via* carbonyl attack, while soft thiol nucleophiles engage in slower *S*-alkylation through methylene attack.[128] This second reaction, forming thioethers, triggers *in situ* $CO_2$ release *via* spontaneous decomposition of the unstable carbonic acid intermediate.

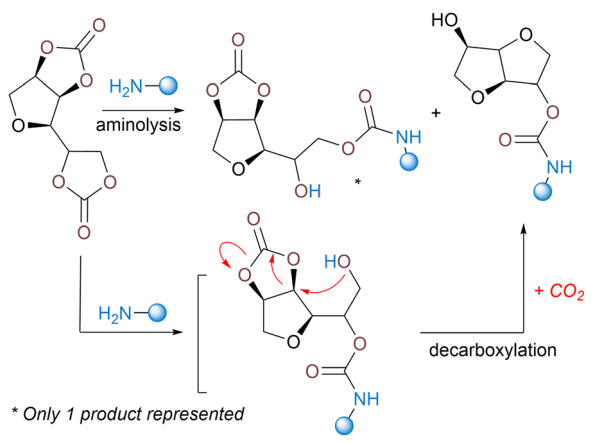


Scheme 4 North's intramolecular decarboxylation concept.

Following these considerations, Detrembleur *et al.* expanded the field of $CO_2$ self-blowing poly(hydroxyurethane)s to diverse formulations (Fig. 7).[128] By mixing stoichiometric amounts of complementary reactive groups found in TMPTC, diamine (jeffamine, *m*-XDA or HMDA) and an aliphatic dithiol ((2,2′(ethylenedioxy)diethanethiol) (EDT)), uniform open-cell foams with densities of 166–320 kg $m^{-3}$ and cell sizes of 0.25–0.98 mm have been fabricated (Fig. 7A). The presence of thioether linkages within the network induces chain mobility, resulting in flexible and resilient foams of low $T_g$ values between 2 and 24.6 °C. In this multi-step foaming protocol, the catalyst plays a primordial role in regulating aminolysis and decarboxylation. While aminolysis proceeds even without a catalyst, *S*-alkylation of thiols requires it. Besides, the reactivity of *S*-nucleophiles is influenced by a balance between acidity and sulfur electron delocalization.[129] Aromatic thiols are more reactive than their aliphatic counterparts and a low basicity organobase, such as $NEt_3$ or the diamine monomers used to fabricate NIPU foams, promotes *S*-alkylation.[130] With much less reactive aliphatic thiols, only nitrogen superbases (DBU, DBN, or TBD) are effective, significantly enhancing the $CO_2$ delivery while also allowing for moderate acceleration in hydroxyurethane formation.[128,131,132] As a result, both reactions occur simultaneously but at different rates, with aminolysis being slightly faster than *S*-alkylation. This difference in thiol reactivity is demonstrated by comparative foaming experiments from Thiol/TMPTC/*m*-XDA formulations ($T$ = 100 °C, $t$ = 3 h, 5 mol% DBU *vs.* cyclic carbonate). The formulation made of the aliphatic thiol (EDT) exhibits a delayed foam expansion – initiated after 30 min – compared to those with aromatic thiols, such as bismuthiol (20 min) or 4,4′-thiobisbenzenethiol (10 min) (Fig. 7B).[130] Unlike the foam made from EDT that is flexible ($T_g$ = 8 °C) and high in density (355 kg $m^{-3}$), those made from aromatic thiols are less dense (203–309 kg $m^{-3}$) and more rigid ($T_g$ of 30–41 °C). Enhancing the thiol functionality of the blowing agent has minimal impact on the morpho-structural characteristics of the foams but significantly improves their thermo-mechanical properties through additional crosslink formation.[133] As demonstrated by Torkelson *et al.*, processing fatty acid-derived biscyclic carbonate (Erisys® GS-120)/Jeffamine® T-403 formulations with di- (EDT), tri- (trimethylolpropane tris(3-mercaptopropionate) (TMPTSH) or tetra-functional pentaerythritol tetrakis(3-mercaptopropionate)thiols delivers foams of similar densities of 240–270 kg $m^{-3}$, cell size averaging from 0.25 to 0.31 mm, cell density of 42–51 × $10^3$ cells per $cm^3$ and low content of open cells for high density materials ($d$ = 530 kg $m^{-3}$). All foams are flexible and highly resilient, with $T_g$s evolving from −30 to −23 °C with the increase of thiol

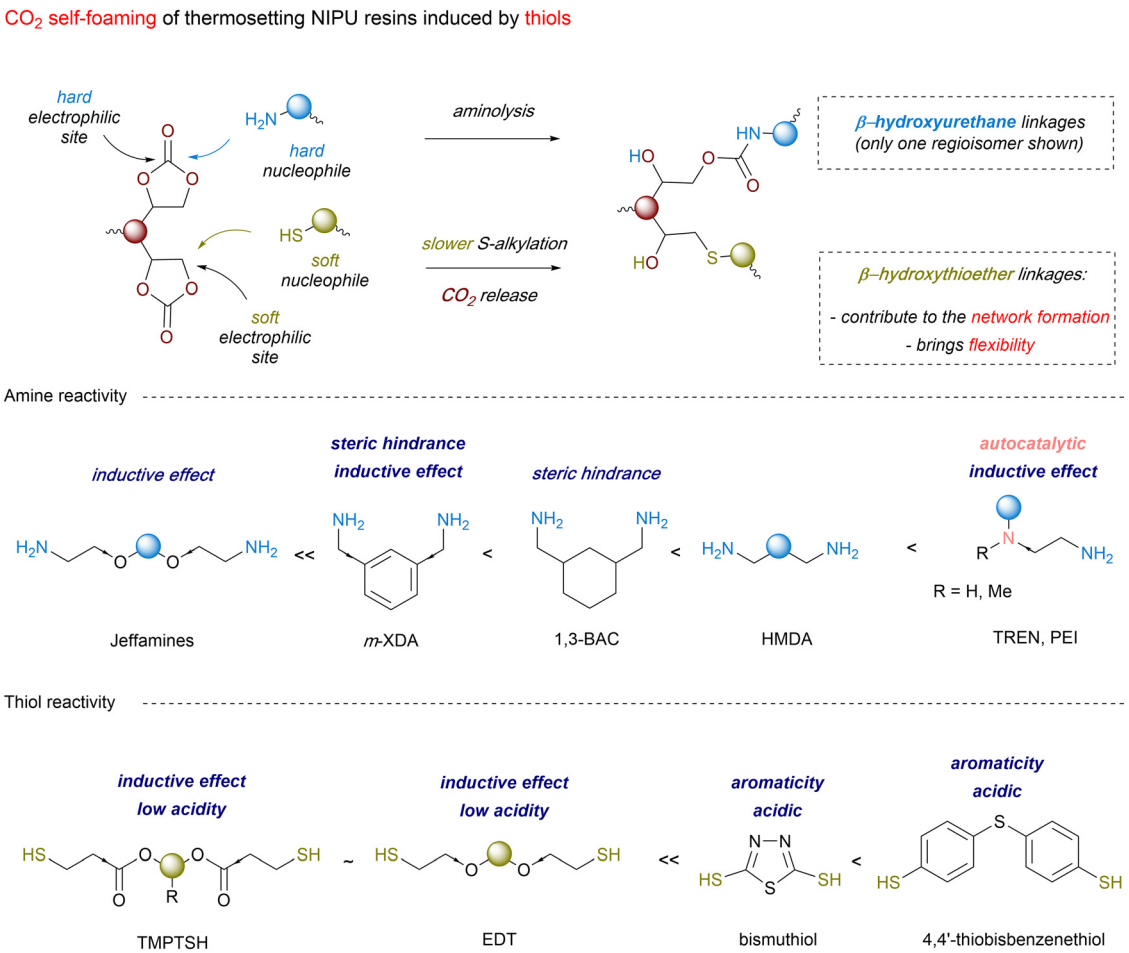


Scheme 5 $CO_2$ self-foaming of thermosetting PHU resin induced by a thiol and influence of the amine and thiol structure on the reactivity.

functionality.[133] This is consistent with a higher crosslinking density restricting chain mobility within the network. Additionally, tri- and tetra-functional thiols lead to foams four- to six-fold more resistant to deformation than those obtained from the EDT blowing agent.

To mitigate the unpleasant smell of thiols, thiols masked under a "dormant" form, being either a thiolactone[134] or a dithiocarbonate,[135] have been proposed as blowing agents (Fig. 8). These heterocycles are more reactive than cyclic carbonates. They undergo rapid ring-opening by amines, creating *in situ* a thiol during the initial stage of the process (Fig. 8A). The foam formation results from the alignment of three divergent and regioselective domino reactions, *i.e.*, the fast thiol generation by aminolysis of the masked precursor, followed by the slower PHU network construction and its blowing *via* *S*-alkylation. For stoichiometric TMPTC/Jeffamine EDR148 formulations, adding 25–30 mol% of thiolactone or dithiocarbonate (*vs.* cyclic carbonate) yields open cells and flexible foams of 167 kg $m^{-3}$ (in 5 h at 80 °C) or 364 kg $m^{-3}$ (in 24 h at 90 °C), respectively (Fig. 8B). Unlike formulations made of dithiocarbonates, DBU is optional with thiolactones. However, the absence of a catalyst leads to foams of higher density (442 kg $m^{-3}$). This trend extends to other formulations replacing EDR148 by *m*-XDA, where foam density increases from 185 kg $m^{-3}$ with DBU to 310 kg $m^{-3}$ without a catalyst. Due to the inherent properties of dithiocarbonates, the resulting NIPU foams exhibit two $T_g$'s, indicative of a two-phase material.[135] Since dithiocarbonates copolymerize with diamines and are more reactive than analogous five-membered cyclic carbonates, it is postulated that low $T_g$ (−45 to −31 °C) polythiourethane segments form early in the curing process. Subsequent chain extension and gelation through polyaddition with TMPTC create PHU sequences with a higher $T_g$ of 11 to 19 °C.

Most previous protocols require a pre-curing step to adjust viscosity and/or prolonged foaming even at high temperatures to achieve an optimal balance between viscosity increase, gelation and foam formation. To shorten the foam fabrication, strategies such as decoupling gelation from foaming or pre-heating the foam components have been proposed. The first solution exploits oscillatory shear rheology to monitor at various temperatures the evolution of the shear loss ($G''$) and shear storage ($G'$) moduli of a non-stoichiometric reactive PHU foam formulation (without a thiol) and maintain tan $\delta$ values (tan $\delta = G''/G'$) above 1, ideally from 2 to 4 (Fig. 7A).[131,136] According to Torkelson, this value range supports uniform bubble growth in formulations made of TMPTC/Jeffamine EDR148[131] or cashew

 

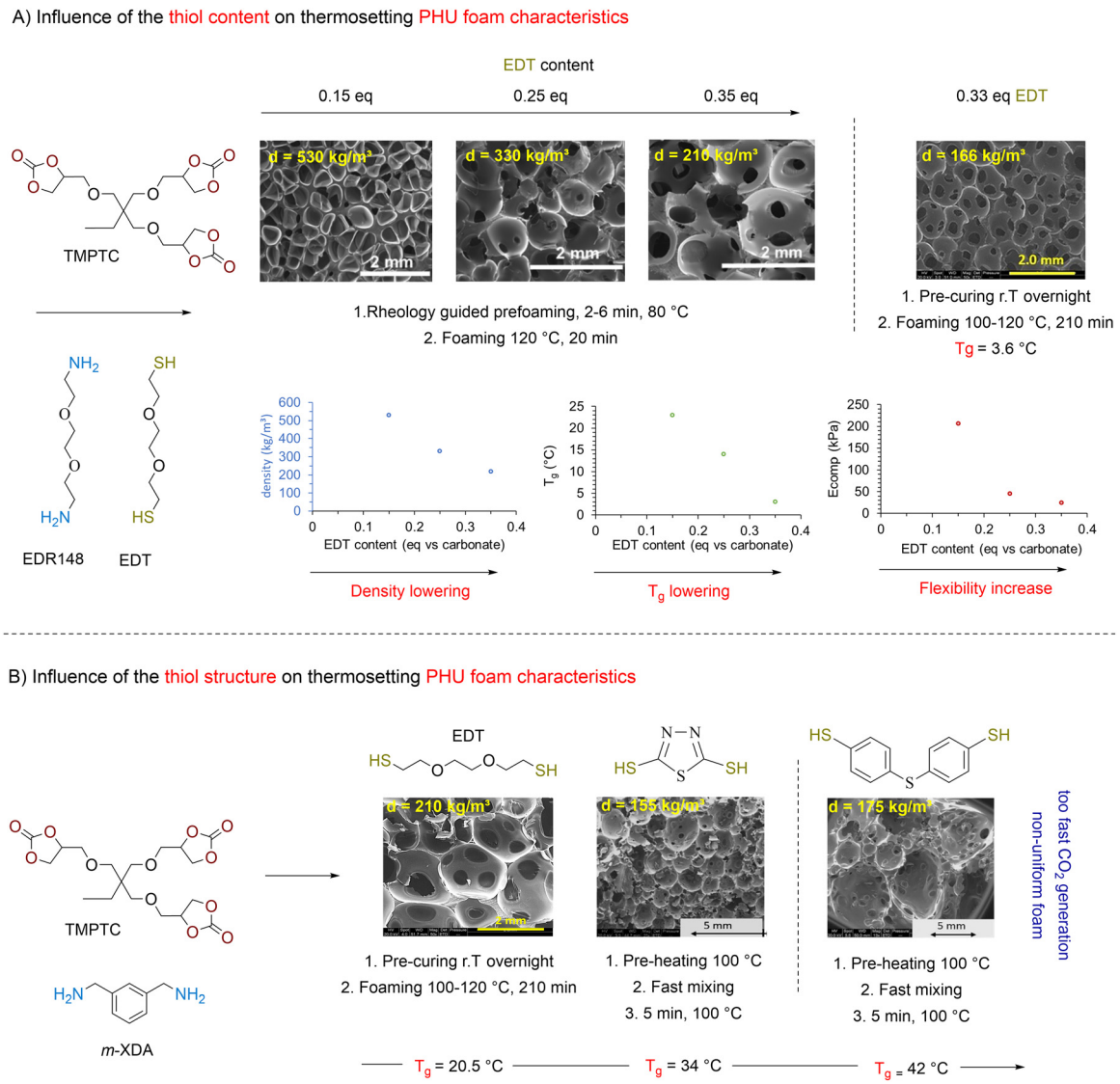


Fig. 7 Thiol-induced foaming of thermosetting PHU resins. (A) Influence of the thiol content on the morpho-structural and mechanical properties of the foams; (B) influence of the thiol structure (aliphatic *vs*. aromatic) on the morphologies and thermal properties of the foams. SEM pictures reproduced (1) from ref. 131 with permission from Elsevier. Copyright © 2023, Elsevier Ltd; (2) from ref. 128 with permission from John Wiley and Sons. Copyright © 2020, Wiley-VCH Verlag GmbH & Co. KGaA, Weinheim; (3) from ref. 130 with permission from the Royal Society of Chemistry. Copyright © 2024, Royal Society of Chemistry Publisher.

nutshell-based cyclic carbonate/Jeffamine T-403.[136] Then, since the matrix is not yet crosslinked, a thiol blowing agent (EDT) is added in the correct proportion to reach stoichiometry in the reactive group while providing sufficient viscosity for effective foaming. The formulation is then cured at elevated temperature (120 °C), forming foams within 20 to 120 min. Interestingly, materials produced using this accelerating foaming method exhibit morphologies and thermal properties comparable to those obtained with the original slower processes.

The second solution involves preheating all foam components separately at 100 °C,[130] before mixing them at this temperature. For a stoichiometric TMPTC/*m*-XDA/EDT formulation, the foam expansion begins after 2 min in the presence of DBU. When aromatic thiols replace EDT, the expansion occurs significantly faster, within 15 sec with bismuthiol and instantaneously with 4,4′-thiobisbenzenethiol even in the absence of a catalyst. If gas generation is fast enough to induce a rapid rise of the foam in 2 to 10 min, a curing of 30 min is required to consume carbonate moieties and create sufficient crosslinked nodes. All foams are uniform with open-cells, with those made from aromatic thiols being less dense (166–185 kg $m^{-3}$) than those derived from EDT (372 kg $m^{-3}$). The foam formation is shortened by increasing the amine content. For example, in catalyst-free 1/1/0.25 TMPTC/*m*-XDA/aromatic thiol formulations, non-stoichiometric conditions – where amine and thiol reactive groups are in excess relative to cyclic carbonates – yield highly crosslinked foams (155–156 kg $m^{-3}$) that can be demolded in just 5 minutes. The versatility of this approach is further exemplified by substituting *m*-XDA with

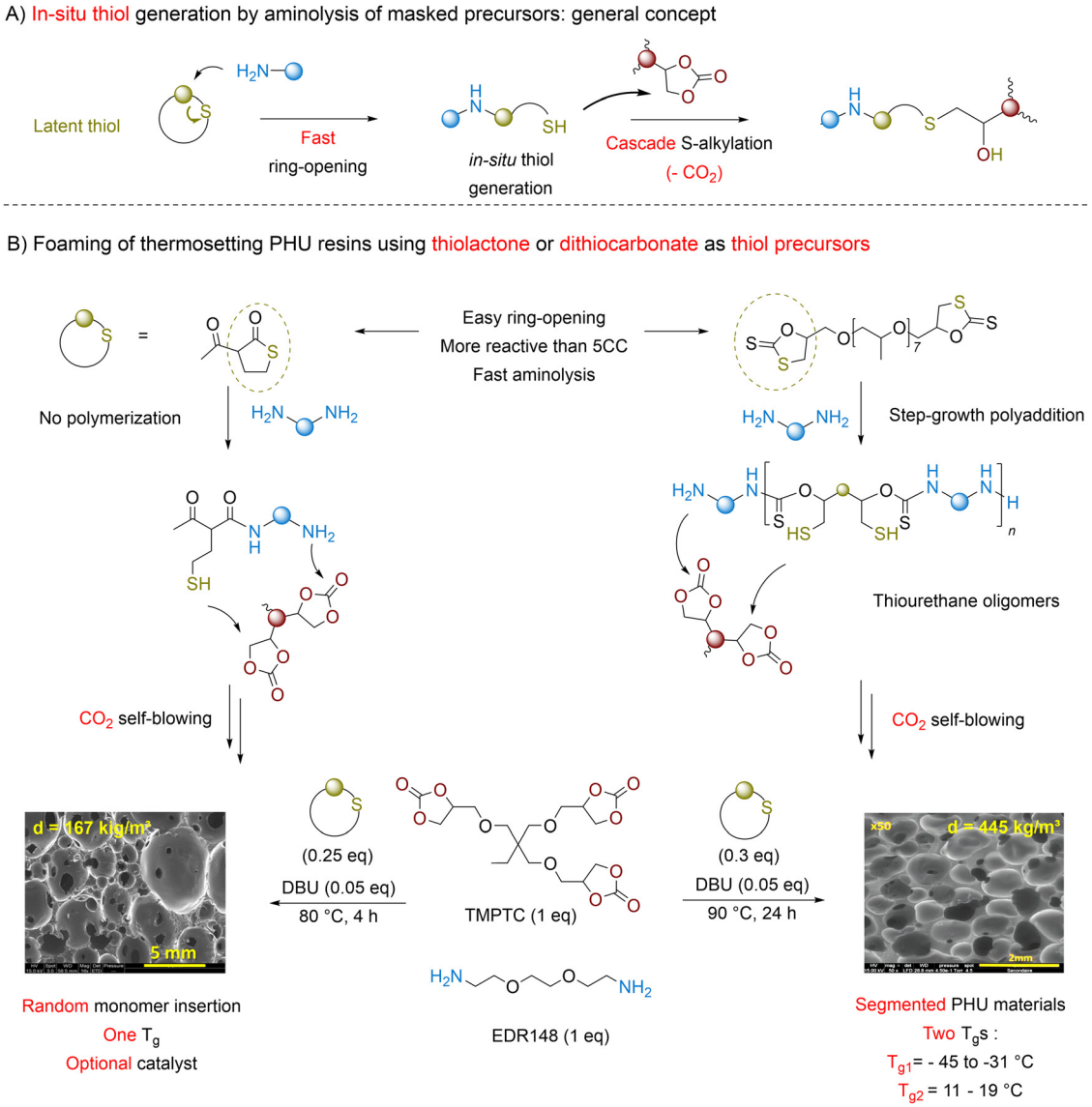


Fig. 8 $CO_2$ self-foaming of PHU thermosetting resins using masked thiols. (A) General domino concept; (B) key differences in PHU foaming using blowing agents masked under the form of a thiolactone or a dithiocarbonate (exemplified for a TMPTC/EDR148 formulation). SEM pictures reproduced from (1) ref. 134 with permission from the American Chemical Society. Copyright © 2022, American Chemical Society; (2) from ref. 135 with permission from John Wiley and Sons. Copyright © 2022, Wiley-VCH Verlag GmbH & Co. KGaA, Weinheim.

Jeffamine EDR148, which results in a homogeneous, low-density foam (155 kg $m^{-3}$).

*Water-induced foaming.* Five-membered cyclic carbonates are less sensitive to hydrolysis than isocyanates. Their decomposition into the corresponding vicinal diol and $CO_2$ occurs slowly and typically requires elevated temperature, a strongly alkaline medium and an excess of water.[137–139] A key distinction from conventional polyurethane (PU) foaming is that the vicinal diol formed during hydrolysis is unreactive toward both amines and cyclic carbonates. As a result, it does not participate in the crosslinking process of the PHU (Fig. 9A).

Thus, achieving self-foaming in PHU systems using water requires precise control over both aminolysis and decarboxylation by carefully adjusting the formulation composition and stoichiometry, water content, temperature (80–100 °C), and catalyst (*e.g.*, DBU or KOH).[140] Following these considerations, PHU foams have been produced by mixing a non-stoichiometric ratio of reactive amine and cyclic carbonate groups, with a fixed [$NH_2$]/[5CC] ratio of 0.75. This ensures that (theoretically) 25% of the cyclic carbonates serve as sacrificial groups to generate $CO_2$ through base-catalyzed hydrolysis. As illustrated for a TMPTC/*m*-XDA formulation using DBU as a catalyst (Fig. 9B), the morpho-structural and thermo-mechanical properties of the foams vary with the processing temperature and the water content. At 100 °C, a low-density foam (153 kg $m^{-3}$) with large open cells averaging 2.3 mm is produced in 3 h using 1 eq. of water *vs.* sacrificial cyclic carbonates. The addition of hydrotalcite as a

 

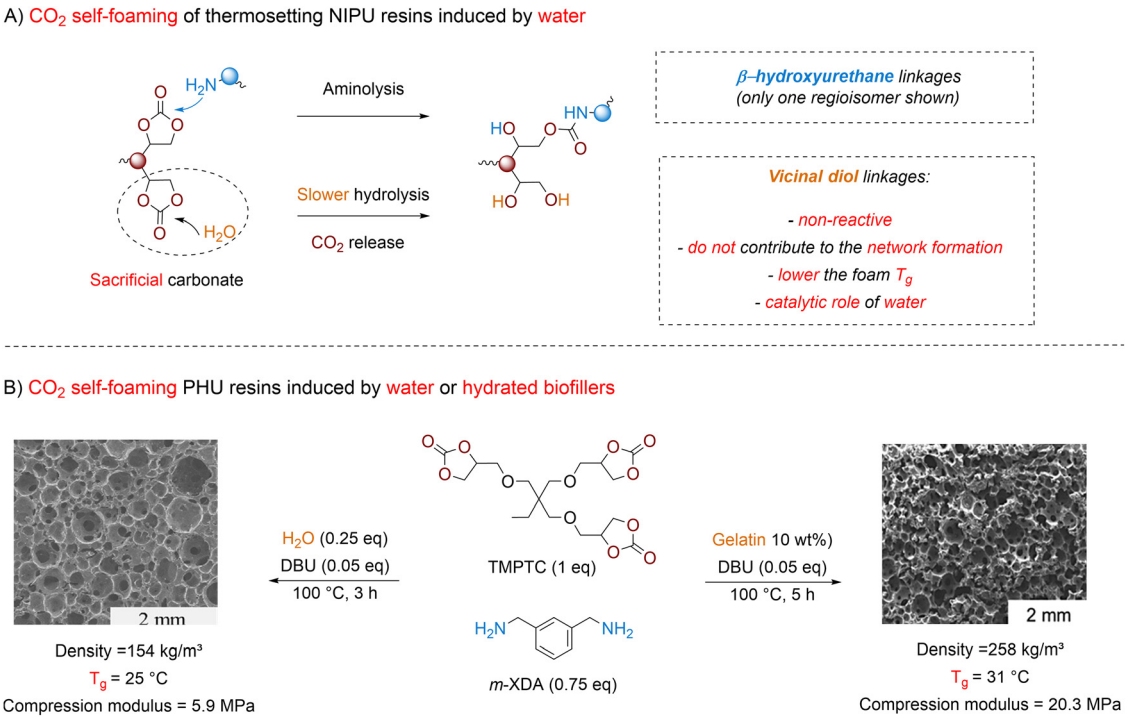


Fig. 9 Water-induced foaming of thermosetting PHU resins. (A) General concept; (B) examples of PHU foams produced using water or a hydrated protein as a blowing agent. SEM pictures reproduced from (1) ref. 140 with permission from John Wiley and Sons. Copyright © 2022, Wiley-VCH Verlag GmbH & Co. KGaA, Weinheim and (2) ref. 142 with permission from the Royal Society of Chemistry. Copyright © 2024, Royal Society of Chemistry Publisher.

nucleation agent and viscosity modifier within the formulation improves the foam uniformity and decreases the cell size to 390 μm without impacting the density. Lowering the temperature to 80 °C slows down the $CO_2$ release and necessitates prolonged curing times of 5 h to prevent foam collapse. This foaming procedure delivers twice denser foam (327–366 kg $m^{-3}$). The slower hydrolysis can be compensated by a fourfold increase in the water amount (*vs.* sacrificial carbonates), yielding foams with lower densities (179 kg $m^{-3}$) and more uniform open cells averaging 0.54 mm. In this foaming strategy, the extent of hydrolysis dictates the amount of vicinal diol produced, which in turn affects the PHU network crosslinking density. This is evidenced by the gel content values ranging from 86% to 95%. As a result of higher chain mobility, $T_g$ values drop from 25 °C to 8 °C when the water content increases from 1 to 4 equivalents at foaming temperatures of 100 °C and 80 °C, respectively. Additionally, the presence of vicinal diol groups induces strong hydroplasticization under ambient humidity. Drying the PHU foams significantly raises their $T_g$'s by 25–40 °C. Although foam density and cell size vary across foaming conditions, their mechanical performance also differs greatly due to varying degrees of crosslinking. For example, the compression modulus ranges from 6.66 MPa for a foam made at 100 °C with 1 eq. of water to just 0.149 MPa for a foam made at 80 °C with excess water. The versatility of the water-induced foaming approach, also applicable to PHU foaming in close molds, is proven by the fabrication of uniform low-density materials (226–480 kg $m^{-3}$) from various formulations, either by replacing *m*-XDA with jeffamine EDR 148 or HMDA, or by valorizing other carbonates (neopentyl or PEG diglycidyl carbonate) and amine (TREN) precursors. Similar to the thiol system, pre-heating the components (*e.g.*, TMPTC and Jeffamine EDR 148) to 100 °C before curing accelerates the foam fabrication in just 30 min with no impact on their morpho-structural and thermal properties compared to similar materials produced *via* the slow foaming procedure. Further improvements use TREN as a reactive curing accelerator. This polyamine has an "aminoethyl amine"-type structure with highly reactive amine groups. When mixed at 30% with another polyamine, it causes very rapid gelation of the network, preventing foam collapse. This results in a stable and uniform low-density material (193–209 kg $m^{-3}$) within only 5 min when formulations are pre-heated to 100 °C.[141]

Interestingly, bio-based fillers derived from biomass waste streams such as proteins (gelatin, keratin, zein), lignin, cellulose or chitosan play a dual role in foam fabrication, acting simultaneously as a "reservoir" releasing water during foaming due to their inherent hydrophilicity and a biofiller improving cell nucleation and initial viscosity.[142] Even a 1 wt% content of the biofiller is sufficient to obtain uniform open-cell foams with medium density between 240 and 320 kg $m^{-3}$ (Fig. 9B). This open-cell porosity arises from the incorporation of bio-based fillers. These solid particles act as nucleation sites at the initial stage of the foaming. They typically increase the number of cells, resulting in thinner and mechanically weaker cell walls. In addition, these rigid particles generate local stress during bubble growth because they can't accommodate the deformation of the

expanding cell membranes, which ultimately promotes cell-wall rupture and the formation of open-cell foams. Well-crosslinked foams with a homogeneous porous structure were obtained with bio-filler contents of up to 30 wt%, demonstrating their potential to reduce production costs, as the bio-fillers originate from low-value biomass waste.

*Room temperature-induced fast foaming.* Conceptually, the foaming of PU benefits from the high exothermicity of the isocyanate/polyol reaction. The heat generated *in situ* creates a "snowball effect" that rapidly raises the temperature of the foam components from r.T. to far above 100 °C (generally >120–180 °C), further accelerating all reactions at play. This promotes the fast network formation within minutes while simultaneously delivering $CO_2$ as the blowing agent. Unlike conventional PUs, the aminolysis of cyclic carbonates only generates a slight exotherm of ~65 °C below the threshold of ~100 °C. To kick-start the foaming from r.T. formulations, an extra "heat boost" is needed. Epoxide[130,141,143] or exovinylene cyclic carbonate[144] (αCC) additives proved to be effective by triggering additional heat generation (Fig. 10).

*Epoxide additives.* The epoxy-amine reaction is recognized for its high exothermicity related to the strain release of the cyclic structure.[145,146] In epoxy resins, it is common to witness an induction period during the curing process with little changes in viscoelastic properties, before a sudden exotherm and a fast increase in viscosity. It has been shown to result from an autocatalytic mechanism relying on the slow appearance of the first hydroxyl groups that further catalyze the network formation. This effect is further intensified by the rapid increase in viscosity, which inhibits efficient heat dissipation. To control the exothermicity during foaming, the hybridization of PHU chemistry through the addition of epoxides has proven effective. In a water-induced foaming process (Fig. 10A), partially substituting 25% of TMPTC with its epoxy precursor (TMPTE) in a TMPCT/*m*-XDA/TREN formulation is sufficient to elevate the temperature from r.T. to over 110 °C, producing a uniform, open-cell, medium-density foam (<300 kg $m^{-3}$) within 3 min.[141] Mechanistically, the tricomponent *m*-XDA/TMPTC/water reaction creates a first elevation of the temperature from r.T. to ~87 °C. This heat rise triggers in cascade the aminolysis of the epoxy additive, leading to a second exothermic event elevating the temperature within the foaming zone to >100 °C. As a trend, increasing the TMPTE content influences both the foam expansion and the material thermo-mechanical properties. Epoxy-rich compositions exhibit significantly higher exothermicity, with temperatures even reaching 180 °C when TMPTC is replaced by 3 eq. of TMPTE. However, the exotherm is delayed, and foam formation slows down with increasing TMPTE content (*e.g.*, 6 min with 3 eq. of TMPTE). Beyond 0.5 eq. of TMPTE, the foam density plateaus around 150 kg $m^{-3}$, likely due to the higher degree of crosslinking (Fig. 10C). Lower epoxide content (≤0.5 eq. *vs.* TMPTC) produces foams with $T_g$'s (~20 °C) and compression moduli (0.5–0.6 MPa) similar to pure expanded PHUs. Conversely, increasing the epoxide concentration leads to materials with epoxy resin-like properties, exhibiting higher $T_g$'s of 35–40 °C and enhanced stiffness ($E$ = 3.7–4.7 MPa). Further research underscores the role of epoxide structure in the exothermic behavior of the foaming process. With aromatic epoxide (DER332), the presence of the electron-withdrawing group nearby the oxirane ring lowers the activation barrier required for its aminolysis, thereby increasing its reactivity compared to aliphatic epoxides (*e.g.*, neopentyl glycol diglycidyl ether).[143] As a result, formulations containing aromatic epoxides exhibit higher exothermic peaks than their aliphatic counterparts. The use of epoxide with aromatic moieties also introduces rigidity into the NIPU chains, further increasing the $T_g$ of the resulting foams and improving their mechanical performances.

Adding epoxy additives to initiate the fast r.T. foaming of PHUs using thiol blowing agents is also applicable (Fig. 10B).[130] However, this strategy necessitates the proper selection of the foam components and the careful adjustment of their composition. For successful foaming, it is essential to use epoxy/cyclic carbonate blends in a 50/50 molar ratio and acidic thiols such as bismuthiol and 4,4-thiobisbenzothiol. Deciphering the foaming mechanism highlights a complex interplay of multiple cascades and parallel reactions. In the initial stage of the process, a quick acid–base reaction takes place between the thiol and the amine, yet protecting the thiol in the form of a non-reactive salt while simultaneously releasing heat. The rise in temperature triggers the aminolysis of the cyclic carbonate and/or the epoxide. When reaching 80–100 °C in 1–2 min, the thiol-amine salt begins to decompose, releasing the reactive thiol. This species engages in competitive decarboxylation of 5CCs, driving foam expansion, and click reaction with the remaining epoxide, helping to maintain an elevated temperature (up to 170 °C) to ensure efficient material curing and prevent foam collapse. The fine-tuning of the formulation enables precise control over the morphology and thermo-mechanical properties of the foams by simply varying the chemical structure of the epoxide and amine components. Uniform rigid foams of 312 kg $m^{-3}$, $T_g$'s of 49 °C and compression modulus of 81 MPa have been produced by employing TMPTC with bismuthiol, aromatic DER332 and *m*-XDA. In contrast, switching to aliphatic epoxides (*e.g.*, butanediol diglycidyl ether, BDGE) and (cyclo)aliphatic amines (such as Jeffamine EDR148 or 1,3-BAC) produces flexible to semi-rigid foams with densities of 227–400 kg $m^{-3}$, low $T_g$ values ranging from −17 to 24 °C, and compression moduli between 0.096 and 23.5 MPa.

*Exovinylene cyclic carbonate additives.* αCCs are five-membered heterocycles that can be efficiently synthesized from $CO_2$ and propargylic alcohols (Fig. 11).[144] Unlike conventional 5CCs, the presence of an exocyclic olefin moiety within the cyclic carbonate structure makes αCCs highly reactive toward *N*-, *O*-, or *S*-nucleophiles,[72,75,147,148] unlocking diverse chemical transformations. In particular, their aminolysis with primary amines yields 5-membered cyclic urethanes (hydroxy-oxazolidones) rapidly.[16,149–151] This reaction proceeds instantaneously at r.T., even without a catalyst, and is characterized by a significant exotherm. Leveraging these unique reactivity features in the

 

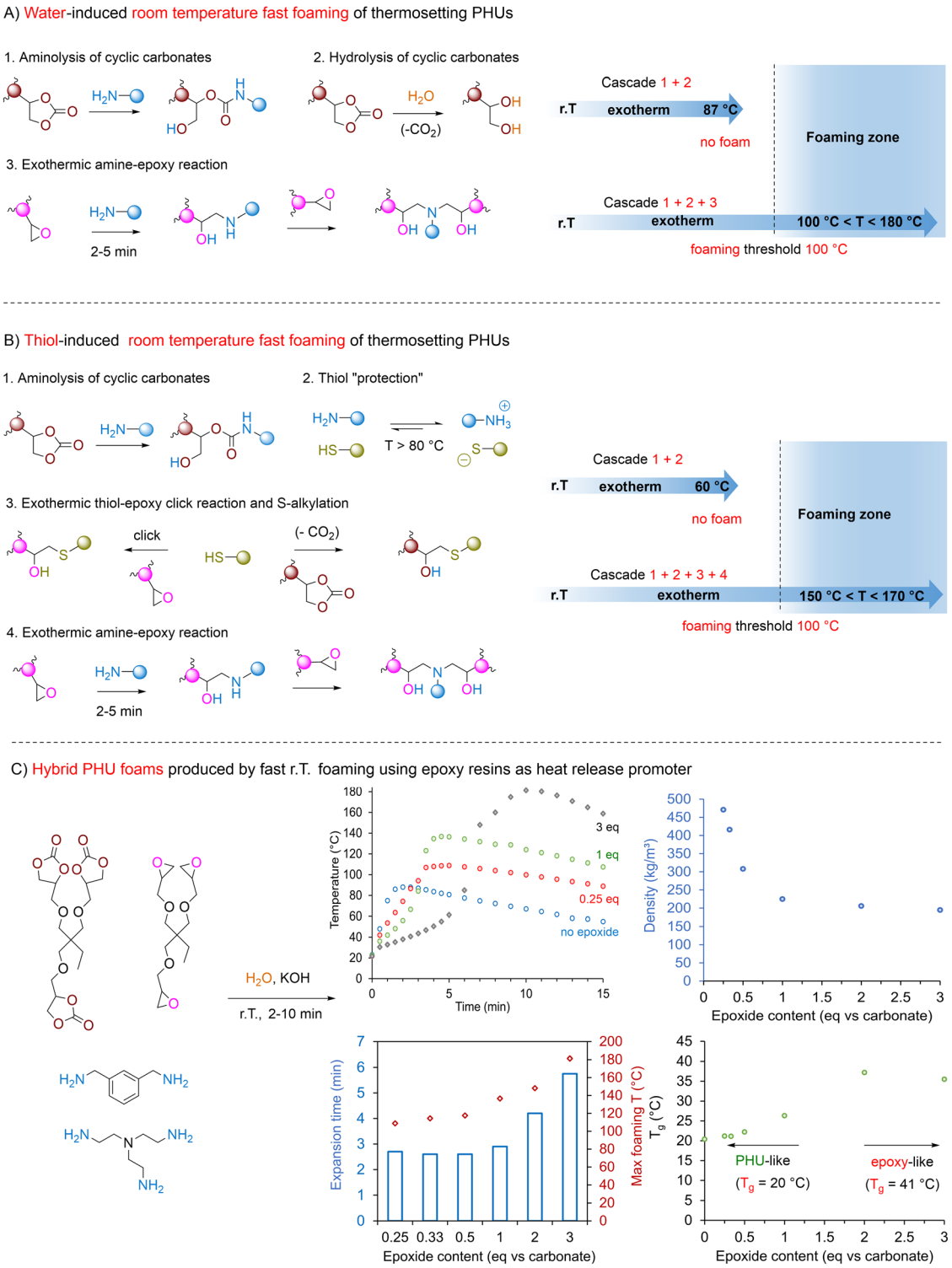


Fig. 10 Fast foaming of NIPUs from r.T. reactive formulations *via* cascade reactions with epoxides as heat release promoters. (A) Cascade reactions in water-induced self-blowing of PHUs; (B) cascade reactions in thiol-induced self-blowing of PHUs; (C) foaming parameters and properties of hybrid epoxy/PHU foams of various compositions produced by the water-induced fast foaming approach with an illustration of (i) the time evolution of the temperature with the epoxide content during foaming, (ii) the time for foam expansion and maximum temperature reached for various epoxide compositions, (iii) the evolution of the foam density with the epoxide content and (iv) the thermal characteristics of the hybrid PHU foams at various epoxide contents.

water-induced $CO_2$ self-foaming of cyclic carbonate/amine formulations allows raising the temperature to 110–130 °C within a few seconds by simply varying the αCC (4,4-dimethyl-5-methylene-1,3-dioxolan-2-one, DMACC) content *vs.* 5CC from 0.1 up to 0.3 eq. (Fig. 11A). However, both the aminolysis of αCC and the decarboxylation of 5CC can terminate NIPU chains, which reduces the crosslinking density of the networks and impacts the foam's morphology. To compensate for the adverse effects of these terminations and achieve an optimal balance between foam expansion and crosslinking, it is essential to use polyfunctional monomers with functionalities higher than two, such as TMPTC and TREN. For example, in a stoichiometric TMPTC/αCC/TREN formulation containing 0.15 eq. of water *vs.* TMPTC, decreasing the αCC content from 0.3 to 0.15 eq. increases the foam density from 173 to 323 kg $m^{-3}$ while no foam is produced below 0.15 eq. Besides, at a fixed αCC content of 0.25 eq. relative to TMPTC, foams with densities of 188–233 kg $m^{-3}$ are obtained and found uniform only when the water content is maintained between 10 and 15%. Substituting DMACC with sterically hindered αCC analogs (bearing cyclohexyl, phenyl, or isobutyl groups) does not significantly alter the exotherm or the foaming process. These analogs lead to the fabrication of homogeneous foams with slightly higher densities (~270–390 kg $m^{-3}$, Fig. 11B). Additionally, the choice of αCC influences the glass transition of the resulting materials, with values ranging between 28 and 38 °C. All foams display an open-cell morphology with a cell size averaging 85–180 μm.

*3.5.2.2. Amine–$CO_2$ adducts.* Taking inspiration from reversible non-aqueous $CO_2$–amine carbon capture technologies, Choong *et al.* have proposed carbamate salts as latent blowing agents for PHU self-foaming applications (Fig. 12A).[152] Alkylamines have a strong affinity for various electrophiles and act as a $CO_2$ acceptor, rapidly forming amine–$CO_2$ adducts even at r.T. Further addition of a nitrogen superbase markedly enhances the reactivity of amine sorbent with $CO_2$, allowing for the formation of amine–$CO_2$-superbase "mixed" (bi)carbamates.[153–155] Spontaneous $CO_2$ desorption and amine/superbase regeneration are generally triggered at high temperature, often exceeding 100 °C. In the quest for liquid polyamine–$CO_2$ adducts allowing for homogeneous mixing at r.T. with cyclic carbonate/amine formulations and tunable $CO_2$ release, Choong *et al.* identified triethylenetetramine (TETA) as a promising candidate.[152] In the absence of a nitrogen superbase, this polyamine absorbs 17.9% of $CO_2$, providing a viscous liquid TETA–$CO_2$ adduct (viscosity = 3500 mPa $s^{-1}$). Adding DBU or DBN not only enhanced the absorption rate of $CO_2$ but also allowed for higher $CO_2$ uptake of 27.6% and 60.4%, respectively. Furthermore, these superbases facilitate $CO_2$ desorption with desorption rate constants of 0.0021–0.0023 $h^{-1}$ at a low temperature of 60 °C compared to 0.009 $h^{-1}$ for the TETA–$CO_2$ adduct at 100 °C. Mixing of TETA–$CO_2$–DBN with two model cyclic carbonates substituted by an ester (M1) or an ether (M2) promotes hydroxyurethane formation (with high carbonate conversion of 93% for M1 and 68% for M2 after 2 h at 60 °C) and expedites $CO_2$ desorption. This is reflected in the increased desorption rate constant values of

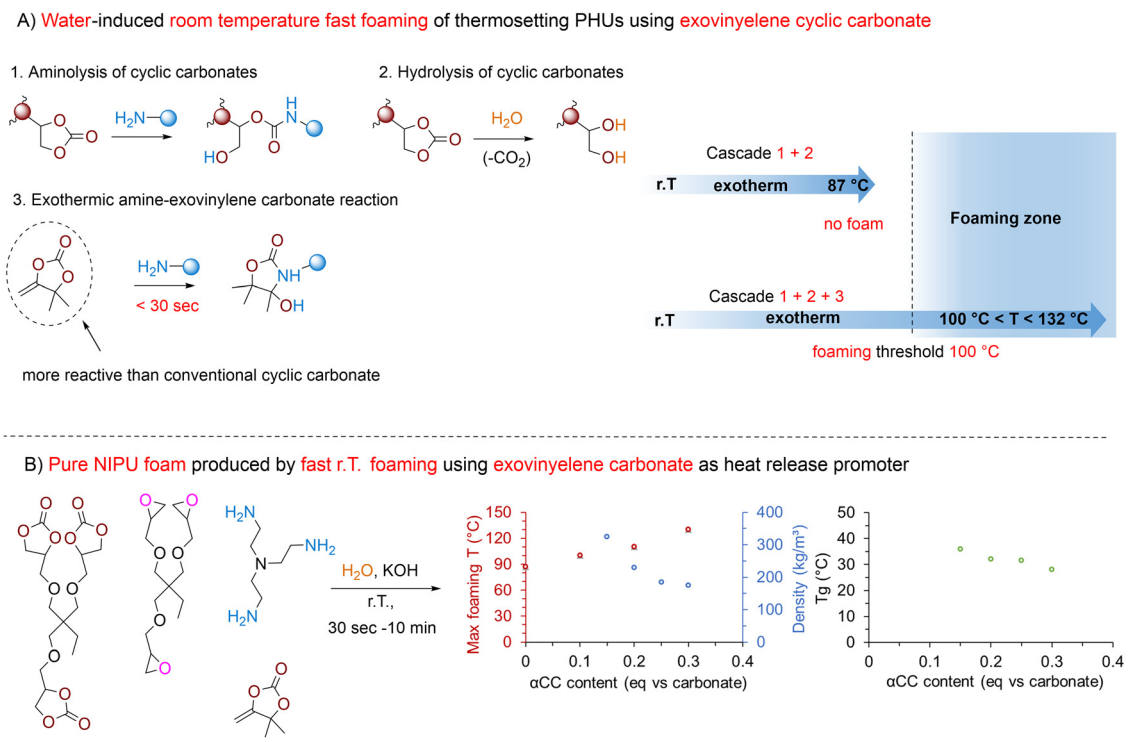


Fig. 11 Fast foaming of NIPUs from r.T. reactive formulations *via* cascade reactions with exovinylene cyclic carbonates as heat release promoters. (A) Cascade reactions in water-induced self-blowing of PHUs; (B) foaming parameters and properties of NIPU foams of various compositions produced by the water-induced fast foaming approach with an illustration of (i) maximum temperature reached for various αCC compositions and related foam densities, (ii) $T_g$ value evolution with the αCC content.

 

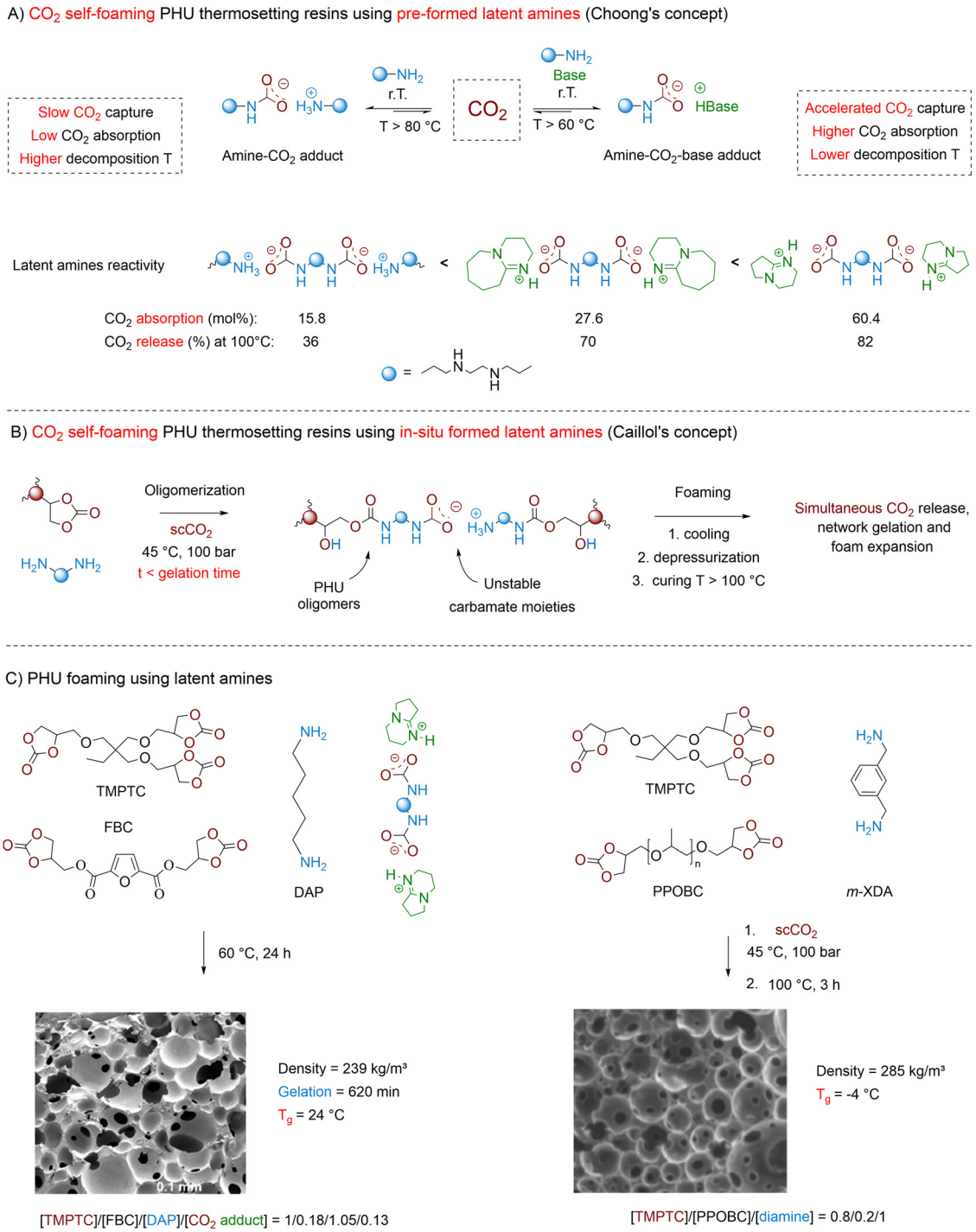


Fig. 12 Latent amine formation either *via* $CO_2$ capture (A) or the oligomerization approach (B) and their thermal decomposition. (C) $CO_2$ self-blown PHU foams produced from cyclic carbonates and latent amines or oligomeric PHU–carbamate adducts. SEM pictures reproduced from ref. 152 and 156 with permission from the American Chemical Society. Copyrights © 2023 and 2025, American Chemical Society.

$0.222\ h^{-1}$ and $0.132\ h^{-1}$ corresponding to $CO_2$ releases of 87% and 77% respectively for M1 and M2 after 24 h at 60 °C. Learning from these model experiments provides guidelines for the fabrication of $CO_2$ self-blowing PHUs using TETA–$CO_2$–DBN as the latent amine. To synchronize $CO_2$ desorption with PHU resin expansion, diamines (*e.g.*, 1,2-bis(2-aminoethoxy)ethane or 1,5-diaminopentane) have been cured at 60 °C for 24 h with a blend of TMPTC and a furan-based biscyclic carbonate (FBC) (80/20 molar ratio). Notably, using TMPTC alone resulted in unsatisfactory foaming due to rapid gelation outpacing $CO_2$ release. By analogy with M1, the ester groups within FBC enhance its reactivity against amines compared to the ether-substituted TMPTC, enabling good control over viscosity increase, gelation, and $CO_2$ release. The use of 13 mol% of TETA–$CO_2$–DBN *vs.* TMPTC leads to uniform open-cell foams

with densities of 203–239 kg $m^{-3}$ and a cell diameter of 232 ± 97 to 314 ± 116 μm (Fig. 12C). These foams exhibit flexibility, as reflected in their $T_g$ values between 16 °C and 24 °C. Reducing the TETA–$CO_2$–DBN content results in denser foamed materials ($d$ = 401 kg $m^{-3}$), while higher concentrations lead to rapid matrix expansion, collapse, and stabilization at 462 kg $m^{-3}$. Increasing the temperature accelerates $CO_2$ desorption, leading to non-homogeneous high-density foams (405 kg $m^{-3}$) with large pores of ~2 mm.

While elegant, Choong's concept is constrained by the limited availability of liquid polyamine–$CO_2$ adducts suitable for PHU foaming and by the utilization of a significant amount of organobases, which are often costly and/or toxic. To address these limitations, Caillol revisited the foaming of thermosetting PHUs through a sequential methodology (Fig. 12B).[156] In the first step, non-crosslinked PHU oligomers synthesized from polyfunctional monomers are infused with $scCO_2$ under moderate conditions (45 °C, 100 bar, 1 h). Rheological analysis confirms that while the viscosity of the reactive formulation increases at 45 °C, no gelation occurs. During this stage, $CO_2$ not only dissolves into the reactive mixture but also promotes the *in situ* formation of a carbamate salt as a latent blowing agent. After the saturation stage and cell depressurization (when cooled to 0 °C), the foaming is initiated by exposing the "infused" resin to elevated temperatures of 100–140 °C for 2–3 h. During this phase, the carbamate salt progressively decomposes and releases $CO_2$ – promoting material expansion – and an amine – enabling further network curing and foam stabilization by reaction with the cyclic carbonate moieties. The success of this methodology is proven by the fabrication of rigid foams (227 kg $m^{-3}$, $T_g$ = 49 °C) with open cells averaging 0.58 ± 0.39 mm from TMPTC/*m*-XDA compositions added with 5 wt% of LAPONITE® fillers serving as a viscosity modifier and nucleation agent. The versatility of the approach is further illustrated by replacing up to 50% of TMPTC with a bis(5-membered cyclic carbonate), *i.e.*, poly(propylene oxide) biscarbonate (PPOBC), which confers flexibility to the foams by the presence of the polyether backbone. This leads to the fabrication of foams with densities ranging from 285 to 491 kg $m^{-3}$ and $T_g$s progressively decreasing to 28 °C for a 50/50 TMPTC/PPOBC molar ratio (Fig. 12C).

*3.5.2.3. Carbonyldiimidazole.* In 2023, Long introduced biscarbonylimidazolides (BCI) as both latent $CO_2$ blowing agents and monomers for the rapid construction of self-blowing NIPU foams devoid of pending hydroxyl groups (Fig. 13).[157] These chemicals undergo β-hydrogen elimination by reaction with amines under basic catalysis, which liberates a carbamic acid at temperatures exceeding 160 °C, which subsequently undergoes entropically driven decarboxylation. The aminolysis of the carbonylimidazolide moiety, running in a parallel fashion, enables the formation of a new carbamate linkage with concomitant release of imidazole condensates (Fig. 13A). NIPU foams have been successfully fabricated within 30 seconds to 15 minutes by simply melting a (cyclo)aliphatic difunctional BCI monomer at 160–180 °C, followed by mixing with either an aliphatic (Jeffamine T403) or an aromatic (4-(4-aminophenoxy)benzene-1,3-diamine,

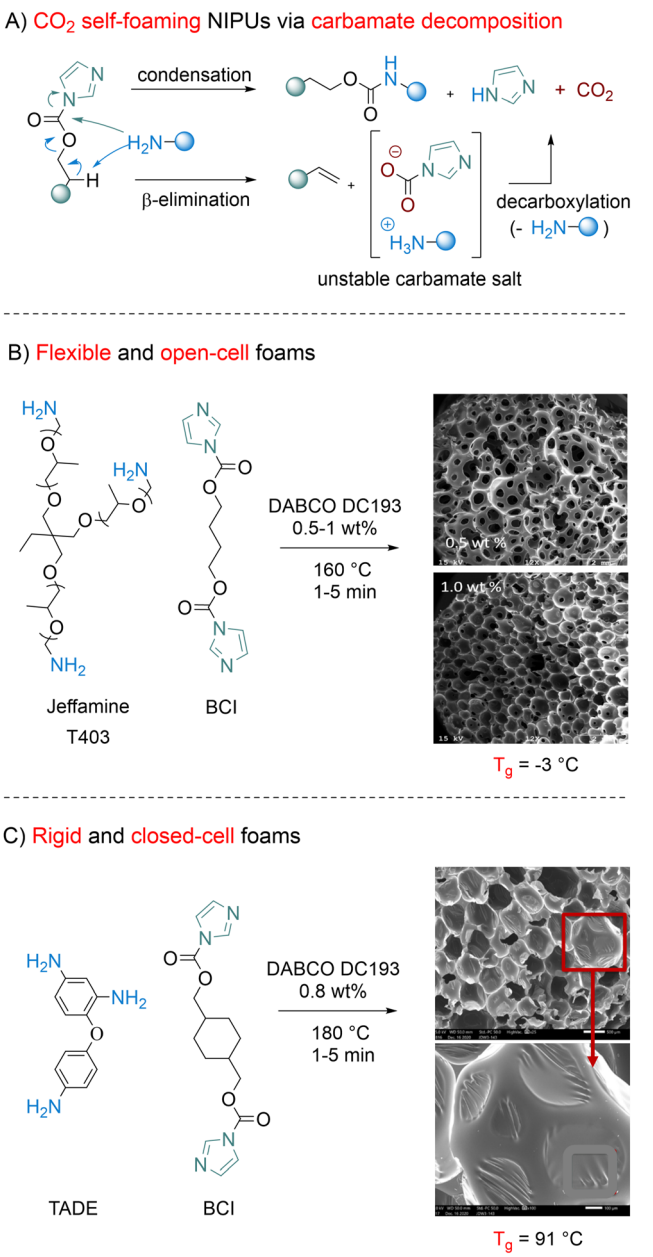


Fig. 13 $CO_2$ self-blown NIPU foams by thermal decomposition of carbamate monomers (A) and flexible (B) or rigid (C) foams produced from biscarbonyldiimidazole monomers and various polyamines. SEM pictures reproduced from ref. 157 with permission from the Royal Society of Chemistry. Copyright © 2023, Royal Society of Chemistry Publisher.

TADE) triamine and their blend in various compositions. Manipulating the surfactant and catalyst content enables precise control over the morpho-structural properties of the foams. Without a surfactant, open-cell foams with cell sizes ranging from 500 μm to 1 mm were produced respectively when aliphatic or aromatic amines are used in combination with an aliphatic BCI monomer (Fig. 13B). Due to its stabilizing effect, the utilization of a silicone-ether type surfactant (DABCO DC193) at 0.8 to 5 wt% content significantly reduces the foam density, and for some formulations, allows for cell closure (Fig. 13C). Controlling the foam

formulations by assorting the BCI and triamine monomers also allowed tuning the mechanical behavior of the foams. The combination of aliphatic precursors leads to flexible materials with low $T_g$ (−3 °C) while mixing (blends of) monomers with cycloaliphatic and aromatic spacers, imparting restricted rotation, delivers rigid porous NIPUs with $T_g$ up to 126 °C. Inherent to this concept is the formation of an equimolar imidazole condensate that requires removal by methanol extraction before foam characterization/utilization. Recent developments, reported in an abstract of papers from the ACS Spring 2024,[158] utilize an orthogonal Michael addition to trap this by-product efficiently. This approach creates *in situ* small molecule additives acting as either flexible plasticizers or rigid fillers.

### 3.6. Porous NIPUs through "emulsion templated-like polymerization"

A series of bio-NIPU foams have been developed by Pizzi through a polycondensation process, which has been further reproduced by other researchers (Fig. 14). Decoding the foaming mechanism is challenging, as this aspect has not been properly addressed in the original publications, and the experimental protocols somehow lacked details and clarity. It is worth noting that the researchers used aqueous solutions of (bio-)monomers/oligomers in combination with glutaraldehyde and carboxylic acids as raw chemicals/crosslinkers. In this regard, we believe they exploited a kind of emulsion templated polymerization process – also referred to as "internal phase emulsion" polymerization – to create porous NIPUs.[159] Conceptually, all foaming procedures exploit a similar methodology. A biomolecule in aqueous solution – selected from glucose,[160,161] tannin,[162–164] xylose[165,166] – is transformed into a (poly)alkylcarbonate by condensation with dimethylcarbonate and then further reacted at 65–90 °C with an excess of diamine, *e.g.*, hexamethylene diamine (70% in water), to create carbamates or NIPU oligomers. The addition of a carboxylic acid (*e.g.*, maleic, citric, malic or aconitic acid)[162]/glutaraldehyde solution upon mixing then initiates the phase-separation qualified as "foaming". We do believe that the foam formation responds to a complex interplay of various phenomena. The acid–base reaction between the carboxylic acid and amines – described as violent by the authors – generates a significant exotherm, causing partial evaporation of water, further expanding the liquid formulation. Concomitantly, the temperature rise promotes the crosslinking of the NIPU with an increase in the polymer viscosity. This results in the formation of a kind of stable emulsion, analogous to "mayonnaise", composed of water droplets surrounded by the NIPU network under construction, whose curing is completed by a final high-temperature treatment ($T$ = 70–103 °C) for 2–10 h (or overnight). During this thermal process, the water evaporates, yet delivering from flexible to rigid bio-NIPU foams. Besides the urethane linkages, amides and imines are identified, attesting to the condensation of amine moieties with carboxylic acids and aldehydes, respectively.[164] The absence of decomposition products of citric acid excludes any participation of carboxylic acid as an endothermic blowing agent. This is further supported by the high decomposition temperature of citric acid, between 160 and 270 °C, which is not reached during the foaming process.

The stability, density and cell morphology of the foams are governed by the contents of carboxylic acid and glutaraldehyde. Generally, increasing the carboxylic acid content (*e.g.*, maleic acid) decreases the foam density. Pizzi has correlated this observation to the higher exotherm produced by the carboxylic acid/amine reaction at higher acid content. This likely enhances the water evaporation during the initial foaming stage, resulting in foams with lower density and larger cells. This is illustrated for glucose-160 or xylose-based[166] NIPU materials, for which an increase of respectively the maleic (to 150%) or citric acid (to 200%) content in the monomer composition (*vs.* the corresponding benchmark samples) reduces the foam density from 130 kg m$^{-3}$ to 80 kg m$^{-3}$ and 467 kg m$^{-3}$ to 303 kg m$^{-3}$. Except for formulations containing citric acid, the use of glutaraldehyde is mandatory to get stable foams. Glutaraldehyde serves as an additional crosslinker, fastening the viscosity increase and gelation of the medium. When being absent, the foam collapses, while at too high a content, the

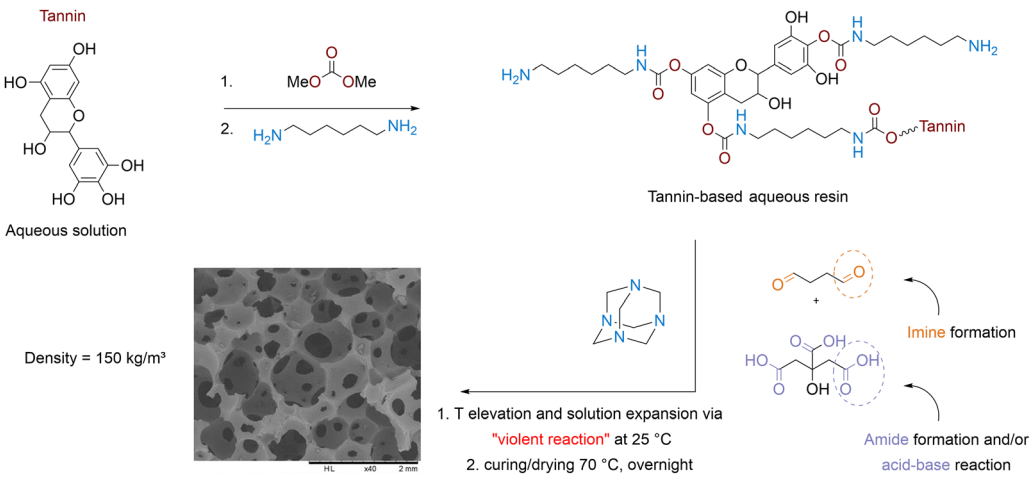


Fig. 14 Pizzi's foaming process of biobased NIPU precursors using glutaraldehyde/citric acid systems. SEM picture reproduced from ref. 164 from MDPI journal.

density increases due to a weakening of the nucleation efficiency upon water evaporation and material drying. This is particularly observed for a tannin-based NIPU with a quasi-doubling of the density (from 150 to 260 kg $m^{-3}$) by doubling the glutaraldehyde content.[160,164] Considering only the publications specifying the NIPU material density, all foams display an open-cell morphology with large pores of heterogeneous size distribution between ~500 μm and ~2 mm.

## Take-home message

**Key differences between conventional PU and NIPU foaming**

*Difference 1 – Foaming process control.* (Self-)Foaming of PUs with physical or chemical blowing agents benefits from the high exothermicity of the isocyanate/polyol reaction, enabling rapid gelation of thermosetting resins and synchronization between PU crosslinking and expansion. Foams are produced within minutes with excellent control of morpho-structural and thermo-mechanical properties. PHU, made by step-growth copolymerization of polycyclic carbonates and polyamines, accounts for >90% of NIPU foams. PHU reactions are however slow and display low exothermicity, making it challenging to control viscosity increase, gelation rate, and blowing agent generation. Proper selection of catalysts, monomers, and the blowing system is essential to align PHU crosslinking with expansion.

Physical blowing of PHU thermosetting resins has been achieved with hydrocarbons, (chloro)fluorocarbons, or water/ethanol mixtures, but prolonged curing (>14 h) at high temperature (>80 °C) is required to prevent material collapse. The addition of co-monomers, such as epoxy or acrylate, can be used to induce cascade exotherms and enable the crosslinking reaction under milder conditions. Concurrently, the $scCO_2$-assisted foaming methodology is the only relevant approach for blowing thermoplastic PHUs.

With chemical foaming agents ($Na_2CO_3$, $NaHCO_3$/citric acid, azodicarbonamide, *etc.*), the foaming process remains slow, poorly managed and lacks versatility. Any variation in one processing parameter (*e.g.*, size of the inorganic carbonate salt, foaming temperature) or in one monomer structure necessitates a complete readjustment of the foaming window. Self-blowing PHUs are prevalent and rely either on $H_2$ release from hydrogenosiloxanes (*e.g.*, Momentive® MH 15) or on $CO_2$ generation from the partial decarboxylation of a foam precursor, such as a cyclic carbonate or carbonated amines. Hydrogenosiloxanes and (masked) thiol additives (used for decarboxylating cyclic carbonates) contribute to PHU crosslinking while reducing their $T_g$'s, thereby enhancing foam flexibility. Similar to conventional PUs, water can induce the partial hydrolysis of cyclic carbonates with the release of $CO_2$. This reaction is accompanied by the formation of unreactive vicinal diol moieties, which do not participate in foam crosslinking but increase its hydrophilicity. To prevent collapse and access uniform foams, the proportion of sacrificial cyclic carbonates should not exceed 25%. Water and also halide salt residues issued from the fabrication of cyclic carbonate monomers act as co-catalysts in PHU formation and accelerate the gelation. With carbonated amines, the control of the foaming process is strongly dependent on the decomposition rate of the amine–$CO_2$ adducts and temperature. This foaming strategy is actually constrained by a limited range of suitable carbamate salts that decompose below 150 °C with kinetics compatible with the PHU network formation. Porous NIPU formation through "emulsion templated-like polymerization" is slow, restricting its utilization. Up to now, PHU chemistry hybridization is the only self-blowing process able to rapidly foam NIPU from r.T. formulations.

*Difference 2 – Foam density and morphology*. In PU thermosetting foams, density (30 kg $m^{-3}$ < $d$ < 250 kg $m^{-3}$), cell size (μm-scale), and porosity type (open or closed cells) are finely controlled through the careful adjustment of formulation parameters, including surfactant, catalyst and blowing agent. Morpho-structural control remains less efficient in PHU foams, which may exhibit non-uniformity and high densities exceeding 100–400 kg $m^{-3}$. These foams typically have open porosity and large cells, with dimensions exceeding 100 μm to 1–2 mm. However, it is important to note that most reports do not utilize surfactants/foam stabilizers to assist foaming and control cell morphology. To date, closed-cell foams have been described for one carbonyldiimidazole/amine self-blowing formulation when used in combination with a surfactant and for the $scCO_2$-assisted physical blowing of thermoplastic PHU. A nearly closed cell morphology was also described in the case of a thiol-assisted self-foamed PHU formulation, although the final density of the foam is relatively high (>500 kg $m^{-3}$). As PHU foams exhibit higher hydrophilicity compared to conventional PU foams, surfactants or foam stabilizers used in PU foams do not display similar performance in PHU foaming. Therefore, identifying appropriate surfactants is paramount for the future optimal control of the morphology of PHU foams. Moreover, it is worth mentioning that progress must be made to precisely quantify the closed-to-open cell ratio, as conventional methodologies such as picnometry have not been properly used to this end in the field of NIPU foams to date.

*Difference 3 – Role of surfactants in controlling foaming*. Silicone-based surfactants play a multifaceted role in PU foam formation by controlling the polyol/isocyanate emulsification, cell nucleation and stabilization, as well as foam density. Their low surface tension decreases the energy barrier to promote air bubble formation during mixing. This so-called "bubble dispersion stage" fixes the number of gas bubbles with no additional bubbles being formed during subsequent foam expansion.[5,167] By adsorbing at the gas–liquid interface, the surfactants reduce the interfacial energy and limit the Ostwald ripening (diffusion of the smallest cells to the larger ones).[168] They also prevent the cell wall drainage, *i.e.* the flowing of the monomers out of the cell wall to the exterior, forming the plateau borders (struts) separating bubbles in a foam.[5,167,169] During the bubble expansion, a gradient in surfactant concentration is created along the cell surface. This triggers the movement of the surfactant from the higher to the lower concentration area (Marangoni effect). As the surfactants move, they drag liquids (monomers or low viscosity oligomers) with them, slowing film drainage. This phenomenon delays/limits cell wall rupture, coalescence and foam collapse, enhancing foam stability and uniformity during rise and curing. When evaluating NIPU foams, directly utilizing silicone-based surfactants that are effective in PU formulations presents a significant challenge in enhancing foaming properties. Indeed, the fundamental differences in the two distinct chemistries arise from monomer structure, miscibility, and polarity, initial viscosity, gelation rates, and also the hydrophilicity of the final polymer matrix. These factors are likely to alter surfactant interfacial behavior and therefore the bubble dispersion stage and cell stabilization. Surfactants specifically adapted for NIPU foaming are still to be discovered.

*Difference 4 – Thermo-mechanical properties*. PHUs lack isocyanate-derived motifs (biuret, allophanate, isocyanurate, uretdione) and often have lower crosslinking density than conventional PU foams. This translates into low $T_g$ and very low stiffness materials. Achieving rigid PHU foams with $T_g$ > 60–80 °C remains a significant hurdle.

*Difference 5 – Hydrophilicity and humidity sensitivity*. The OH-rich PHU backbone is intrinsically more hydrophilic than PU, making PHU foams susceptible to plasticization when exposed to humidity, affecting their mechanical properties and reducing their $T_g$ value.[170]

*Difference 6 – Industrial deployment*. Most PU foam manufacturing processes are based on two-component diisocyanate/polyol formulations poured onto a conveyor belt, injected into molds or sprayed onto walls. These established technologies rely on the precise control of the initial viscosity of the reactive formulation and its homogeneous mixing, typically achieved using high-shear static mixers or high-pressure mixing heads. This mixing step is critical as it ensures the proper blending of the foam ingredients with the blowing agent and stabilizer, forming an emulsion that dictates the quality and morpho-structural characteristics of the foam. Foams are generally produced in 1 to 5 minutes at a temperature stabilized at 40–60 °C to ensure operational stability of

 

the manufacturing process. To date, there is no report on testing NIPU foaming on pilot industrial lines using these technologies, and no NIPU foam can be found on the market yet. Within the frame of the fundamental developments reported here, only small-scale samples are usually investigated (few grams). Increasing the volume of the reactive formulation is known to impact the foaming parameter (*e.g.*, viscosity, exothermicity) and thus the final properties of the foams (cell size, density, open/closed cell ratio). Scaling up the foaming processes is foreseen as a crucial step forward to better define the industrial applicability of the reported systems.

**Main challenges for NIPU foaming**

*Challenge 1 – Low temperature, fast foaming*. Hybridization of the NIPU technology has recently enabled the fast foaming (below 5 min) of NIPU from r.T. thermosetting formulations. To broaden the spectrum of NIPU foam structures, properties and thus applications, it is crucial to expand the scope of highly reactive co-monomers that function as heat-release promoters (*e.g.*, acrylates). However, this expansion should be accompanied by careful consideration of their large-scale availability, origin, cost, and toxicity.

*Challenge 2 – Morpho-structural control of NIPU foams*. Achieving NIPU foams with ultra-low densities ($<50$ kg m$^{-3}$), closed porosity, small cell sizes, and high cell densities similar to conventional PUs (notably used for thermal insulation) will require several advancements. Improvements include the identification and use of surfactants to stabilize cell structures and/or suitable nucleating agents (fillers) to promote nucleation sites and generate a high number of cells. Optimizing processing conditions, such as emulsifying a physical blowing agent into the reactive formulation with adequate stabilizers or ensuring effective filler dispersion *via* high shear mixing, should enable the production of foams responding to these criteria. The wide range of surfactants and nucleating agents already developed for isocyanate-based foam chemistry can provide a valuable starting point for controlling the morpho-structural properties of NIPU foams. Further optimization of the morpho-structural properties of NIPU foams might be attained by adapting these well-established additives to the specific reactivity and physico-chemical characteristics of NIPU formulations.

*Challenge 3 – NIPU foams with tunable thermo-mechanical properties*. Specific adjustments of both the NIPU microstructure and foam formulation composition are required here. Improvements involve exploiting the PHU hydroxyl groups for further chemical transformation to increase the crosslinking density of the foams, ideally during their formation by using simple and cost-effective methods. Mechanical performances can also be enhanced by utilizing monomers that introduce rigidity and/or improve thermal resistance through specific interactions. For example, aminotelechelic oligoamides or hydroxyoxazolidone precursors can promote hydrogen bonding, while (poly)aromatic- or lignin-derived monomers can facilitate $\pi$–$\pi$ stacking. Similarly, the controlled dispersion of fillers such as chitin or cellulose nanofibers up to the percolation threshold may yield interpenetrated NIPU networks with superior mechanical strength. Accelerated aging and durability testing of NIPU foams have still to be considered. These tests simulate long-term use of the foams by exposing them to harsh conditions like elevated temperatures (thermo-oxidation), high humidity, UV and chemical agents to predict any variation in their thermo-mechanical properties (*e.g.*, hardness, compression resistance, resilience, *etc.*).

*Challenge 4 – Suppressing or decreasing the hydrophilicity of PHU foam*. This objective can be accomplished through various approaches. One potential method involves modifying the dangling hydroxyl (OH) groups with appropriate hydrophobic groups. Ideally, this modification should occur during the foaming process, as post-modification may not be relevant for industrial applications. This approach necessitates the identification of a chemoselective transformation that specifically targets hydroxyl groups and is compatible with the foaming conditions and the presence of amines. However, identifying a reactant able to react selectively with the OH moieties during foaming is extremely challenging and requires significant chemical engineering, particularly when simple and inexpensive transformations are desired. A relevant example for PHU hydrophobization by Shaplov *et al.* is the acetalization of their pending OH groups by aldehydes.[171] However, this was only achieved on pre-formed PHU in solution, and the possibility to realize it *in situ* during PHU foaming remains challenging. Instead of transforming the existing OH groups, a promising strategy for hydrophobization involves incorporating reactive hydrophobic (nano)fillers into the foaming formulation. This has been recently demonstrated by Liu *et al.* by adding hydrophobic thiol-functionalized polyhedral oligomeric silsesquioxane (POSS-SH) to water-induced self-blown NIPU formulations.[171] Besides imparting hydrophobicity to the NIPU matrix, this POSS-SH served as additional crosslinked nodes. This strategy is similar to the one reported by Gong *et al.*, who highlighted that the dispersion of hydrophobic reduced graphene oxide significantly suppressed atmospheric moisture absorption by the PHU foams.[172] The final proposed approach involves incorporating silicone-based surfactants into the NIPU formulations. If designed appropriately, these surfactants will stabilize the gas bubble/cell interface by covering the cell surface with a hydrophobic segment. Consequently, they will serve as protective coatings on the cell surface within the NIPU foams, thereby enhancing their humidity resistance.

*Challenge 5 – Retrofitting of industrial infrastructures*. Implementing the foaming of NIPUs on existing industrial PU manufacturing lines requires significant adjustments. This includes the judicious selection of non-isocyanate PU chemistries to precisely control reaction kinetics to align with industrial processes; the efficient mixing/emulsification of all foam ingredients (monomers, blowing agent, stabilizers, catalyst and additives) into a homogeneous mixture *via* high-pressure mixing or high shear static mixers; the proper control of the initial formulation viscosity and mixing temperature, allowing the deposition, spraying or high-pressure injection and flowing of the formulation onto conveyors, onto walls or into closed molds, respectively. Although the fast NIPU foaming has recently been achieved *via* the hybrid formulations, the developments remain at the lab scale. Testing these NIPU foaming processes on pilot industrial lines is now necessary to identify the remaining technological barriers that need to be overcome to transfer the technology to industry. This will also necessitate the large-scale production of monomers (*e.g.*, cyclic carbonates), still not commercially available at a large scale.

## 4. How to address the end-of-life of NIPU foams?

In the transition towards a circular economy preserving resources and lowering the environmental footprint of the products, waste polyurethane foams can be given a second life through recycling.[173] There exist multiple options for treating and transforming end-of-life (EoL) PU foams. The most common is chemical recycling, with the end products (recyclates) being reintroduced into the production cycle of second-generation PUs (foams) as reusable chemicals (mainly polyols). These methods, reviewed recently by Malucelli *et al.* for conventional PU made from isocyanates,[174] could virtually apply to all varieties of NIPUs, as illustrated for the recovery of small molecules from PHU thermosets *via* base-catalyzed methanolysis.[175] As PU foams are generally thermosetting materials, they are also revalorized *via* a downcycling scenario – also named physical recycling – into new products. Generally, waste PU foams are mechanically converted into powders, flakes, or small particles and reused as additives/fillers in new (PU) matrices.[174] Recently, Dichtel introduced carbamate exchange catalysts[176,177] or exploited residual foam catalysts,[178] allowing for the conversion of thermoset PU

foams into covalent adaptable networks (CANs). Leveraging the melt-processability of the so-produced PU CAN and the use of a suitable blowing agent, he opened a new foam-to-foam recycling perspective *via* extrusion foaming.[176] This CAN behavior is present and even facilitated in non-isocyanate polyhydroxyurethanes,[179–183] and is exploited now to reprocess waste NIPU foams into films, adhesives, or structural composites.

### 4.1. Chemolysis of NIPU foams

To date, the chemical recycling of NIPU foams has been reported only through high-pressure glycolysis, alkaline hydrolysis or hydroglycolysis and is exemplified with carbonated lignin/priamine-derived materials blown with Momentive (Fig. 15).[117] These chemolytic methods break down the urethane linkages, releasing polyols, amine and $CO_2$. When using cyclocarbonated lignins, the presence of additional labile ether and acyclic carbonate linkages within its chemical structure further aids in the foam decomposition. Glycolysis using ethylene glycol shows limited decomposition efficiency, even at 220 °C, with ~30–40% of the foams being degraded after 3–6 h. Alkaline hydrolysis using 0.1 M KOH under the same conditions achieves significantly higher degradation, around 65–70%. The most effective approach is a hybrid hydroglycolysis system combining 10 wt% ethylene glycol with a 0.2 M KOH aqueous solution, which increases foam decomposition up to 90%. In this study, the authors focused only on characterizing, recovering and reusing lignin for the production of second-generation foams. Through in-depth characterization, the hydroglycolysis procedure yields an ethylene glycol-modified lignin structure with a high hydroxyl content, favoring the reformation of cyclic carbonate units by condensation with DMC, and molar mass comparable to native lignin, ensuring its total solubility within the foam formulation. These features are better suited for the revalorization of recycled lignin into second-generation foams. Lignin recovered through alkaline hydrolysis undergoes structural modification and can therefore only be reincorporated at a content of about 10–20% into new foam formulations. In contrast, lignin obtained *via* hydroglycolysis can be reintroduced at up to 100% in fresh formulations, enabling the production of foams with densities (251 kg $m^{-3}$), compressive modulus (1.51 MPa) and compressive strength (0.126 MPa at 10% deformation) that are essentially identical to those of the original foams.

### 4.2. Covalent adaptable network NIPU foams

Covalent adaptable networks (CANs) provide an emerging solution to overcoming the end-of-life of thermosets. CANs are dynamic polymer systems capable of rearranging their network structures through reversible bonds and/or exchange reactions triggered by external stimuli, *e.g.*, heat and pressure.[184–188] In dissociative CANs, temporary scission of the crosslinked nodes upon heating reduces the network density and enables structural rearrangement. Conversely, associative CANs, also named vitrimers, maintain a constant network connectivity by forming new bonds simultaneously as existing ones break. In the absence of degradative side reactions, these dynamic thermosets can thus be repaired, reprocessed, and recycled without drastically compromising their material performance. For more details on CANs, we invite the reader to refer to the recently published user guide of Ladmiral, which serves as a vade mecum for neophytes.[184]

**4.2.1. Fundamentals of PHU foams with CAN behavior.** PHUs possess a microstructure that makes them intrinsic CAN materials (Fig. 16A). The presence of pendant hydroxyl groups along the polymer backbone enables transcarbamoylation reactions, *i.e.* the intramolecular reversible scission of hydroxyurethane

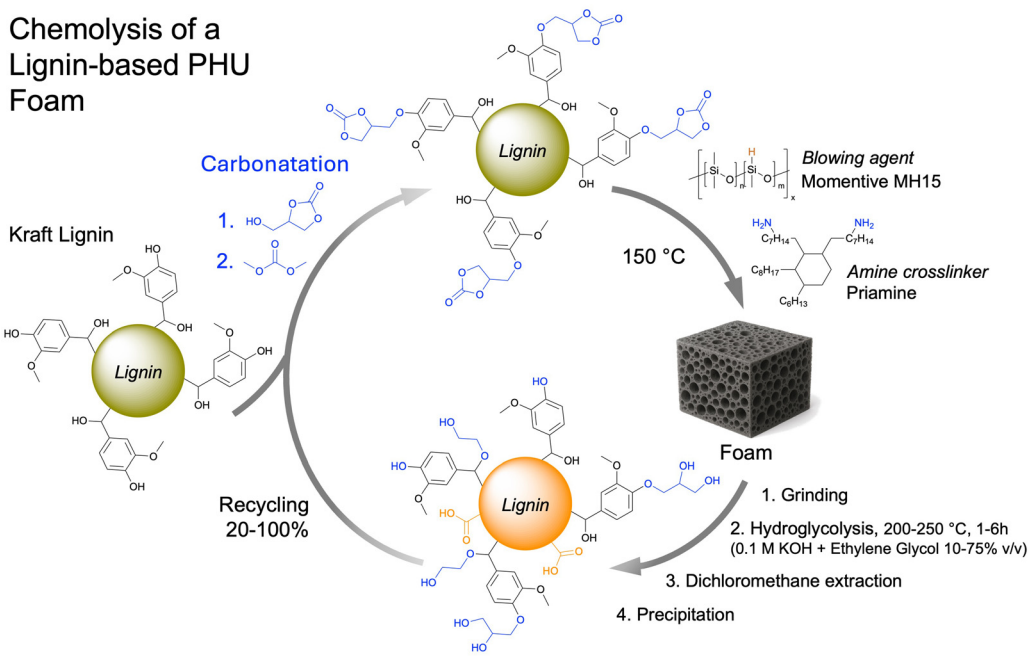


Fig. 15 Closed-loop chemical recycling of lignin-based NIPU foams.

 

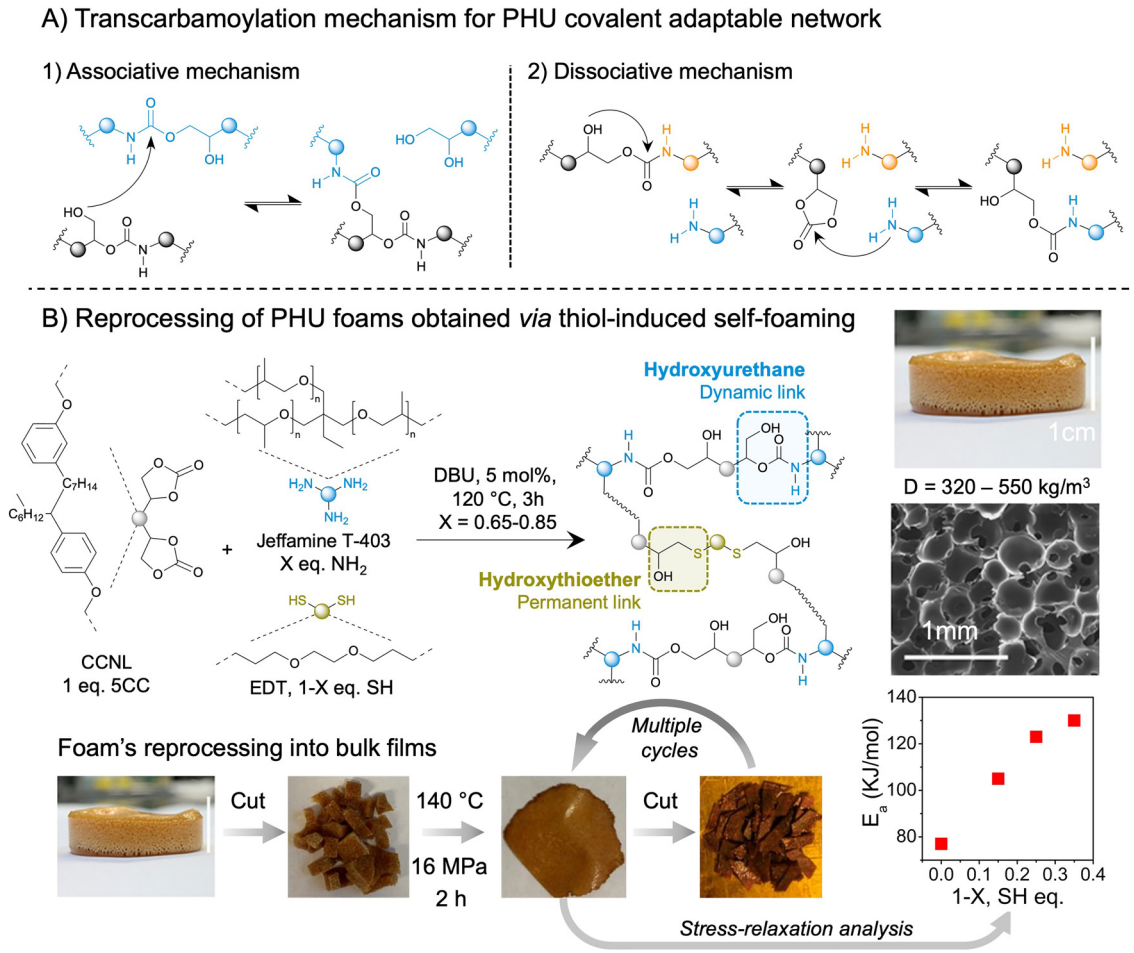


Fig. 16 Concept of covalent adaptable networks (CANs) (A) and (B) reprocessing of $CO_2$ self-blown PHU foams produced with thiol blowing agents into films. SEM pictures and foam micrographs reproduced from ref. 136 with permission from the American Chemical Society. Copyright © 2023, American Chemical Society.

linkages back to the native cyclic carbonate and amine as well as the intermolecular transcarbamoylation leading to associative exchanges between neighboring polymer segments.[179] These features have been exploited to recycle PHU foams of various compositions into second-life films,[133,134,136,189] structural coatings,[134] adhesives[134,190] and potentially dimensionally stable elastomers.[133] Generally, PHUs foamed with water[140,190] or (masked) thiol blowing agents[133,134,136,189] undergo reprocessing *via* compression molding at $T > 160$ °C, in 2–3 h under >10 MPa pressure (Fig. 16B). Bases that promote foam formation, such as DBU, also serve as reprocessing catalysts, although other catalysts may facilitate exchange reactions.[180] Two main factors govern the foam reprocessing, *i.e.*, the permanent *vs.* non-permanent linkage composition of the PHU network, notably for systems using a thiol as a blowing agent, and the hydroplasticization[190] of PHU. Insights into the role of thiols in the process dynamics are reported in detail for a model PHU foam made of carbonated cashew nutshell liquid, Jeffamine T-403 and EDT (Fig. 16B).[136] It reveals that the introduction of up to 35% of permanent hydroxythioether linkages, formed *via* *S*-alkylation, within the dynamic PHU networks, does not hinder the foam-to-film repurposing. This agrees with the modified Flory–Stockmayer theory for vitrimer gelation, which states that effective reprocessing without facing creep is possible as long as non-permanent linkages remain below 50 mol%.[191] However, the content and functionality of the thiol blowing agent impact the reprocessing efficiency. An increase of either the dithiol (EDT) content within the formulation[189] or the thiol functionality of the crosslinker[133] affects the interchain diffusion (segmental relaxation) necessary for the transcarbamoylation reactions. This translates into higher temperatures needed to overcome this diffusion barrier and enable effective reprocessing. This results in a doubling of the apparent activation energy value ($E_a$), which rises from 77 kJ mol$^{-1}$ for the reprocessing of a pure PHU film to 130 kJ mol$^{-1}$ for a film containing 35 mol% of permanent hydroxythioether linkages. Inspired by the moisture-healing ability of PHUs, a recent study shows that humidity aids foam-to-film recycling.[190] This improvement is attributed to water disrupting hydrogen bonds, enhancing chain mobility, and facilitating the network rearrangement. Comparing dry-conditioned and moistened $CO_2$ self-blown PHU foams (made by water-induced self-foaming of TMPTC/HMDA formulations)

attests to this benefit. Dry foams can only be reprocessed under harsh conditions, *i.e.*, *T* of 170 °C for 4 h with a 5-ton pressure, while analogous moistened foams that have absorbed 11.7% of water at 80% relative humidity are reshaped into films at just 140 °C in 2 h under the same pressure.

**4.1.2. Design for recyclability.** Smart editing of the PHUs by in-chain insertion of additional labile ester or disulfide linkages offers another effective lever to enhance foam recyclability. Transesterification between the OH groups of PHU chains and ester bonds – embedded within the network *via* the proper design/selection of the carbonate monomer[133] or the crosslinker – might be exploited. It has been reported as inactive for temperatures up to 160 °C. However, it becomes operative at a higher *T* of 180 °C, helping restore sufficient chain mobility to enable efficient foam-to-film reshaping. Disulfides, which usually dissociate at ~100 °C, can be incorporated into foams (Fig. 17).[190] Their presence enables a faster foam-to-film reprocessing under less demanding conditions than conventional PHU CANs. This is demonstrated for water-induced self-blown PHU foams made from TMPTC and HMDA, cystamine or their blends, for which network dynamicity is directly correlated with the disulfide content. Notably, foams composed entirely of cystamine, a renewable disulfide diamine, can be reprocessed at 90 °C in just 30 min under 5 tons, representing conditions that are substantially milder than the ones required to reshape a 100% HMDA-based foam (170 °C, 4 h, 5 tons). For cystamine/HMDA blends, the reprocessing temperature increases with the HMDA content, rising from 120 °C to >140 °C as the HMDA composition in the blend increases from 25% to 75%. Importantly, for the PHU foams with or without cystamine, their reshaping was further facilitated and accelerated when they were previously equilibrated in a humidity chamber at 80% relative humidity. Hydroplasticization further facilitated the rearrangement of the network in a simple, cost-effective manner without resorting to elevated temperatures or catalysts.

**4.1.3. Foam-to-film recycling.** While PHU foams can be effectively repurposed into films by compression molding, slight variations in thermo-mechanical properties and crosslinking densities are observed between the two types of materials. Like all PHU thermosets, the consumption of cyclic carbonates *via* aminolysis, *S*-alkylation or hydrolysis is often incomplete due to restricted monomer mobility, which arises from the change in viscosity and strong interchain hydrogen bonding during curing. This limitation is even more pronounced in foaming systems, where the formation and growth of gas-filled cells further hinder chain mobility and reduce access to reactive groups. As a trend, during reprocessing by thermal compression molding, these residual carbonate moieties can react, contributing to further network gelation. This results in reprocessed films with a higher crosslinking density

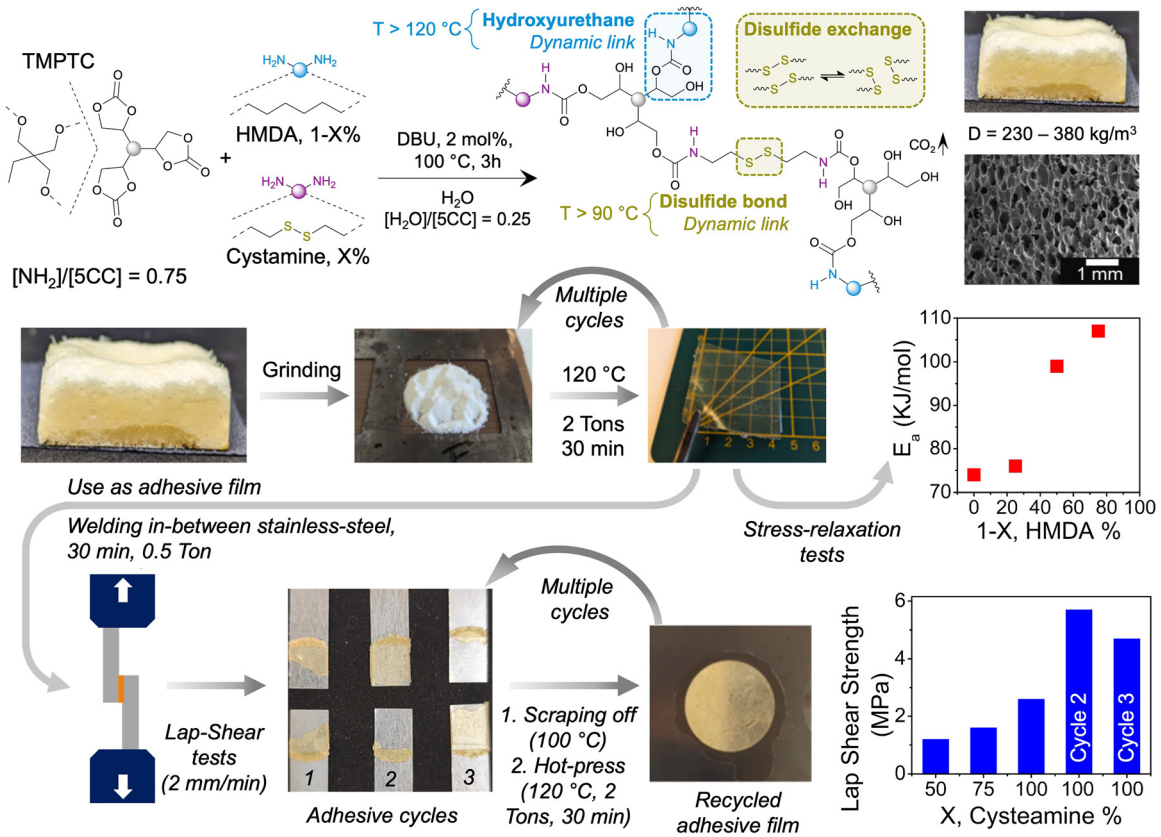


Fig. 17 Recycling of waste PHU foams containing additional dynamic disulfide linkages into films and adhesives. SEM pictures and other micrographs reproduced from ref. 190 with permission from Elsevier. Copyright © 2025, Elsevier Ltd.

 

compared to the original foams, as shown by the evolution of the gel content from 80–85% to 89–90% after three recycling cycles.[189] In addition, the consumption of residual carbonate groups eliminates their plasticizing effect, leading to an increase in the $T_g$'s of the films compared to the foams – *e.g.*, from 6 °C at 15% hydroxythioether linkage content up to 15 °C at 35%.[189] The rubbery plateau modulus of the films also rises after each reprocessing cycle (*e.g.*, from 0.34 to 0.41 MPa between the first and third recycling), in line with the progressive consumption of unreacted carbonate groups in the thermoset but also the formation of urea linkages much favored at high reprocessing temperatures.

**4.1.4. Foam-to-adhesive recycling.** The PHU foam-to-film transformation opens new possibilities for using the resulting films as high-performance CAN adhesives that combine the strong adhesion of thermosets with the reversible bonding and debonding ability of hot-melt adhesives. As shown by Detrembleur *et al.* for designing and welding structural coatings *via* hot-pressing onto nylon fabrics of films recycled from flexible $CO_2$ self-blown foams,[134] the concept has been extended to bonding various substrates, such as glass or steel, with cystamine-containing adhesives reshaped from the same foams (Fig. 17).[190] When bonding steel at 120 °C for 10–30 min under a pressure of 0.5 tons, adhesion performance improves with higher disulfide content, as shown by the lap shear adhesion value increasing from 1.2 ± 0.7 MPa to 2.6 ± 0.2 MPa as the cystamine content increases from 50% to 100%, with cohesive failure observed. At higher disulfide contents, the highly dynamic network allows bond rearrangements, further improving PHU adhesive–substrate contact. Reuse tests involving multiple bonding and debonding cycles demonstrated even greater performance, with lap shear adhesion reaching up to 5.7 ± 1.0 MPa for 100% cystamine adhesives. This enhancement results from increased crosslinking of the PHU network during repeated cycles, along with fewer defects due to better stress redistribution within the material. Notably, these cystamine-rich adhesives outperform commercial hot-melt EVA and thermosetting PU glues and approach the performance of cyanoacrylate-based Superglue®, which provides an adhesion strength of 6.2 ± 0.7 MPa. On glass substrates, the lap shear adhesion is lower, ranging from 0.8 to 0.9 MPa, yet it remains competitive with commercial adhesives (1.1 to 1.3 MPa).

## 5. What are the emerging applications of NIPU foams?

Over the last 5 years, NIPU foaming has witnessed a significant acceleration, especially with the adoption of physical or self-blowing methods, which have driven the emergence of products for cutting-edge applications. Despite being in their infancy, the elaboration of these practical applications is

**Take-home message**

**Key differences between the end-of-life options of conventional PUs and NIPUs**

*Difference 1 – Chemical recycling*. Chemolysis is the preferred method for decomposing thermosetting PU foams. Hydrolysis, glycolysis, aminolysis, ammonolysis, acidolysis, and phosphorolysis yield high-value, high-purity chemicals with diverse functionalities and physico-chemical properties. Among these methods, glycolysis of flexible PU foams has advanced to pilot-plant and industrial-scale operations. The chemical recycling of NIPU foams, apart from the hydroglycolysis of lignin-derived foams reported by Stemberg, remains nonexistent. Besides, data on the long-term hydrolytic stability of PHU foams are still lacking and could provide useful insights for future developments.

*Difference 2 – Physical recycling*. High-temperature, high-pressure injection/compression molding techniques are effective for reprocessing PU foams of low crosslinking degree into structural parts, *e.g.*, covers for motors and pumps, dashboard or door panels, *etc.* Thermosetting PU foams of high crosslinking degrees are generally ground into powders, particles or flakes that further serve as fillers for other resins or are rebonded with PU adhesives into the form of covers for tires, athletic mats, car linings, and carpet underlays, among other uses. Physical recycling of NIPU foams is limited to PHUs and exploits their covalent adaptable network properties to easily upcycle foams into films, structural composites and high-performance adhesives for metal, wood, glass and fabrics.

**Main challenges for NIPU recycling**

*Challenge 1 – New chemical recycling strategies*. Recycling waste NIPU foams faces challenges due to variations in NIPU chemical structures, crosslinking degree, and crystallinity. Specific recycling strategies should maximize yield and purity of recovered chemicals while minimizing by-products, environmental impact, and energy consumption. Conventional hydrolysis, glycolysis, aminolysis, or ammonolysis should be prioritized, but other chemolysis approaches could be engineered, especially for PHUs with pending OH moieties. Biodegradation using urethanases or designing NIPUs with labile linkages for facilitated recycling should also be considered for longer-term deployment.

*Challenge 2 – New physical recycling strategies*. Going beyond the simple grinding of waste PU foams would capitalize on mechanochemistry. Mechanochemical recycling involves applying high-shear mechanical forces, *e.g.*, *via* ball milling, to break covalent bonds in the NIPU network, promoting fragmentation, depolymerization or modification (*e.g.*, hydroxyl group formation) reactions. This methodology might be applied to NIPU foams and its utility in producing (functional) powders or oligomers that might then be reused as fillers, chemical feedstocks, or precursors for new materials evaluated.

*Challenge 3 – Foam-to-foam recycling*. Existing industrial "foam-to-foam" recycling methods for conventional PUs shred foams and rebind particles into new materials like carpet underlays. Implementing foam-to-foam recycling for NIPUs, especially thermosetting PHU foams, will exploit their CAN properties. Using suitable catalysts for transurethanization or urethane bond dissociation, or designing NIPU foams for easy recycling with labile linkages, could lead to reprocessable materials. Second-generation foams with new morpho-structural characteristics might be produced through extrusion-foaming with physical blowing agents.

*Challenge 4 – Integration within the current recycling streams*. Short-term recycling of NIPUs should be standardized with existing PU methodologies to ensure their integration into industrial recycling streams. In this context, glycolysis, aminolysis and eventually ammonolysis, which are largely deployed to decompose conventional PUs, should be adapted to NIPUs. Mechanical grinding of NIPU foams into powder and their reuse as fillers or other foam components should be evaluated.

essential not only to validate the potential of these foams and benchmark their value with existing solutions but also to uncover performance limitations that can guide future material optimization.

### 5.1. Fire retardant foams

Without flame retardants, conventional PU foams are highly flammable materials, producing a significant level of smoke during burning that contains $CO_2$, toxic gases (HCN, $NO_x$, CO), hydrocarbons (benzene, xylene, toluene, carbazole, *etc.*)[192] and other hazardous chemicals (phenyl- or *p*-toluene-isocyanates, isoquinoline, nitriles, *etc.*).[193] Their high flammability arises from their inherently porous structure, facilitating oxygen diffusion within the foam, and their intrinsically low limiting oxygen index (LOI) of 18% (LOI indicates the minimum oxygen concentration required to sustain combustion).[194] Foam density also plays a significant role in the fire resistance properties.[195,196] Low-density materials limit heat transfer from the surface to the core, leading to shorter ignition times. The open-cell structure of PU foams, the absence of aromaticity in the PU skeleton and the presence of hydrocarbon or $H_2$ blowing agents within closed cells are additional factors worsening the resistance of the foam to fire.[195,196] NIPU foams display flammability similar to conventional PU counterparts, as illustrated by LOI values as low as 17.5% or 22.3% for materials made from glucose[161] or xylose-derived[166] monomers, respectively, far away from 27%, the value at which the foam is considered fire-resistant. This ignitability is reduced by the insertion of aromatic monomers within the NIPU network.[162] These aromatic species, like tannic acid or tannin, undergo carbonization in the condensed phase, creating a char that shields the underlying material from oxygen diffusion/exposition. The LOI values then increase to 24–25.5%,[161,163] still below the 27% threshold deemed fire resistant but sufficient to make the materials self-extinguishing. Flame-retardant properties of tannin-based NIPU foams are achieved by adding an inorganic salt, such as $Al(OH)_3$ (Fig. 18).[163] Upon exposure to heat, this salt undergoes endothermic decomposition with concomitant water vapor release. The combined effects of endothermic decomposition, absorption of heat, and water vapor release create a protective interface of $Al_2O_3$ between the burning material and the surrounding environment, restricting oxygen contact and retarding the flame propagation rate. This translates into an LOI value of >27%, providing NIPU (bio)foams with fire retardancy (Fig. 18).

Phosphorus-based flame retardants have also been exploited to fabricate fire-resistant PHU foams. Among them, phytic acid stands out as a multi-action flame retardant.[197] When exposed to flame or heat, it decomposes in the gas phase into phosphorus-containing radicals ($HPO^{\bullet}$, $PO^{\bullet}$ and $HPO_2^{\bullet}$), which scavenge reactive OH and H radicals. This mechanism suppresses the thermo-oxidative degradation of polymers and reduces the formation of combustible volatiles. Additionally, the decomposition of phytic acid releases water vapor and other non-reactive gases, further diluting oxygen in the combustion zone. In the condensed phase, its degradation produces acids such as polyphosphoric acid, which catalyze the formation of intumescent char layers. The high efficiency of phytic acid in improving fire resistance is illustrated by an LOI of 29.1% for low-density closed-cell PHU foams (131 kg $m^{-3}$) synthesized from cycloaliphatic biscyclic carbonates, *m*-XDA, and PEI using HFO-1233zd as a physical blowing agent.[105] Novel trends explore now the utilization of phosphorus-containing biscyclic carbonates as analogs to 9,10-dihydro-9-oxa-10-phosphaphenanthrene-10-oxide to serve as reactive flame retardants. The insertion of these monomers at only 2 wt% into a PHU self-foaming formulation is sufficient to reduce the total smoke release during combustion by 31%.[198]

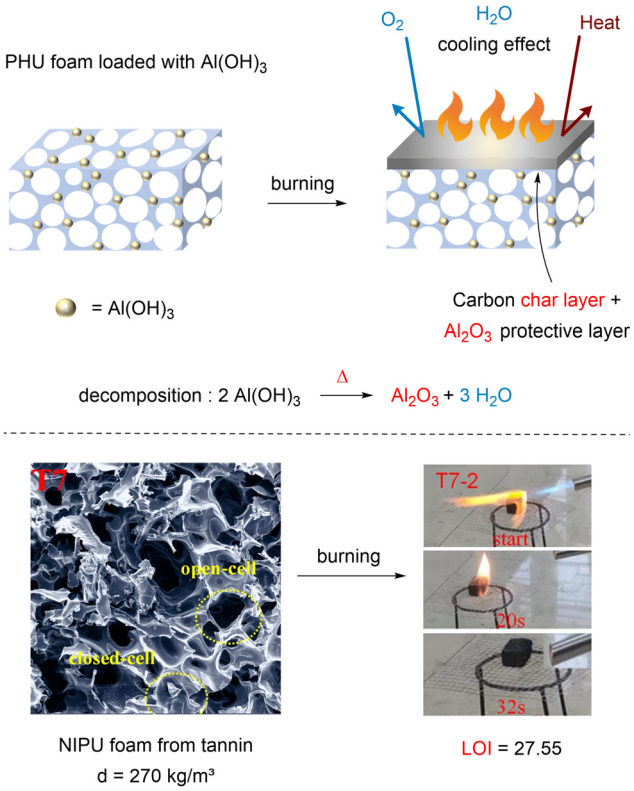


Fig. 18 Fire-retardant tannin-based NIPU foams formed by the use of $Al(OH)_3$. SEM picture and burning tests reproduced from ref. 163 with permission from Elsevier. Copyright © 2023, Elsevier Ltd.

### 5.2. Heat storage and thermal insulation

**5.2.1. Heat storage.** Thermal energy storage (TES) technologies have emerged as a key solution for regulating heat and improving energy efficiency across various applications, including thermal regulation in buildings, batteries for electric vehicles, clothing, solar heating and air conditioning.[199–203] The simplest TES system stores and releases latent heat through endothermic/exothermic solid–solid, solid–liquid, solid–gas, or liquid–gas phase transitions of phase change materials (PCMs),[201] which can be organic (such as waxes) or inorganic (such as salt hydrates). Various approaches exist to stabilize the shape of PCMs, one of the most efficient being their encapsulation in porous materials. In particular, polymeric foams offer a compelling platform to enhance melt-freeze cycling durability and shape-stabilization of PCMs in net $CO_2$ emission reduction and

 

energy efficiency applications. By controlling their morpho-structural properties, Allen valorized bio-derived $CO_2$ self-blown PHU foams to phase-stabilize both paraffinic (hexadecane, heptadecane, and octadecane) and inorganic salt hydrate ($CaCl_2 \cdot 6H_2O$) PCMs with melting temperatures in the ambient range of 18 to 30 °C.[204] The large open-cell morphologies (cell diameter of ~300 μm, density not specified) of the foams allow for infusing and filling the voids with waxes with a loading of ~60 wt%. These PHU foam-encapsulated paraffinic PCM systems exhibited two stable melt-freeze thermal cycles with enthalpies of melting and freezing between 136 and 165 J $g^{-1}$ and calculated stored energies of ~128 MJ $m^{-3}$, ~112 MJ $m^{-3}$ and ~107 MJ $m^{-3}$, respectively, for hexadecane, octadecane and heptadecane. When hydrated salt comes at play, its supercooling upon freezing hinders the direct fabrication and utilization of the PHU foams/$CaCl_2 \cdot 6H_2O$ system for thermal storage. This issue can be circumvented by the addition of $BaCO_3$ during the foam fabrication. When dispersed in the foam, this barium salt acts as a nucleating agent that reacts with $CaCl_2 \cdot 6H_2O$ to form a precipitate that strongly reduces the supercooling of the neat salt hydrate. $CaCl_2 \cdot 6H_2O$ has been loaded at 86 wt% in the $BaCO_3$ containing open-cell PHU foam (cell diameter of ~320 μm). Unlike the TES made from wax PCMs, the $BaCO_3$ PHU foam-encapsulated $CaCl_2 \cdot 6H_2O$ system has been found stable to 48 thermal melt-freeze cycles, with enthalpies of melting and freezing between 133 and 138 J $g^{-1}$ and heat storage capacity (231.5 ± 4.5 MJ $m^{-3}$) twice higher than the one reported for organic PCMs. Despite holding great promise for new applications, the open porosity of the foams may cause inherent long-term leakage of the PCM, while the hygroscopic nature of the PHUs can potentially soften the foams and impact the thermal behavior of the PCM.

**5.2.2. Thermal insulation.** PU foams are among the most efficient high-performance insulation materials, offering excellent energy savings while occupying minimal space. Their high thermal insulation performances are reflected by a low thermal conductivity ($\lambda$) being the sum of four heat transfer modes, *i.e.*, conduction through the solid PU matrix, gas conduction in the cells, radiative transfer and convection.[205] The $\lambda$ value is significantly influenced by the density and the morpho-structural characteristics of the foams and the nature of the blowing agent. $\lambda$ generally decreases with an increased gas volume fraction, *i.e.*, by lowering the foam density and by using blowing agents with low thermal conductivity/high specific heat capacity, $\lambda$ can be reduced. A reduction in cell size at identical foam density, meaning an increase in cell density, creates more interfaces and scattering events, thereby limiting infrared radiation, while closing the cells minimizes or even suppresses internal convection. A reference value for commercial insulation PU foams is within the range of 20–30 mW $m^{-1}$ $K^{-1}$. Capitalizing on these guidelines, attempts to design PHU foams suitable for thermal insulation applications have been reported. Supercritical $CO_2$-assisted foaming of bio-based thermoplastic PHUs produces low-density foams (110–176 kg $m^{-3}$) with closed cells (100%) averaging 6–10 μm in diameter and exhibiting high cell densities ($1.5 \times 10^{10}$ – $1.75 \times 10^{11}$ cells per $cm^3$).[100] While these structural characteristics are favorable to obtain decent thermal insulation properties, $\lambda$ remains relatively poor, ranging from 50 to 64 mW $m^{-1}$ $K^{-1}$ after 1 year of foam equilibration. These relatively high values are attributed to the selection of $scCO_2$ as the blowing agent, which possesses a low specific heat capacity, non-ideal for insulation purposes, but also to the rapid diffusion of $CO_2$ out of the cells and its replacement by air. Later, Berthé reported lower thermal conductivity values of 43–47 mW $m^{-1}$ $K^{-1}$ for thermoplastic PHUs synthesized from various aromatic cyclic carbonate monomers and foamed using acetone.[77] The reduced $\lambda$ values are correlated to the combined effects of replacing $CO_2$ with acetone as the blowing agent and the quite low foam density (~70 kg $m^{-3}$). However, the morpho-structural characteristics of the foams remain non-optimal, with 85% of the cells being interconnected and too large in diameter (125–150 μm). Following these seminal works, Zhang *et al.* recently advanced PHU foams to a level of thermal insulation performance comparable to conventional PU foams.[105] By formulating thermosetting PHUs from reactive cycloaliphatic bis-cyclic carbonates, *m*-XDA and PEI blended with HFO-1233zd, their foamed materials reached $\lambda$ values of 26.5 mW $m^{-1}$ $K^{-1}$. This enhanced thermal performance has been ascribed to the synergistic effect of a low foam density (139 kg $m^{-3}$), closed-cell morphology (although the cell size averages 500–600 μm) and the intrinsically low thermal conductivity and very low rate of permeation through the cell walls of the chlorofluorocarbon-blowing agent.[206] The addition of cellulose nanocrystal fillers slightly reduces $\lambda$ to 25.8 mW $m^{-1}$ $K^{-1}$ in line with a small decrease in the foam density (131 kg $m^{-3}$) and the barrier effect of the filler on gas diffusion, which is expected to provide long-term thermal insulation performances, even if not demonstrated by the authors. Very recently, thermally insulating rigid PHU foams ($d$ = 210–462 kg $m^{-3}$, $T_g$'s > 80–90 °C) have been fabricated from cyclocarbonated lignin and Jeffamine T-403 monomers, using water or thiol-functional POSS fillers as blowing agents. Unlike comparative foams made using water, the cage-like structure of the POSS filler allows for the nonreinforcement of the PHU matrix (compressive strength = 4.21 MPa). At 1% content, the POSS filler also facilitates the formation of more uniform foams with smaller cell sizes, effectively entrapping air and diminishing both radiative and conductive heat transfer across cell walls. This is reflected in a λ of 40.3 mW $m^{-1}$ $K^{-1}$, *i.e.*, a value significantly lower than the thermal conductivity measured for an analogue water-induced self-blown PHU foam produced without a filler ($\lambda$ of 59 mW $m^{-1}$ $K^{-1}$).[207]

### 5.3. Electromagnetic interference shielding

Electromagnetic interference (EMI) is a common problem that affects electronic components and communication or navigation systems. It is especially critical in sectors such as the military, aerospace, medical, and automotive industries. EMI results from the interaction of an electrical field with a magnetic field, forming electromagnetic waves (EM). These waves radiate in the surrounding environment and create electric and electromagnetic noises disturbing or even compromising the well-functioning of nearby systems such as smartphones, GPS

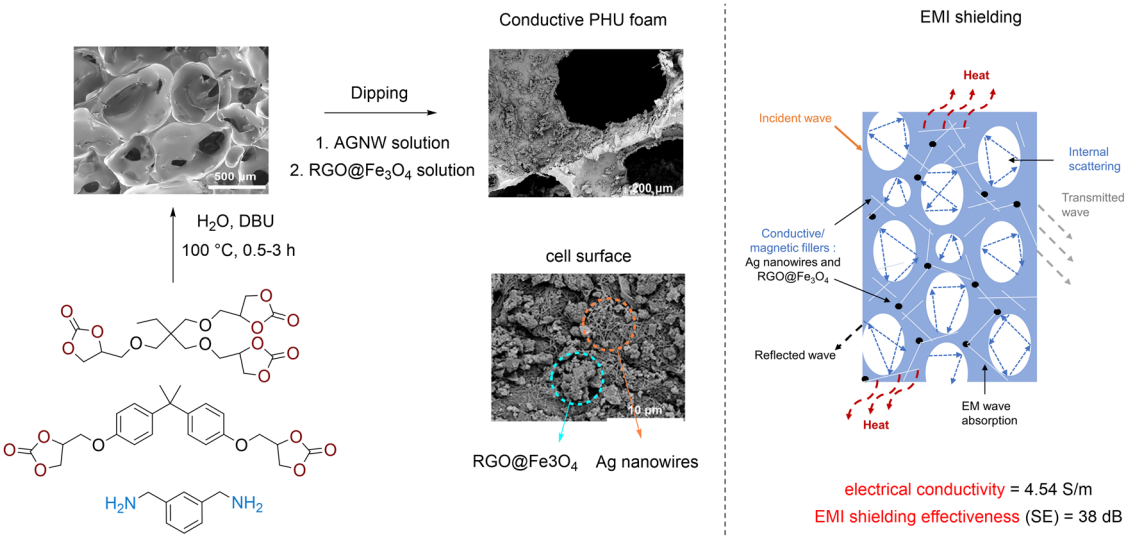


Fig. 19 Conductive PHU/AgNW/RGO@$Fe_3O_4$ composite foams for EMI shielding applications. Content partly reproduced from ref. 172 with permission from the American Chemical Society. Copyright © 2025, American Chemical Society.

devices, wireless tools, radars, or medical imaging equipment like X-rays and MRIs.[208] Long-term exposure to EMI may also carry potential health risks, *e.g.*, miscarriage.[209] In this context, electromagnetic interference shielding across a wide range of frequencies is essential to protect electronic devices from parasitic signals. Traditional shielding films or coatings embedding magnetic and conductive particles primarily block EMI through reflection at the material interface, potentially causing secondary EM pollution.[210,211] In contrast, modified polymer foams demonstrate superior EMI shielding performances.[212–215] Their porous structure, combined with the presence of conductive fillers, promotes multiple internal reflections of EM waves, yet dissipates the energy in the form of heat through an attenuation process and limits the emissions of secondary EM waves (Fig. 19). Uniform open cell $CO_2$ self-blown PHU foams made from TMPTC, bisphenol A diglycidyl carbonate, and *m*-XDA using water as a blowing agent have served as a scaffold to fabricate EMI shielding materials *via* a sequential immersion strategy (Fig. 19).[172] First, insulation PHU foams have been transformed into a conductive material *via* deep coating in an EtOH solution containing silver nanowires (AgNWs) until the percolation threshold is surpassed. After 12 cycles, a maximum of 39.5 wt% of AgNWs has been incorporated within the porous materials, the filler being homogeneously dispersed all along the cell walls. In the second step, the conductive foams are impregnated with reduced graphene oxide@$Fe_3O_4$ composites. This filler, distributed at a 5–20 wt% loading across the cell walls, provides magnetic dipoles for EM radiation absorption. While the virgin PHU foam shows poor shielding efficiency due to its inherent electrical insulation properties, the incorporation of AgNWs yields a highly conductive foam (electrical conductivity of 4.54 S $m^{-1}$) with an electromagnetic interference shielding effectiveness (SE) of 38 dB, surpassing the 20 dB of commercially available solutions. The addition of reduced graphene oxide@$Fe_3O_4$ filler further improves the EMI shielding by improving electromagnetic wave penetration and absorption loss. The best performance is observed with 5 wt% of reduced graphene oxide@$Fe_3O_4$, leading to a remarkable SE of 66 dB. This work represents the sole example of PHU-based foams where synergistic effects between dielectric loss from AgNWs and magnetic loss from $Fe_3O_4$ significantly boost EMI shielding performances.

### 5.4. Antibacterial foam dressing for wound healing

Hydrophilic PU foams have emerged as advanced care materials for the healing of chronic wounds caused by injuries, diabetes or burns. When used as dressings, they can absorb a large amount of exudate, reducing the risk of maceration, while maintaining an ideal moist/dry environment, promoting faster tissue regeneration.[216–220] Their easy loading ability with bioactive ingredients such as Ag nanoparticles also imparts them with antimicrobial properties, minimizing bacterial infections and preventing healing complications. The intrinsic hydrophilic features of PHUs inspired Chen to design self-blowing open-cell foams (cell size of ~300 µm) for antibacterial and wound healing applications from cyclocarbonated lignin, a mixture of polyetheramines, PMH blowing agent and silver nanoparticles (Fig. 20).[120] The biocompatibility of the resulting foams is demonstrated through hemolysis tests on blood cells. The observed hemolysis below 3% indicates minimal disruption of red blood cells in the bloodstream and a low release of free hemoglobin, well within acceptable biocompatibility criteria. Besides, the foams showed no cytotoxicity, with fibroblast viability exceeding 100% after 24 h, further meaning the dressing is conducive for cell growth. The presence of Ag nanoparticles (10%) imparts to the foams antimicrobial properties with a bactericidal efficiency of 95% and 99% after 8 h exposure for *S. aureus* and *E. coli* (Fig. 20B–D), respectively. Finally, the wound healing potential of Ag-loaded PHU foams is attested *in vivo* in mice. Compared to commercial Tegaderm® films, the

 

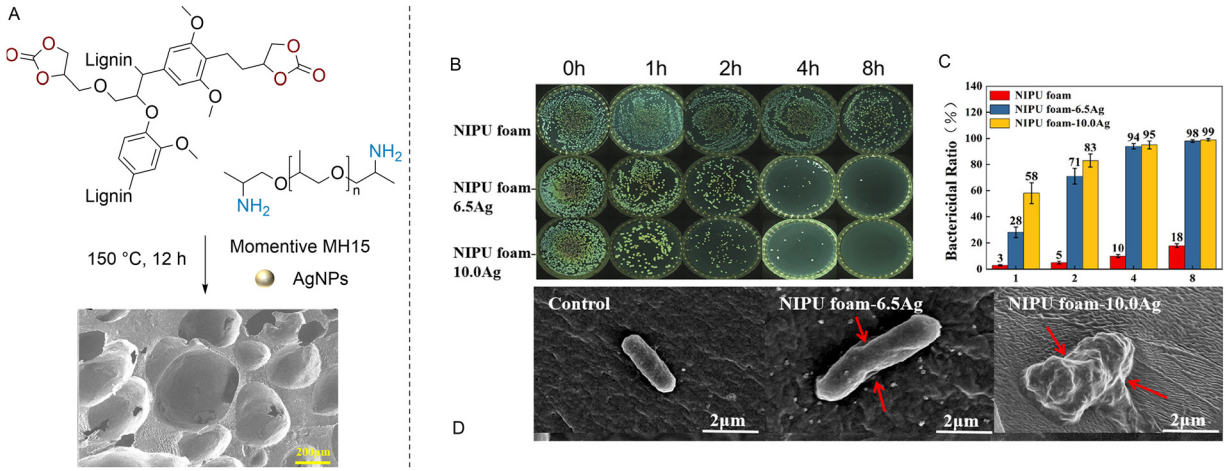


Fig. 20 $H_2$ self-blown PHU foams loaded with 6.5 or 10 wt% (*vs.* carbonated lignin) of Ag nanoparticles for antibacterial and wound healing applications. (A) Foam formulation; (B) antibacterial effect of AgNP-loaded PHU foams on *E. coli*; (C) bactericidal efficiency with time and (D) morphology of *E. coli* before and after 4 h of coculture on (AgNP-loaded) NIPU foams. Content partly reproduced from ref. 120 with permission from the American Chemical Society. Copyright © 2024, American Chemical Society.

PHU dressings exhibited superior wound healing performance, as evidenced by enhanced collagen deposition and blood vessel proliferation, which accelerated the regeneration of fibrous connective tissue, resulting in faster wound closure.

### 5.5. Sensing and pollutant capture

Exposure to pollutants such as formaldehyde, heavy metals, drugs, pesticide residues, *etc.* has become a major scourge of our modern society. Consequently, the removal of these substances from our environment represents a significant challenge. Porous materials[221,222] and open-cell PU foams offer a promising solution by functioning as sponges that trap pollutants.[223–225] Incorporating fluorophores (*e.g.*, polyaromatic groups,[226–228] lanthanide complexes,[229,230] organic dyes[231]) within the foam leads to modified porous materials serving as fluorescent sensors for both the detection and quantification of pollutants. PHU foams, especially those self-blown using water or a physical blowing agent, exhibit a non-conventional fluorescence behavior with a multicolor emission even without the use of fluorescent probes.[105,232] This non-conventional fluorescence behavior arises from aggregation-induced emission (AIE) luminogens that are naturally present within the foams. The AIE phenomenon is promoted by the abundance of hydroxyl groups along the PHU skeleton, prone to hydrogen bonding, yet favoring clusteroluminescence. Analytes or molecules interacting with these clusters may affect the fluorescence of the PHU foam. Consequently, the modification of the multicolor emission of PHU foams is advantageously exploited for multipurpose sensing applications.[232] Functional open-cell foams (290 kg $m^{-3}$) were specifically designed from TMPTC, EDR and the PEI polyamine using water as a blowing agent. The presence of multiple (reactive) amine moieties within the polymer backbone imparts formaldehyde-capturing and metal-complexing capabilities to the foam, leading to notable changes in both its thermo-mechanical and clusteroluminescence properties. The irreversible reaction between residual primary amines and formaldehyde[139] (7 days of exposure at r.T.) reduces the pollutant concentration by 2/3 and forms stable adducts. These structural changes increase the foam $T_g$ from −3 °C to 8 °C and form higher-order aggregates. These changes induce a red shift in fluorescence emission, with a maximum signal shifting from 450 to 495 nm upon excitation at a wavelength ($\lambda_{ex}$) of 380 nm. Formaldehyde capture is further evidenced by a fluorescence color shift in the foam from cyan to green at $\lambda_{ex}$ = 454 nm. These PHU foams have also been used for metal ion sensing applications in water solutions (Fig. 21). Among a broad list of cations, foams could complex $Cu^{2+}$, $Fe^{2+}$, $Fe^{3+}$ and $Hg^{2+}$ ions as highlighted by quenching efficiencies of the fluorescence emission spectra of 73.2% to 90.5%. Monitoring the quenching of the fluorescence intensity (upon excitation at 380 nm) at various ion concentrations allowed for the precise quantification of the metal cation, with maximum foam/$Cu^{2+}$, $Fe^{2+}$ or $Fe^{3+}$ binding efficiencies of respectively 81, 196.6 and 60.2 mg $g^{-1}$. The utility of these nonconventional fluorescent foams is further illustrated by the ratiometric sensing and quantification of tetracycline, a bacteriostatic antibiotic active against various pathogens such as *Streptococcus*, *Staphylococcus*, *etc.* This drug forms a complex with the foam by H-bonding, which translates into an increase of the $T_g$ from −3° to 11 °C and a red shift from 452 nm to 518 nm of the fluorescence emission spectrum upon excitation at 380 nm (for a drug concentration of 1.25 × $10^{-4}$ mol $L^{-1}$ in water). Like metal ions, the quantification of drug residues has been realized by monitoring the decrease in intensity of the emission spectra, which revealed a limit of detection of the drug at a concentration as low as 3.17 × $10^{-8}$ mol $L^{-1}$. Exposing the PHU foam to an increasing concentration of drug results in a multicolor fluorescence evolution from blue to green to yellow upon UV exposure ($\lambda_{ex}$ = 454 nm). This inspired the development of a smartphone-based detection device equipped with an RGB color scanning app to monitor fluorescence color changes, enabling rapid, on-site visual detection of tetracycline in aqueous solutions. When reshaped into PHU films, these hydrophilic, non-conventional fluorescent PHU

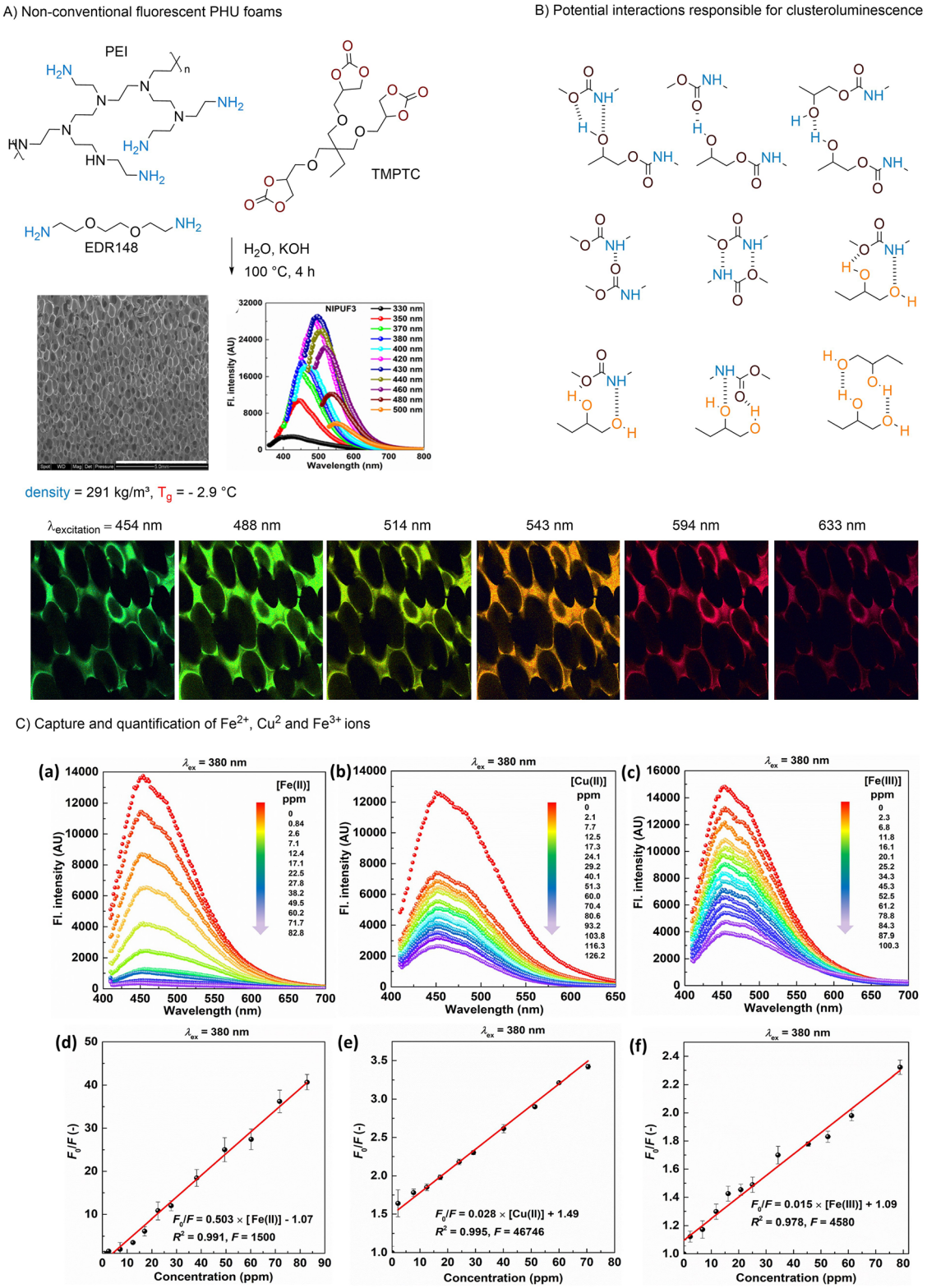


Fig. 21 Non-conventional fluorescent $CO_2$ self-blown PHU foams for metal capture and quantification (A). Potential interactions responsible for clusteroluminescence and SEM image of the foams at various excitation wavelengths (B). Capture of $Fe^{2+}$, $Cu^{2+}$ and $Fe^{3+}$ ions by foams and quantification of their concentration *via* fluorescence (C). Content partly reproduced from ref. 232 with permission from John Wiley and Sons. Copyright © 2024, Wiley-VCH Verlag GmbH & Co. KGaA, Weinheim.

**Take-home message**

**Key differences between conventional PU and NIPU applications**

*Difference 1 – Soft and rigid foams*. PU foaming, a well-established and versatile technology, offers tailored foam solutions for comfort and insulation applications. Adjusting formulation and foaming processes allows for the production of soft elastomeric to rigid foams with controllable properties like crosslink density, cell porosity, thermal stability, resilience, flexibility, and thermal or acoustic insulation. In contrast, NIPU foaming chemistries and processes are still under development, challenging precise control over key foam characteristics like cell morphology, size, and density. Designing high $T_g$ materials and mitigating hydroplasticization of PHU foams also pose difficulties. Open-cell flexible NIPU foams are accessible and exhibit excellent resilience and flexibility, promising seating and cushioning applications. Thermal insulating NIPU foams have been fabricated, but their performance is not yet comparable to commercial PU materials.

*Difference 2 – (Multi)functional foams*. Advanced multi-functional PU foams find applications beyond comfort and insulation, including structural panels, electronic shielding, environmental filtration, biomedical dressings, antimicrobial foams, tissue engineering scaffolds, and smart materials. Emerging NIPU foam applications, limited to PHU materials, utilize their unique hydrophilic nature and clusteroluminescence for diverse functionalities. These foams can sense and quantify pollutants from wastewater, and when infused with phase change materials, they serve as efficient heat storage systems for r.T use. Furthermore, their exceptional biocompatibility and hemocompatibility render them highly appealing for the development of novel biomaterials.

*Difference 3 – Fire resistance*. NIPU foams lack thermally stable isocyanurate structures found in conventional PU foams, promoting char formation and limiting oxygen diffusion during combustion. Achieving a limiting oxygen index value above 27% requires the addition of specific flame retardants.

**Main challenges for NIPU applications**

*Challenge 1 – Performance improvement*. Enhancing fatigue resistance and elasticity of flexible NIPU foams for cushioning, furniture, seats, and mattresses requires producing low-density materials ($<80$ kg m$^{-3}$) with reduced cell size and controlled network crosslinking. Rigid insulating NIPU foams with closed cells, high cell density, and a density below 40–50 kg m$^{-3}$ are crucial to reduce thermal conductivity below 25 mW m$^{-1}$ K$^{-1}$, provided a low-specific heat capacity blowing agent is used. Given the high $T_g$ properties required for this application, a meticulous and challenging selection of monomers, as well as additives (*e.g.* surfactants, nucleating agents), is essential, accompanied by the intricate task of designing solvent-free formulations.

*Challenge 2 – Aging*. The long-term stability and durability of optimized NIPU foams should be evaluated through standardized accelerated aging tests. These tests assess dimensional stability, surface cracking, morpho-structural changes and mechanical performance loss under various stresses. Resistance to UV, photo-oxidation, moisture, chemical/humidity exposure and heat must be systematically examined to ensure reliable long-term performance.

*Challenge 3 – Fire resistance*. Combining nanofillers like nanoclays and expandable graphite is expected to enhance foam fire resistance by synergistically stabilizing the char layer and reducing dripping. Chemical modifications like PHU phosphorylation or targeted surface treatments might further improve fire resistance. Choosing the most efficient flame retardant should minimize loading, preserving the thermo-mechanical and morpho-structural properties of the foam. Reactive additives should be preferred to limit migration outside the foam.

*Challenge 4 – Compliance with industrial and regulatory obligations*. Any new NIPU material reaching similar performances or outperforming conventional PU foams will have to comply with a series of standardized tests and specifications (ASTM, ISO) tailored to the targeted application, ensuring technical, safety, and regulatory compliance.

foams can be utilized for monitoring relative humidity while simultaneously determining the $T_g$'s of the PHU matrix. The fluorescence response of the PHU film is indeed influenced by the disruption of intramolecular hydrogen bonds caused by water molecules, directly impacting the clusteroluminescence of the material. Linear correlations between relative fluorescence intensity and RH and with $T_g$'s of NIPU are indeed observed, facilitating the efficient and rapid monitoring of RH and hydroplasticization.[233]

## 6. Conclusions and perspectives

The last decade has seen significant progress in non-isocyanate polyurethane chemistry and advanced NIPU materials design. While accessing high molar mass thermoplastic NIPUs remains difficult, most synthetic methods are especially suitable for producing thermosetting resins, like those used in traditional PU foams. Virtually, NIPUs, more particularly poly(hydroxyurethane)s made from the step-growth copolymerization of polycyclic carbonates with polyamines, have the potential to serve as alternatives to conventional PU foams. However, the polymerization kinetics of these PHU systems are generally slower than those of the traditional isocyanate/polyol (foaming) process. The microstructure of PHUs also differs from that of conventional PUs by the presence of dangling OH groups and the absence of biuret, allophanate, isocyanurate and uretdione linkages. All these structural motifs derived from the isocyanate chemistry play a crucial role in imparting the excellent thermo-mechanical properties of PU foams. Therefore, transferring a PU foaming process to PHUs is not straightforward and requires adjustments to account for these differences.

Precise control of the viscosity of the formulation, the gelation and curing rates of the PHU matrix, and the release of the blowing agent (whether endogenous or exogenous) is critical for timely gas generation and matrix curing. This coordination ensures an efficient expansion of the matrix, minimizes cell drainage and foam collapse, and ultimately guarantees the dimensional stability of the final materials. Although the aminolysis of cyclic carbonates proceeds relatively slowly, it readily occurs within the temperature range of 80–140 °C. To ensure proper foaming under these conditions, physical blowing agents with high boiling points (e.g., (fluoro)hydrocarbons) and moderate vapor pressure, or chemical blowing agents with a controllable decomposition rate (*e.g.*, $Na_2CO_3$), are preferred.

In self-foaming processes, the blowing agent, usually $H_2$ or $CO_2$, is generated *in situ* by the decomposition of one of the foam components (*e.g.*, Momentive or the cyclic carbonate) contributing to the formation of the polymer matrix. As a trend, this decomposition reaction should be slightly delayed relative to the formation of urethane linkages to ensure the gas delivery when the matrix is sufficiently viscous and close to gelation.

In $CO_2$ self-blowing PHUs, the decarboxylation of the cyclic carbonates is initiated and adjusted either by adapting the concentration of the additive (water or thiol), the nucleophilic character of the thiol and the nature/content of the base catalyst. As Momentive and thiol participate in polymer network formation, their content in the formulation influences the thermo-mechanical properties of the final material. Usually, both components introduce flexibility within the network, favoring the fabrication of flexible foams. When water is used as an additive, part of the cyclic carbonate moieties are sacrificed to generate $CO_2$ *in situ*. To ensure sufficient network crosslinking, preventing the foam collapse, and decent mechanical properties of the foam, the level of sacrificial cyclic carbonates should not exceed 25%.

Catalysts, generally organobases, influence the foaming process of NIPUs by regulating the kinetics of all reactions at play. The control of these kinetics may be affected by ''external'' factors, especially for PHU foaming. Water, used to promote the *in situ* release of $CO_2$, and/or halide salts, used to catalyze the production of cyclic carbonates by $CO_2$/epoxide coupling, accelerate the gelation of the matrix. Water plays a dual role. It disrupts hydrogen bonds between PHU chains, increasing chain mobility, and enhances the electrophilicity of the carbonyl site by H-bonding, thereby facilitating amine attack and hydroxyurethane linkage formation. Cyclic carbonates are usually not purified before PHU synthesis and are thus contaminated by the catalyst. The halide salt residues may interact with the oxygen atom of the carbonyl, further influencing the aminolysis rate of the carbonate ring. This underlines the necessity to consider the co-catalytic role of these halide salt residues when optimizing foaming processes.

The foaming reactions of PHUs or other NIPUs display generally insufficient exothermicity, resulting in a prolonged curing procedure at elevated temperature to obtain stable foams. To address this limitation, hybridizing NIPU chemistry with additives such as epoxides or exovinylene cyclic carbonates, serving as heat-release promoters, offers a promising solution. These additives undergo highly exothermic reactions with amines, enabling the formulation to rapidly reach the foaming threshold within minutes, even under r.T. conditions. Compared to aliphatic epoxides, aromatic epoxides promote higher exotherms upon aminolysis and their use tends to improve the rigidity of the PHU foams. Exovinylene cyclic carbonates allow for rapid foam expansion ($\sim$1 min). This hybridization approach not only enhances process efficiency but also paves the way to retrofitting existing industrial PU manufacturing lines where foaming should be very fast (*i.e.*, within minutes). Importantly, self-blown NIPU foams of high potential bio-based contents (>90 wt%) are also easily accessible by valorizing carbon dioxide and bio-based products (*e.g.*, vegetable oil derivatives, sugars) as raw materials, as well as abundant biowastes as biofillers (*e.g.*, lignin derivatives, cellulose, keratin, chitosan, *etc.*).

Most foaming methodologies produce materials with densities typically >100–150 kg $m^{-3}$ and open-cell structures. Access to very low-density materials (<50 kg $m^{-3}$) with high cell density, small cell diameters and close porosity is necessary to match the performances and specifications of conventional foams, such as those used in thermal insulation panels. In this context, controlling the morpho-structural properties of NIPU foams will result from a complex interplay between surfactant properties and synchronization between the kinetics of gas generation/escape and NIPU curing. To date, most of the NIPU foaming approaches don't use surfactants or exploit surfactants that have not been specifically designed for NIPU foaming. Without surfactants or with the use of poorly efficient surfactants, the gas–liquid interface cannot support any mechanical stress. Upon blowing agent release, the rising internal pressure drives rapid cell expansion, thinning the interface and leading to cell wall rupture. This further creates open porosity and even foam collapse if NIPU formation/solidification is not synchronized with bubble growth.

Silicone surfactants specifically tailored for NIPU are expected to control the initial bubble dispersion stage by stabilizing the air bubble/liquid interface created upon monomer mixing. Then, during the cell expansion step by release of the blowing agent, a surface tension gradient will be generated at the gas–liquid interface, slowing down the drainage flow rate of the thinning cell wall by the Marangoni effect. In low viscosity NIPU matrices lacking effective stabilization and mechanical resistance of the cell walls, the fast drainage leads to rapid cell rupture and foam collapse. Conversely, controlling the release of the blowing agent and the solidification of the NIPU, for instance by manipulating catalysis, should enable a finite cell expansion rate that provides sufficient time for surfactant diffusion and accommodation to alterations in the cell/polymer interface. The appropriate regulation of these phenomena should enable the formation of highly uniform low-density foams with closed-cell porosity, contingent upon the identification of suitable stabilizers.

Inherent to PHUs, the presence of OH moieties along the polymer skeleton makes the final material intrinsically hydrophilic. PHUs tend to easily absorb humidity, leading to plasticization with a significant drop in the foam's $T_g$ values (up to 40 °C). Therefore, achieving rigid PHU foams with $T_g$ > 80 °C remains challenging, even when using aromatic monomers, and foam properties can change upon exposure to different humidity conditions. The plasticization of PHU foams remains a substantial bottleneck, as it hinders the development of PHU foams that can effectively compete with PU foams in similar applications, resulting in less favorable performance. When similar applications are targeted, solutions addressing this issue, *e.g.*, by suppressing or transforming the pending OH moieties, or conceptualizing new NIPU foaming strategies, should be considered in future works. PHU foams can also be advantageous in applications where hydrophilicity is required, as more hydrophobic PU foams may not be the ideal products. This has been demonstrated in designing wound dressings capable of absorbing large volumes of exudate and in developing shape-memory materials.[156] Further applications necessitating this hydrophilicity characteristic should be identified and investigated to facilitate the penetration of PHU foams into this specific foam market.

Today, addressing the end-of-life of NIPU foams is key to creating sustainable materials. The challenges and priorities

 

Table 1 Selection guide of monomers, blowing agent and heat release promoters for PHU foams

| | | |
|---|---|---|
| Monomers for PHU foams | Polycyclic carbonates | 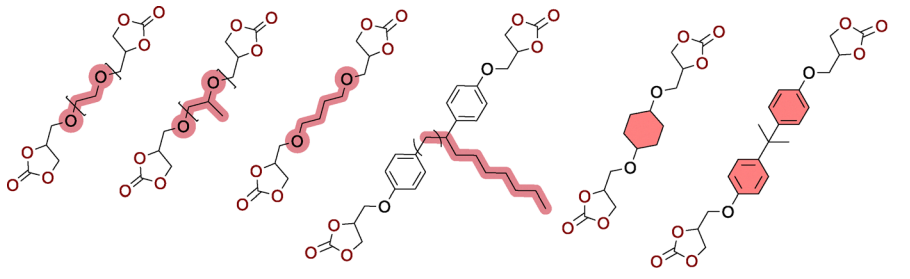  |
| | Polyamines | 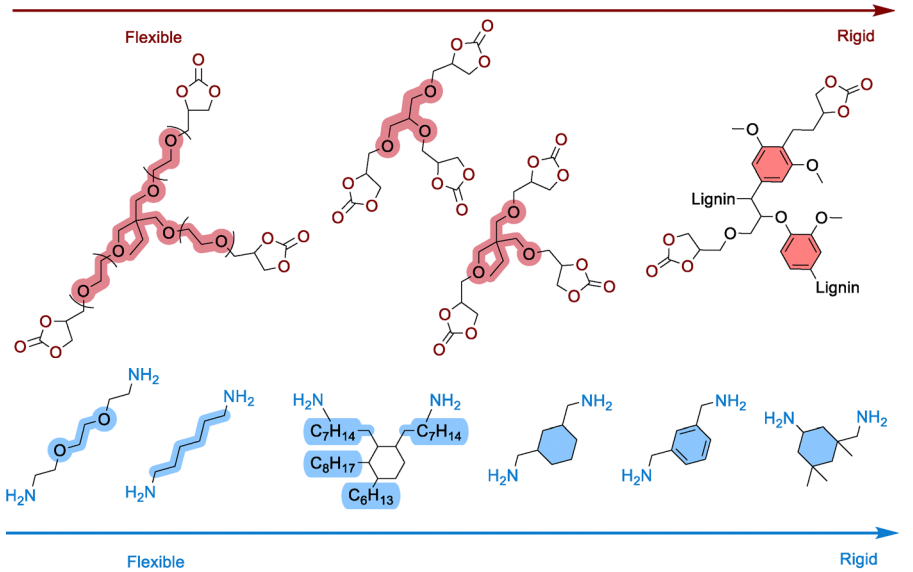  |
| Heat release promoters (r.T. foaming) | Polyepoxides | 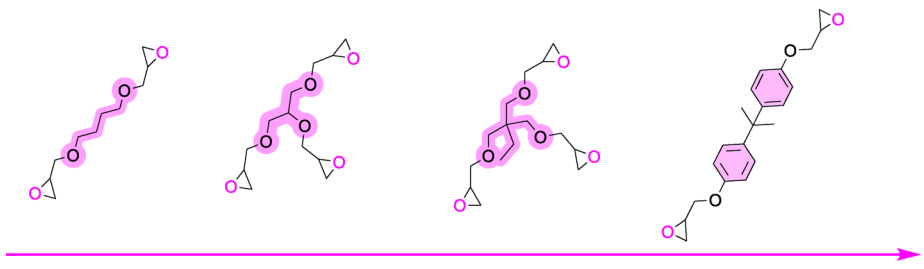  |
| Blowing agent[a] | Polythiols ($CO_2$ self-foaming) | 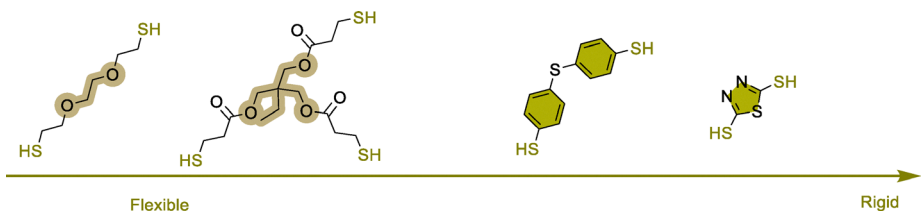  |

Water-induced $CO_2$ self-foaming PHUs: formation of non-reactive vicinal diols upon hydrolysis of cyclic carbonates, the content of sacrificial cyclic carbonates should not exceed 25% to maintain network integrity. $H_2$-induced self-foaming PHUs: use 1–5 wt% of Momentive MH15, Momentive brings flexibility to PHU foams. Latent amine blowing agents (*i.e.* amine/$CO_2$ adducts): suffer from high decomposition temperature. [a] Other blowing systems: chemical and physical blowing agents do not affect the PHU microstructure, closed-cell porosity is accessible using $scCO_2$ as a blowing agent, but this method is limited to the foaming of thermoplastics.

Table 2 NIPUs from carbonate–amine polyaddition (PHU), foaming procedures and general foam properties

| NIPU type | Blowing technique | Blowing agent | | Foaming procedure | Density (kg m$^{-3}$) | Cell size and morphology (μm) | $T_g$ (°C) | Mechanical properties |
|---|---|---|---|---|---|---|---|---|
| Thermo-plastics | Physical foaming | $scCO_2$ | | Impregnation: 40 °C, 300 bar<br>Foaming: 80 °C[100] | 110–180 | Narrow distribution<br>Closed cell<br>3–10 | −2 to −6 ($T_m$ ~ 88 °C) | Rigid<br>Compression modulus 1.8–4.75 MPa (strain 80%) |
| | | | | Impregnation: 80 °C, 300 bar<br>Foaming: 80 °C[101] | 200–400 | Broad distribution<br>Closed cell<br>9–23 | 30 | Rigid<br>Compression modulus 0.123–0.149 MPa (strain 25%) |
| | | Acetone | | ($T_g$ − 5) °C<br>Vacuum[77] | 35 | Open cell<br>125–150 | 80–110 | Highly rigid<br>Compression modulus 0.23–0.30 MPa (strain 15%) |
| Thermosets | Physical foaming | HFC (Solkane®365) | | 80 °C, 14 h[104] | 140–220 | Open cell<br>135–170 | 1 | Flexible<br>Compression modulus 0.0175 MPa (strain 40%) |
| | | HFO (1233zd) | | 80 °C, 14 h[105] | 140 | Closed cell<br>800 | 39 | Rigid<br>Compression modulus 0.15–0.35 MPa |
| | Chemical foaming | $NaHCO_3$ | $CO_2$<br>$H_2O$ | 150 °C, 6 min[107] | 140–480 | Open cell<br>15–330 | NA | NA |
| | | $NH_4HCO_3$<br>citric acid | $CO_2$<br>$H_2O$ | 80 °C, 15 min[109] | NA | NA | 42 | Rigid<br>Compression modulus NA |
| | | Azo-compound<br>ZnO | $N_2$<br>CO<br>$NH_3$ | 120 °C, 30 min, then 60 °C, 30 min[113] | 230–440 | Open cell<br>150–300 | 5–7 | Flexible<br>Compression modulus 0.19–0.20 MPa (strain 50%) |
| | Self-foaming | Poly(methyl-hydrogeno-siloxane) | $H_2$ | 80–150 °C<br>TBD catalysis[114,117,118] | 190–330 | Closed cell and open cell | −18 to 100 | Flexible to rigid<br>Compression modulus 0.0005–0.003 MPa (strain 20%)<br>0.80–0.130 (strain 10%) |
| | | | | r.T. (foaming: 3–7 days)<br>Thiourea catalysis[115] | 270–300 | Open cell<br>140–1300 | 0–11 | Flexible<br>Compression modulus 0.02–0.075 MPa (strain 30%) |
| | | | | 50 °C, overnight<br>120 °C, 2 h<br>6-membered cyclic carbonates[116] | 170–350 | Open cell<br>210–1350 | 7–27 | Flexible to rigid<br>Compression modulus 0.14–0.215 MPa (strain 50%) |
| | | Thiol induced | $CO_2$ | 100 °C<br>Alkyl thiol, DBU catalysis[128,133,134,136] | 140–175 | Open cell<br>250–980 | −30 to 25 | Flexible<br>Compression modulus 0.008–0.065 MPa (strain 50%) |
| | | | | 100 °C<br>Aromatic thiol (foaming: 5–10 min)[130] | 200–300 | Open cell<br>900–1300 | 8–45 | Flexible to rigid<br>Compression modulus 0.35–0.4 MPa (strain 50%) |
| | | | | 80–100 °C, 4 h<br>"Masked" thiol DBU or no catalysis[134,135] | 170–440 | Open cell<br>500–2000 | −25 to 15 | Flexible<br>Compression modulus 0.001–0.21 MPa (strain 10%) |
| | | | | r.T. (foaming: 3–10 min)<br>Exotherm inducer: epoxy[130] | 220–400 | Open cell<br>310–540 | −17 to 49 | Flexible to rigid<br>Compression modulus 0.096–81 MPa (strain 50%) |
| | | Water induced | $CO_2$ | 80–100 °C<br>DBU or KOH catalysis[140,232,235] | 150–370 | Open cell<br>230–5400 | −7.1 to 25 | Flexible to semi-rigid<br>Compression modulus 0.03–0.149 MPa (strain 70%) |
| | | | | r.T. (foaming: 3–10 min)<br>Exotherm inducer: epoxy[141,143] | 150–300 | Open cell<br>420–920 | −7 to 47 | Flexible to rigid<br>Compression modulus 0.0067–1.9 MPa (strain 6%) |
| | | | | r.T. (foaming: 1–10 min)<br>Exotherm inducer: αCC carbonate[144] | 170–390 | Open cell<br>85–180 | −4 to 36 | Flexible to rigid<br>Compression modulus 0.02–8.9 MPa (strain 12%, 40% humidity) |
| | | Amine–$CO_2$ adduct | $CO_2$ | 60 °C<br>1 step process: liquid amine/$CO_2$ adduct + 5CC[152] | 200–460 | Open cell<br>180–2000 | 14–24 | Flexible<br>Compression modulus NA |
| | | | | 100–140 °C<br>2 step process: – Prepolymerization, $scCO_2$ impregnation[156] | 270–450 | Open cell<br>330–910 | −3 to 0 (wet)<br>28–49 (dried) | Flexible<br>Compression modulus 0.000025 (wet) – 9 MPa dried) (strain 50%) |

identified in conventional PU recycling by Malucelli provide a relevant framework that should also be considered for NIPUs, particularly when aiming to integrate into the same waste streams (including collection and sorting).[174] Well-established, industrially viable recycling strategies based on physical and chemical recycling should then be adapted to NIPUs. The intrinsic CAN behavior of PHUs allows physical reprocessing of foams *via* compression molding into various second-life materials (films, adhesives). By taking inspiration from recent discoveries by Dichtel, the CAN properties of PHUs pave the way to the future direct reuse of EoL polyurethane foams as a raw material for new foam fabrication through extrusion-foaming (foam-to-foam recycling).[176] Chemical recycling of NIPU foams, *via* hydroglycolysis, should focus on the design of efficient catalysts to transform waste foams into ready-to-reuse high-quality recycled raw materials, which in turn can be reincorporated in a loop into new foam formulations. Future recycling concepts should integrate the "designed-for-recycling" approach, leading to new added-value chemicals, far beyond conventional polyol or polyamine "liquors" typically formed *via* hydrolysis, glycolysis or aminolysis of PUs. Finally, life cycle assessment (LCA) of NIPU foams over the entire value chain, *i.e.*, from monomer synthesis to material recycling, is essential to confirm their potential for reducing environmental impacts. As it stands, the only existing LCA of PHU bulk materials reveals a clear negative impact on three key indicators, *i.e.*, fossil fuel consumption, greenhouse gas (GHG) emissions and water consumption.[234] Energy consumption is 14.3% higher for PHUs than for conventional PUs. However, the emergence of r.T. foaming solutions for NIPU should lead to significant improvements in this key indicator. GHG emission penalty is expected to decrease by using renewable chemicals. This is particularly evident for PHUs for which a large diversity of cyclic carbonate precursors are now accessible from biogenic $CO_2$ and bio-renewable raw epoxides. By considering biogenic chemicals in the simulation, a reduction in GHG emissions of 11.5% to 16.1% has been predicted for PHU production compared to PUs. Finally, the negative contribution of PHU towards water consumption stems from its inherently demanding use as a solvent during the depolymerization process. This underlines the strong need to improve/optimize the recycling scenario of NIPUs and adapt the protocols to the decomposition of foams. The emergence of predictive machine learning and artificial intelligence tools could play an important role in the future, not only in the development of environmentally friendlier solutions but also in facilitating the selection of monomers to guide the design of materials with specifications tailored on demand to the requirements of the targeted application. Pending the deployment of these tools, a "monomer selection guide" (Table 1) and two tables summarizing the morpho-structural and mechanical properties of NIPU foams, distinguishing PHUs (Table 2) from other types of non-isocyanate PUs (Table 3), are provided below.

Predicting the fabrication costs of NIPU foams presents a significant challenge due to the ongoing absence of mass production for certain key reactants, such as cyclic carbonates in PHU materials. Although there is no techno-economic study of NIPU foam production yet, a preliminary Aspen techno-economic simulation suggests that the production cost of PHU thermoplastic could approach a level of competitiveness comparable to conventional fossil-based flexible polyurethane (PU).[234] In the proposed scenario, the thermoplastic was obtained by copolymerizing in dimethylformamide (DMF) a bis(cyclic carbonate), synthesized from 1,3-butadiene and carbon dioxide ($CO_2$), with a mixture of diamines, *i.e.*, amino-telechelic poly(butadiene-*co*-acrylonitrile) (PBN) and *p*-xylylenediamine (*p*-XDA). The minimum selling price (MSP) was estimated at 5.37 USD per kg, assuming a 20% internal rate of return. This MSP was higher than that of conventional PUs (3.53–4.49 USD per kg). Total production costs were primarily driven by raw materials, contributing to 59% of the overall cost. Operating expenses accounted for an additional 16%, while the remaining costs were attributed to taxes, utilities, and capital expenditures. With respect to the reactant cost, amines, particularly PBN, accounted for 62% of the total. A sensitivity analysis revealed that a reduction in amine prices or the replacement of PBN with less expensive alternatives, lower capital expenditures, and increased plant capacity could significantly decrease MSPs. Notably, scaling production to industrially relevant capacities up to 9000 t per year would facilitate economies of scale, resulting in an MSP reduction of 0.88 USD $kg^{-1}$. Cumulatively, these changes could reduce the MSP of PHU to a production cost of 4.19 USD per kg.

Table 3 NIPUs from transurethanization and polycondensation, foaming procedures and general foam properties

| NIPU type | Blowing technique | Blowing agent | Foaming procedure | Density (kg $m^{-3}$) | Cell size and morphology (μm) | $T_g$ (°C) | Mechanical properties |
|---|---|---|---|---|---|---|---|
| Thermosets | Physical | Water/ethanol | 73–120 °C, 2 h[106] | 55–950 | Open cell 140–3000 | −20 to −18 | Highly flexible Compression modulus 0.0007–0.003 MPa (strain 25%) |
| Amino-telechelic oligo-NIPU Epoxide crosslinker | Self-foaming | Poly(methylhydrogeno-siloxane) $H_2$ | r.T. −100 °C[121] | 130–400 | Open cell 210–430 | Self-foaming | Flexible Compression modulus 0.001–0.005 MPa (strain 50%) |
| Thermosets Amonio-telechelic oligo-NIPU Glutaraldehyde crosslinker | "Emulsion-like" templated | Citric acid, glutaraldehyde, water — | r.T. −160 °C[166] 2 step process: oligomerization, curing 80–160 °C for 2–10 h[160,164] | 80–470 | Open cell 200–2000 | NA–112 | Flexible to rigid Compression modulus 0.0015–1.2 MPa (strain 50%) |

These preliminary techno-economic analyses suggest that, under optimized conditions, PHU-based materials could approach cost competitiveness with conventional fossil-based polyurethanes. More broadly, they underscore the strong long-term potential of NIPU chemistry, positioning it as a promising and forward-looking platform for the development of next-generation polyurethane materials.

## Conflicts of interest

There are no conflicts to declare.

## Data availability

As this paper is a tutorial review, no primary research results, software or code have been included and no new data were generated or analysed.

## Acknowledgements

The authors thank the European Commission for its support in the frame of the European Union's Horizon 2020 research and innovation program under the Marie Skłodowska-Curie grant agreement no. 955700. B. G. thanks the FNRS for funding the CO2smos project (PDR – ID application 40028664). C. D. thanks the Region Wallonne for funding the WEL-T Advanced Grant "CHEMISTRY" project (application WEL-T-CR-2023 A – 02) and the Win2Wal project "ECOFOAM" (convention 2010130). C. D. and J. M. R. are FNRS Research Directors and thank FNRS for financial support and the European Regional Development Fund (ERDF-FEDER) for general support in the frame of UP_PLASTICS portfolio. H. S. thanks the European Union's Horizon 2020 in the frame of the Research and Innovation Program under the Grant TED2021-129852B-C22 funded by MCIU/AEI/10.13039/501100011033 and by the European Union NextGenerationEU/PRTR and the Grant PID2022-138199NB-I00 funded by MCIU/AEI/10.13039/501100011033. T. V. and H. C. would like to acknowledge the French government funding managed by the National Research Agency under the France 2030 program, reference ANR-23-PEXD-0008, project GreenFOAM.

## References

1 MarketsandMarkets, Polyurethane Foams Market – Global Forecast to 2030, 2024.
2 A. Mohammadi, A. Doctorsafaei, M. Ghodsieh and S. Beigi-Boroujeni, *Polymeric Foams: Fundamentals and Types of Foams (Volume 1)*, American Chemical Society, 2023, vol. 1439, pp. 143–159, SE–7.
3 N. V. Gama, A. Ferreira and A. Barros-Timmons, *Materials*, 2018, **11**, 1841.
4 M. Ates, S. Karadag, A. A. Eker and B. Eker, *Polym. Int.*, 2022, **71**, 1157–1163.
5 J. Peyrton and L. Avérous, *Mater. Sci. Eng., R*, 2021, **145**, 100608.
6 E. Delebecq, J.-P. Pascault, B. Boutevin and F. Ganachaud, *Chem. Rev.*, 2013, **113**, 80–118.
7 G. Coste, C. Negrell and S. Caillol, *Eur. Polym. J.*, 2020, **140**, 110029.
8 F. Monie, T. Vidil, B. Grignard, H. Cramail and C. Detrembleur, *Mater. Sci. Eng., R*, 2021, **145**, 100628.
9 A. Ghosh, J. T. Orasugh, S. S. Ray and D. Chattopadhayay, *Polymeric Foams: Fundamentals and Types of Foams (Volume 1)*, American Chemical Society, 2023, vol. 1439, pp. 4–63.
10 S. Merenyi, *With an Introduction and Future Prospects Regarding the Area of Chemicals Legislation*, GRIN Verlag (2012), Article 20123656293538, REACH: regulation (EC) No 1907/2006: consolidated version.
11 B. Grignard, S. Gennen, C. Jérôme, A. W. Kleij and C. Detrembleur, *Chem. Soc. Rev.*, 2019, **48**, 4466–4514.
12 A. Delavarde, G. Savin, P. Derkenne, M. Boursier, R. Morales-Cerrada, B. Nottelet, J. Pinaud and S. Caillol, *Prog. Polym. Sci.*, 2024, **151**, 101805.
13 X. Ou, Y. Niu, Q. Liu, L. Li, F. Wei, Y. Cui, Y. Zhou and F. Yan, *Prog. Polym. Sci.*, 2024, **149**, 101780.
14 A. Mouren and L. Avérous, *Chem. Soc. Rev.*, 2023, **52**, 277–317.
15 F. D. Bobbink, A. P. van Muyden and P. J. Dyson, *Chem. Commun.*, 2019, **55**, 1360–1373.
16 T. Habets, B. Grignard and C. Detrembleur, *Prog. Polym. Sci.*, 2025, **165**, 101968.
17 T. Theerathanagorn, T. Kessaratikoon, H. U. Rehman, V. D'Elia and D. Crespy, *Chin. J. Chem.*, 2024, **42**, 652–685.
18 A. Gomez-Lopez, F. Elizalde, I. Calvo and H. Sardon, *Chem. Commun.*, 2021, **57**, 12254–12265.
19 L. Maisonneuve, O. Lamarzelle, E. Rix, E. Grau and H. Cramail, *Chem. Rev.*, 2015, **115**, 12407–12439.
20 C. Carré, Y. Ecochard, S. Caillol and L. Avérous, *ChemSusChem*, 2019, **12**, 3410–3430.
21 S. El Khezraji, H. Ben Youcef, L. Belachemi, M. A. Lopez Manchado, R. Verdejo and M. Lahcini, *Polymers*, 2023, 15.
22 P. Singh, M. Kour, G. Varshney and R. Kaur, *Polymer*, 2025, **333**, 128658.
23 F. Orabona, F. Recupido, G. C. Lama, K. Polaczek, F. Taddeo, T. Salmi, M. Di Serio, L. Verdolotti and V. Russo, *Green Chem.*, 2025, **27**, 7403–7444.
24 C. C. N. D. Lim, M. J. H. Ong, M. Wu, C.-L. K. Lee and P. Sen Choong, *ACS Eng. Au*, 2024, **4**, 493–518.
25 M. L. Chaudhary and R. K. Gupta, *Non-Isocyanate Polyurethanes: Chemistry, Progress, and Challenges*, American Chemical Society, 2025, vol. 1507, pp. 5–91.
26 L. Gu, X. Wang, X. Chen, X. Zhao and F. Wang, *J. Polym. Sci., Part A: Polym. Chem.*, 2011, **49**, 5162–5168.
27 W. Kuran, A. Rokicki and D. Romanowska, *J. Polym. Sci., Polym. Chem. Ed.*, 1979, **17**, 2003–2011.
28 O. Ihata, Y. Kayaki and T. Ikariya, *Angew. Chem., Int. Ed.*, 2004, **43**, 717–719.
29 K. Soga, S. Hosoda and S. Ikeda, *J. Polym. Sci., Polym. Chem. Ed.*, 1974, **12**, 729–736.
30 O. Ihata, Y. Kayaki and T. Ikariya, *Macromolecules*, 2005, **38**, 6429–6434.

 

31 K. Soga, W.-Y. Chiang and S. Ikeda, *J. Polym. Sci., Polym. Chem. Ed.*, 1974, **12**, 121–131.
32 K. Soga, S. Hosoda and S. Ikeda, *Die Makromol. Chem.*, 1974, **175**, 3309–3313.
33 D. Zhang, Y. Zhang, Y. Fan, M.-N. Rager, V. Guérineau, L. Bouteiller, M.-H. Li and C. M. Thomas, *Macromolecules*, 2019, **52**, 2719–2724.
34 J. Futter, L. F. Richter, S. Hörl, M. Kränzlein and B. Rieger, *Angew. Chem., Int. Ed.*, 2025, **64**, e202502727.
35 L. Rubino, V. Patamia, A. Rescifina, M. Galimberti and V. Barbera, *Sci. Rep.*, 2024, **14**, 23521.
36 J. Kušan, H. Keul and H. Höcker, *Macromolecules*, 2001, **34**, 389–395.
37 B. Lebedev, V. Veridusova, H. Höcker and H. Keul, *Macromol. Chem. Phys.*, 2002, **203**, 1114–1125.
38 B. V. Lebedev, T. A. Bykova, E. G. Kiparisova, A. M. Kochetkov, H. Höcker, J. Kusan and H. Keul, *Macromol. Chem. Phys.*, 1999, **200**, 1863–1869.
39 B. V. Lebedev, N. N. Smirnova and E. G. Kiparisova, *Macromol. Chem. Phys.*, 1997, **198**, 41–58.
40 S. Neffgen, H. Keul and H. Höcker, *Macromolecules*, 1997, **30**, 1289–1297.
41 G. Rokicki and A. Piotrowska, *Polymer*, 2002, **43**, 2927–2935.
42 M. L. Chaudhary and R. K. Gupta, *Non-Isocyanate Polyurethanes: Chemistry, Progress, and Challenges*, American Chemical Society, 2025, vol. 1507, pp. 4–59.
43 S. Li, J. Zhao, Z. Zhang, J. Zhang and W. Yang, *RSC Adv.*, 2015, **5**, 6843–6852.
44 N. Kébir, M. Benoit and F. Burel, *Eur. Polym. J.*, 2018, **107**, 155–163.
45 B. Ochiai and T. Utsuno, *J. Polym. Sci., Part A: Polym. Chem.*, 2013, **51**, 525–533.
46 B. Sharma, L. Ubaghs, H. Keul, H. Höcker, T. Loontjens and R. van Benthem, *Polymer*, 2004, **45**, 5427–5440.
47 S. Li, J. Zhao, Z. Zhang, J. Zhang and W. Yang, *Polymer*, 2015, **57**, 164–172.
48 F. Meng and D. Tang, *ACS Appl. Polym. Mater.*, 2023, **5**, 5600–5608.
49 P. Dongdong and T. Hengshui, *J. Appl. Polym. Sci.*, 2014, **132**, 41377.
50 D. Wołosz, P. G. Parzuchowski and A. Świderska, *Eur. Polym. J.*, 2021, **155**, 110574.
51 N. Wybo, E. Cherasse, A. Duval and L. Avérous, *J. Mater. Chem. A*, 2025, **13**, 11557–11572.
52 N. G. Jaques, E. Grau, A. Llevot, T. Vidil, M. A. R. Meier and H. Cramail, *Macromol. Chem. Phys.*, 2025, **226**, e00207.
53 C. Duval, N. Kébir, A. Charvet, A. Martin and F. Burel, *J. Polym. Sci., Part A: Polym. Chem.*, 2015, **53**, 1351–1359.
54 B. Sharma, H. Keul, H. Höcker, T. Loontjens and R. van Benthem, *Polymer*, 2005, **46**, 1775–1783.
55 Z. Chen, N. Hadjichristidis, X. Feng and Y. Gnanou, *Macromolecules*, 2017, **50**, 2320–2328.
56 S. Xie, Y. Li, Y. Chai, Q. Chen, M. North and H. Xie, *ACS Macro Lett.*, 2024, **13**, 14–20.
57 D. Wu, R. T. Martin, J. Piña, J. Kwon, M. P. Crockett, A. A. Thomas, O. Gutierrez, N. H. Park, J. L. Hedrick and L. M. Campos, *Angew. Chem., Int. Ed.*, 2024, **63**, e202401281.
58 M. Blain, L. Jean-Gérard, R. Auvergne, D. Benazet, S. Caillol and B. Andrioletti, *Green Chem.*, 2014, **16**, 4286–4291.
59 M. Blain, H. Yau, L. Jean-Gérard, R. Auvergne, D. Benazet, P. R. Schreiner, S. Caillol and B. Andrioletti, *ChemSusChem*, 2016, **9**, 2269–2272.
60 F. Monie, T. Vidil, E. Grau, B. Grignard, C. Detrembleur and H. Cramail, *Macromolecules*, 2024, **57**, 8877–8888.
61 M. Blain, A. Cornille, B. Boutevin, R. Auvergne, D. Benazet, B. Andrioletti and S. Caillol, *J. Appl. Polym. Sci.*, 2017, **134**, 44958.
62 P.-L. Yang, S.-H. Tsai, Y.-Y. Han, H.-W. Chao, K.-N. Chen and D. S.-H. Wong, *Ind. Eng. Chem. Res.*, 2024, **63**, 17430–17440.
63 J.-Z. Hwang, C.-L. Chen, C.-Y. Huang, J.-T. Yeh and K.-N. Chen, *J. Polym. Res.*, 2013, **20**, 195.
64 P.-L. Yang, S.-H. Tsai, K.-N. Chen and D. S. Wong, *Polymers*, 2023, **15**, 2499.
65 A. Cornille, M. Blain, R. Auvergne, B. Andrioletti, B. Boutevin and S. Caillol, *Polym. Chem.*, 2017, **8**, 592–604.
66 O. Lamarzelle, P.-L. Durand, A.-L. Wirotius, G. Chollet, E. Grau and H. Cramail, *Polym. Chem.*, 2016, **7**, 1439–1451.
67 O. Lamarzelle, G. Hibert, S. Lecommandoux, E. Grau and H. Cramail, *Polym. Chem.*, 2017, **8**, 3438–3447.
68 H. Tomita, F. Sanda and T. Endo, *J. Polym. Sci., Part A: Polym. Chem.*, 2001, **39**, 3678–3685.
69 R. H. Lambeth, S. M. Mathew, M. H. Baranoski, K. J. Housman, B. Tran and J. M. Oyler, *J. Appl. Polym. Sci.*, 2017, **134**, 44941.
70 J. Liu, P. Miao, X. Leng, J. Che, Z. Wei and Y. Li, *Macromol. Rapid Commun.*, 2023, **44**, 2300263.
71 D. J. Fortman, J. P. Brutman, C. J. Cramer, M. A. Hillmyer and W. R. Dichtel, *J. Am. Chem. Soc.*, 2015, **137**, 14019–14022.
72 C. Ngassam Tounzoua, B. Grignard and C. Detrembleur, *Angew. Chem., Int. Ed.*, 2022, **61**, e202116066.
73 S. Gennen, B. Grignard, T. Tassaing, J. Ø. Christine and C. Detrembleur, *Angew. Chem., Int. Ed.*, 2017, **56**, 10394–10398.
74 J. Wu, Q. Guo, H. Hong, R. Xie and N. Zhu, *J. CO2 Util.*, 2022, **65**, 102192.
75 S. Dabral, U. Licht, P. Rudolf, G. Bollmann, A. S. K. Hashmi and T. Schaub, *Green Chem.*, 2020, **22**, 1553–1558.
76 B. Quienne, R. Poli, J. Pinaud and S. Caillol, *Green Chem.*, 2021, **23**, 1678–1690.
77 A. Datta Sarma, S. V. Zubkevich, F. Addiego, D. F. Schmidt, A. S. Shaplov and V. Berthé, *Macromolecules*, 2024, **57**, 3423–3437.
78 F. Magliozzi, G. Chollet, E. Grau and H. Cramail, *ACS Sustainable Chem. Eng.*, 2019, **7**, 17282–17292.
79 P. Helbling, F. Hermant, M. Petit, T. Vidil and H. Cramail, *Macromol. Chem. Phys.*, 2023, **224**, 2300300.
80 V. Aomchad, À. Cristòfol, F. Della Monica, B. Limburg, V. D'Elia and A. W. Kleij, *Green Chem.*, 2021, **23**, 1077–1113.
81 L. Guo, K. J. Lamb and M. North, *Green Chem.*, 2021, **23**, 77–118.

82 C. Muzyka, D. V. Silva-Brenes, B. Grignard, C. Detrembleur and J.-C. M. Monbaliu, *ACS Catal.*, 2024, **14**, 12454–12493.
83 M. Alves, B. Grignard, R. Méreau, C. Jérôme, T. Tassaing and C. Detrembleur, *Catal. Sci. Technol.*, 2017, **7**, 2651–2684.
84 M. Usman, A. Rehman, F. Saleem, A. Abbas, V. C. Eze and A. Harvey, *RSC Adv.*, 2023, **13**, 22717–22743.
85 M. Decostanzi, Y. Ecochard and S. Caillol, *Eur. Polym. J.*, 2018, **109**, 1–7.
86 A. Cornille, Y. Ecochard, M. Blain, B. Boutevin and S. Caillol, *Eur. Polym. J.*, 2017, **96**, 370–382.
87 B. Bizet, E. Grau, J. M. Asua and H. Cramail, *Macromol. Chem. Phys.*, 2022, **223**, 2100437.
88 F. M. de Souza, Y. Desai and R. K. Gupta, *Polymeric Foams: Fundamentals and Types of Foams (Volume 1)*, American Chemical Society, 2023, vol. 1439, p. 1.
89 A. Wong, R. K. M. Chu, S. N. Leung, C. B. Park and J. H. Zong, *Chem. Eng. Sci.*, 2011, **66**, 55–63.
90 C. B. Park, D. F. Baldwin and N. P. Suh, *Polym. Eng. Sci.*, 1995, **35**, 432–440.
91 G. C. DSouza, H. Ng, P. Charpentier and C. C. Xu, *ChemBioEng Rev.*, 2024, **11**, 7–38.
92 G. Harikrishnan, T. U. Patro and D. V. Khakhar, *Ind. Eng. Chem. Res.*, 2006, **45**, 7126–7134.
93 X. Cao, L. James Lee, T. Widya and C. Macosko, *Polymer*, 2005, **46**, 775–783.
94 L. J. Lee, C. Zeng, X. Cao, X. Han, J. Shen and G. Xu, *Compos. Sci. Technol.*, 2005, **65**, 2344–2363.
95 A. Kausar, *Polym. Plast. Technol. Eng.*, 2018, **57**, 346–369.
96 M. Nofar, J. Utz, N. Geis, V. Altstädt and H. Ruckdäschel, *Adv. Sci.*, 2022, **9**, 2105701.
97 S. P. Nalawade, F. Picchioni and L. P. B. M. Janssen, *Prog. Polym. Sci.*, 2006, **31**, 19–43.
98 M. Dong, G. Wang, X. Zhang, D. Tan, D. Jaya Prasanna Kumar, J. Ren, H. Colorado, H. Hou, Z. Toktarbay and Z. Guo, *Adv. Compos. Hybrid Mater.*, 2023, **6**, 207.
99 M. Sauceau, J. Fages, A. Common, C. Nikitine and E. Rodier, *Prog. Polym. Sci.*, 2011, **36**, 749–766.
100 B. Grignard, J.-M. Thomassin, S. Gennen, L. Poussard, L. Bonnaud, J.-M. Raquez, P. Dubois, M.-P. Tran, C. B. Park, C. Jerome and C. Detrembleur, *Green Chem.*, 2016, **18**, 2206–2215.
101 H.-I. Mao, C.-W. Chen, H.-C. Yan and S.-P. Rwei, *J. Appl. Polym. Sci.*, 2022, **139**, e52841.
102 F. N. Olang, *US pat.*, US 2012/0183694 A1, 2012.
103 O. Figovsky, R. Potashnikov, A. Leykin, L. Shapovalovs and S. Sivokon, *US pat.*, US 2015/0024138 Al, 2013.
104 H. Blattmann, M. Lauth and R. Mülhaupt, *Macromol. Mater. Eng.*, 2016, **301**, 944–952.
105 H. Ren, Q. Liao, Z. Zhou, S. Gao, Y. Wang, X. Du, B. Yuan and H. Zhang, *Polymer*, 2025, **334**, 128740.
106 V. Valette, N. Kébir, F. Burel and L. Lecamp, *eXPRESS Polym. Lett.*, 2023, **17**, 974–990.
107 C. Amezúa-Arranz, M. Santiago-Calvo and M.-Á. Rodríguez-Pérez, *Eur. Polym. J.*, 2023, **197**, 112366.
108 X. Xi, A. Pizzi, C. Gerardin and G. Du, *J. Renew. Mater*, 2019, **7**, 301–312.
109 T. Dong, E. Dheressa, M. Wiatrowski, A. P. Pereira, A. Zeller, L. M. L. Laurens and P. T. Pienkos, *ACS Sustain. Chem. Eng.*, 2021, **9**, 12858–12869.
110 C. H. Tran, J.-H. Park, S.-Y. Lee, B. Han, W. S. Jae, H. S. Lee, H. Paik and I. Kim, *Polymer*, 2025, **323**, 128217.
111 J. A. Reyes-Labarta and A. Marcilla, *J. Appl. Polym. Sci.*, 2008, **107**, 339–346.
112 J. A. Reyes-Labarta and A. Marcilla, *Ind. Eng. Chem. Res.*, 2012, **51**, 9515–9530.
113 D. Kiełkiewicz, A. Siewniak, R. Gaida, M. Greif and A. Chrobok, *Molecules*, 2024, **29**, 3908.
114 A. Cornille, S. Dworakowska, D. Bogdal, B. Boutevin and S. Caillol, *Eur. Polym. J.*, 2015, **66**, 129–138.
115 A. Cornille, C. Guillet, S. Benyahya, C. Negrell, B. Boutevin and S. Caillol, *Eur. Polym. J.*, 2016, **84**, 873–888.
116 G. Coste, D. Berne, V. Ladmiral, C. Negrell and S. Caillol, *Eur. Polym. J.*, 2022, **176**, 111392.
117 J. Sternberg and S. Pilla, *Nat. Sustain.*, 2023, **6**, 316–324.
118 J. Sternberg and S. Pilla, *Green Chem.*, 2020, **22**, 6922–6935.
119 K. Evancho, R. S. Reiner, B. M. Bujanovic, S. Pilla and J. Sternberg, *RSC Adv.*, 2025, **15**, 38056–38068.
120 J. Li, X. Xu, X. Ma, M. Cui, X. Wang, J. Chen, J. Zhu and J. Chen, *ACS Appl. Bio Mater.*, 2024, **7**, 1301–1310.
121 V. Valette, N. Kébir, F. B. Tiavarison, F. Burel and L. Lecamp, *React. Funct. Polym.*, 2022, **181**, 105416.
122 J. H. Clark, T. J. Farmer, I. D. V. Ingram, Y. Lie and M. North, *Eur. J. Org. Chem.*, 2018, 4265–4271.
123 R. G. Pearson, *J. Am. Chem. Soc.*, 1963, **85**, 3533–3539.
124 P. Tundo, F. Trotta, G. Moraglio and F. Ligorati, *Ind. Eng. Chem. Res.*, 1988, **27**, 1565–1571.
125 M. Selva and P. Tundo, *J. Org. Chem.*, 2006, **71**, 1464–1470.
126 M. Selva, A. Perosa, D. Rodríguez-Padrón and R. Luque, *ACS Sustainable Chem. Eng.*, 2019, **7**, 6471–6479.
127 P. Tundo, M. Musolino and F. Aricò, *Green Chem.*, 2018, **20**, 28–85.
128 F. Monie, B. Grignard, J. M. Thomassin, R. Mereau, T. Tassaing, C. Jerome and C. Detrembleur, *Angew. Chem., Int. Ed.*, 2020, **59**, 17033–17041.
129 B. Grignard, P. Mampuys, J. Escudero, D. Masullo, F. Lemière, B. U. W. Maes and C. Detrembleur, *Polym. Chem.*, 2022, **13**, 6599–6605.
130 M. Bourguignon, B. Grignard and C. Detrembleur, *Polym. Chem.*, 2024, **16**, 192–203.
131 N. S. Purwanto, Y. Chen, T. Wang and J. M. Torkelson, *Polymer*, 2023, **272**, 125858.
132 B. Lecart, C. Baumsteiger, F. Monie, A. Di Maria, C. Detrembleur, A. Richel and H. Vanderschuren, *Green Chem.*, 2023, **25**, 9282–9291.
133 N. S. Purwanto, Y. Chen and J. M. Torkelson, *Eur. Polym. J.*, 2024, **206**, 112775.
134 F. Monie, B. Grignard and C. Detrembleur, *ACS Macro Lett.*, 2022, **11**, 236–242.
135 G. Coste, C. Negrell and S. Caillol, *Macromol. Rapid Commun.*, 2022, **43**, 1–10.
136 N. S. Purwanto, Y. Chen and J. M. Torkelson, *ACS Appl. Polym. Mater.*, 2023, **5**, 6651–6661.

 

137 L.-F. Xiao, Q.-F. Yue, C.-G. Xia and L.-W. Xu, *J. Mol. Catal. A: Chem.*, 2008, **279**, 230–234.
138 M. Metzger, B. Strehle, S. Solchenbach and H. A. Gasteiger, *J. Electrochem. Soc.*, 2016, **163**, A1219.
139 M. Bourguignon, B. Grignard and C. Detrembleur, *ACS Appl. Mater. Interfaces*, 2021, **13**, 54396–54408.
140 M. Bourguignon, B. Grignard and C. Detrembleur, *Angew. Chem., Int. Ed.*, 2022, **61**, e202213422.
141 M. Bourguignon, B. Grignard and C. Detrembleur, *J. Am. Chem. Soc.*, 2024, **146**, 988–1000.
142 D. Trojanowska, F. Monie, G. Perotto, A. Athanassiou, B. Grignard, E. Grau, T. Vidil, H. Cramail and C. Detrembleur, *Green Chem.*, 2024, **26**, 8383–8394.
143 M. Chaib, S. Thakur, H. Ben Youcef, M. Lahcini and R. Verdejo, *Eur. Polym. J.*, 2025, **229**, 113843.
144 M. Makarov, M. Bourguignon, B. Grignard and C. Detrembleur, *Macromolecules*, 2025, **58**, 1673–1685.
145 J. A. Marsella and W. E. Starner, *J. Polym. Sci., Part A: Polym. Chem.*, 2000, **38**, 921–930.
146 Z. Ran, X. Liu, X. Jiang, Y. Wu and H. Liao, *Thermochim. Acta*, 2020, **692**, 178735.
147 F. Siragusa, E. Van Den Broeck, C. Ocando, A. J. Müller, G. De Smet, B. U. W. Maes, J. De Winter, V. Van Speybroeck, B. Grignard and C. Detrembleur, *ACS Sustainable Chem. Eng.*, 2021, **9**, 1714–1728.
148 F. Ouhib, B. Grignard, E. Van Den Broeck, A. Luxen, K. Robeyns, V. Van Speybroeck, C. Jerome and C. Detrembleur, *Angew. Chem., Int. Ed.*, 2019, **58**, 11768–11773.
149 L. Crane, T. Habets, B. Grignard, J.-C. M. Monbaliu, P. Stiernet and C. Detrembleur, *ACS Sustain. Chem. Eng.*, 2025, **13**, 16107–16116.
150 L. Narducci, T. Habets, Q. Grossman, B. Grignard, M. A. R. Meier and C. Detrembleur, *Macromolecules*, 2025, **58**, 6452–6465.
151 T. Habets, F. Siragusa, B. Grignard and C. Detrembleur, *Macromolecules*, 2020, **53**, 6396–6408.
152 P. Sen Choong, Y. L. E. Hui and C. C. Lim, *ACS Macro Lett.*, 2023, **12**, 1094–1099.
153 L. Biancalana, G. Bresciani, C. Chiappe, F. Marchetti and G. Pampaloni, *New J. Chem.*, 2017, **41**, 1798–1805.
154 P. V. Kortunov, L. S. Baugh, M. Siskin and D. C. Calabro, *Energy Fuels*, 2015, **29**, 5967–5989.
155 J. K. Mannisto, L. Pavlovic, T. Tiainen, M. Nieger, A. Sahari, K. H. Hopmann and T. Repo, *Catal. Sci. Technol.*, 2021, **11**, 6877–6886.
156 K. Gouveia, J. Vauloup, M. Colpaert, C. Ocando, P. Lacroix-Desmazes, V. Ladmiral, S. Caillol and J. M. Raquez, *ACS Appl. Polym. Mater.*, 2025, **7**, 6113–6124.
157 J. I. Sintas, J. D. Wolfgang and T. E. Long, *Polym. Chem.*, 2023, **14**, 1497–1506.
158 T. Sintas, J. Wolfgang and T. E. Long, in *ACS Spring 2024 – Sessions*, 2024, p. 3990633.
159 M. S. Silverstein, *Prog. Polym. Sci.*, 2014, **39**, 199–234.
160 X. Xi, A. Pizzi, C. Gerardin, H. Lei, X. Chen and S. Amirou, *Polymers*, 2019, **11**, 1802.
161 X. Chen, J. Li, X. Xi, A. Pizzi, X. Zhou, E. Fredon, G. Du and C. Gerardin, *Polym. Degrad. Stab.*, 2020, **175**, 109121.
162 D. L. Smith, D. Rodriguez-melendez, S. M. Cotton, Y. Quan, Q. Wang and J. C. Grunlan, *Polymers*, 2022, **14**, 5019.
163 Y. Zhao, Q. Zhang, H. Lei, X. Zhou, G. Du, A. Pizzi and X. Xi, *Int. J. Biol. Macromol.*, 2024, **258**, 128994.
164 X. Chen, X. Xi, A. Pizzi, E. Fredon, X. Zhou, J. Li, C. Gerardin and G. Du, *Polymers*, 2020, **12**, 750.
165 P. Singh and R. Kaur, *Mater. Lett.*, 2023, **331**, 133433.
166 P. Singh and R. Kaur, *J. Polym. Environ.*, 2023, **31**, 743–753.
167 A. K. Malhotra and D. T. Wasan, *Chem. Eng. Commun.*, 1987, **55**, 95–128.
168 P. W. Voorhees, *J. Stat. Phys.*, 1985, **38**, 231–252.
169 B. E. Obi, in *Polymeric Foams Structure-Property-Performance A Design Guide*, ed. B. E. Obi, William Andrew Publishing, Oxford, 2018, pp. 131–188.
170 C. F. Frias, A. C. Fonseca, J. F. J. Coelho and A. C. Serra, *Prog. Org. Coatings*, 2024, **187**, 108100.
171 S. V. Zubkevich, M. Makarov, R. Dieden, L. Puchot, V. Berthé, S. Westermann, A. S. Shaplov and D. F. Schmidt, *Macromolecules*, 2024, **57**, 2385–2393.
172 C. Pu, J. Yang, S. Jin, Y. Zhou and W. Gong, *ACS Appl. Polym. Mater.*, 2025, **7**, 7600–7611.
173 P. M. Stathatou, C. E. Athanasiou and M. J. Realff, *J. Am. Chem. Soc.*, 2025, **147**, 32299–32308.
174 G. Rossignolo, G. Malucelli and A. Lorenzetti, *Green Chem.*, 2024, **26**, 1132–1152.
175 Y. Chen, M. Laporte and J. M. Torkelson, *J. Polym. Res.*, 2024, **31**, 264.
176 S. Kim, K. Li, A. Alsbaiee, J. P. Brutman and W. R. Dichtel, *Adv. Mater.*, 2023, **35**, 2305387.
177 D. T. Sheppard, K. Jin, L. S. Hamachi, W. Dean, D. J. Fortman, C. J. Ellison and W. R. Dichtel, *ACS Cent. Sci.*, 2020, **6**, 921–927.
178 S. Kim, L. M. Felsenthal, O. Sala, O. Welz, M. Bergeler, A. Alsbaiee and W. R. Dichtel, *J. Am. Chem. Soc.*, 2025, **147**, 35655–35663.
179 X. Chen, L. Li, K. Jin and J. M. Torkelson, *Polym. Chem.*, 2017, **8**, 6349–6355.
180 C. Bakkali-Hassani, D. Berne, P. Bron, L. Irusta, H. Sardon, V. Ladmiral and S. Caillol, *Polym. Chem.*, 2023, **14**, 3610–3620.
181 X. Chen, L. Li, T. Wei, D. C. Venerus and J. M. Torkelson, *ACS Appl. Mater. Interfaces*, 2019, **11**, 2398–2407.
182 Y.-W. Huang and J. M. Torkelson, *Macromolecules*, 2025, **58**, 5356–5367.
183 L. M. Nuñez Tapia, P. Y. Batista Peguero, E. Poisson, L. Bischoff, A. Ledoux and F. Burel, *Chem. Eng. J.*, 2025, **520**, 166382.
184 D. Berne, S. Laviéville, E. Leclerc, S. Caillol, V. Ladmiral and C. Bakkali-Hassani, *ACS Polym. Au*, 2025, **5**, 214–240.
185 R. G. Ricarte and S. Shanbhag, *Polym. Chem.*, 2024, **15**, 815–846.
186 V. Zhang, B. Kang, J. V. Accardo and J. A. Kalow, *J. Am. Chem. Soc.*, 2022, **144**, 22358–22377.
187 G. M. Scheutz, J. J. Lessard, M. B. Sims and B. S. Sumerlin, *J. Am. Chem. Soc.*, 2019, **141**, 16181–16196.
188 B. R. Elling and W. R. Dichtel, *ACS Cent. Sci.*, 2020, **6**, 1488–1496.

189 N. S. Purwanto, Y. Chen, T. Wang and J. M. Torkelson, *Polymer*, 2023, **272**, 125858.
190 V. D. Lechuga-Islas, E. Gillissen, M. Bourguignon, B. Grignard and C. Detrembleur, *Chem. Eng. J.*, 2025, **516**, 163998.
191 L. Li, X. Chen, K. Jin and J. M. Torkelson, *Macromolecules*, 2018, **51**, 5537–5546.
192 S. T. McKenna and T. R. Hull, *Fire Sci. Rev.*, 2016, **5**, 3.
193 K. Sałasińska, M. Leszczyńska, M. Celiński, P. Kozikowski, K. Kowiorski and L. Lipińska, *Materials*, 2021, **14**, 1184.
194 H. Singh and A. K. Jain, *J. Appl. Polym. Sci.*, 2009, **111**, 1115–1143.
195 J. Zhang, G. H. Yeoh and I. I. Kabir, *Fire*, 2025, **8**, 64.
196 A. Yadav, F. M. de Souza, T. Dawsey and R. K. Gupta, *Ind. Eng. Chem. Res.*, 2022, **61**, 15046–15065.
197 Y. Liu, A. Zhang, Y. Cheng, M. Li, Y. Cui and Z. Li, *Polym. Test.*, 2023, **124**, 108100.
198 G. Coste, M. Denis, R. Sonnier, S. Caillol and C. Negrell, *Polym. Degrad. Stab.*, 2022, **202**, 110031.
199 A. Sharma, V. V. Tyagi, C. R. Chen and D. Buddhi, *Renew. Sustain. Energy Rev.*, 2009, **13**, 318–345.
200 S. Ben Romdhane, A. Amamou, R. Ben Khalifa, N. M. Saïd, Z. Younsi and A. Jemni, *J. Build. Eng.*, 2020, **32**, 101563.
201 K. Pielichowska and K. Pielichowski, *Prog. Mater. Sci.*, 2014, **65**, 67–123.
202 A. H. Alami, H. M. Maghrabie, M. A. Abdelkareem, E. T. Sayed, Z. Yasser, T. Salameh, S. M. A. Rahman, H. Rezk and A. G. Olabi, *J. Energy Storage*, 2022, **54**, 105204.
203 Y. Jing, Z. Zhao, X. Cao, Q. Sun, Y. Yuan and T. Li, *Nat. Commun.*, 2023, **14**, 8060.
204 M. Lee, S. D. Dahlhauser, C. Lucci, B. S. Donohoe, R. D. Allen and N. A. Rorrer, *Adv. Funct. Mater.*, 2025, **35**, 1–13.
205 L. J. Gibson and M. F. Ashby, *Cellular Solids: Structure and Properties*, Cambridge University Press, 2nd edn, 1997.
206 B. Hadała, B. Zygmunt-Kowalska, M. Kuźnia, A. Szajding and T. Telejko, *Thermochim. Acta*, 2024, **731**, 179659.
207 J. Zhu, Y. Gao, M. Zhang, K. Shen, J. Chen, C. Jin, G. Wu and G. Liu, *Chem. Eng. J.*, 2025, **525**, 170558.
208 S. B. Kondawar and P. R. Modak, in *Materials for Potential EMI Shielding Applications Processing, Properties and Current Trends*, ed. K. Joseph, R. Wilson, Elsevier, 2020, pp. 9–25.
209 D.-K. Li, H. Chen, J. R. Ferber, R. Odouli and C. Quesenberry, *Sci. Rep.*, 2017, **7**, 17541.
210 A. A. Isari, A. Ghaffarkhah, S. A. Hashemi, S. Wuttke and M. Arjmand, *Adv. Mater.*, 2024, **36**, 2310683.
211 J. Kruželák, A. Kvasničáková, K. Hložeková and I. Hudec, *Nanoscale Adv.*, 2021, **3**, 123–172.
212 M. Panahi-Sarmad, M. Noroozi, M. Abrisham, S. Eghbalinia, F. Teimoury, A. R. Bahramian, P. Dehghan, M. Sadri and V. Goodarzi, *ACS Appl. Electron. Mater.*, 2020, **2**, 2318–2350.
213 B. Zhao, M. Hamidinejad, S. Wang, P. Bai, R. Che, R. Zhang and C. B. Park, *J. Mater. Chem. A*, 2021, **9**, 8896–8949.
214 M. Panahi-Sarmad, M. Noroozi, X. Xiao and C. B. Park, *Ind. Eng. Chem. Res.*, 2022, **61**, 1545–1568.
215 H. M. S, P. Joseph and S. George, *Nanoscale Adv.*, 2025, **7**, 4510–4534.
216 N. M. Petryk, N. L. B. Thai, L. V. Saldanha, S. T. Sutherland and M. B. B. Monroe, *ACS Appl. Mater. Interfaces*, 2025, **17**, 26402–26415.
217 W. Liang, N. Ni, Y. Huang and C. Lin, *Polymers*, 2023, **15**, 4301.
218 N. Sienkiewicz, *Thermal Insulation and Radiation Control Technologies for Buildings*, ed. J. Kośny and D. W. Yarbrough, Springer International Publishing, Cham, 2022, pp. 217–240, ISBN 978-3-030-98692-6.
219 S. Li, Y. Zhang, X. Ma, S. Qiu, J. Chen, G. Lu, Z. Jia, J. Zhu, Q. Yang, J. Chen and Y. Wei, *Biomacromolecules*, 2022, **23**, 1622–1632.
220 Y. Ding, Z. Sun, R. Shi, H. Cui, Y. Liu, H. Mao, B. Wang, D. Zhu and F. Yan, *ACS Appl. Mater. Interfaces*, 2019, **11**, 2860–2869.
221 S. Wang, H. Li, H. Huang, X. Cao, X. Chen and D. Cao, *Chem. Soc. Rev.*, 2022, **51**, 2031–2080.
222 Q. Liu, Q. Sun, J. Shen, H. Li, Y. Zhang, W. Chen, S. Yu, X. Li and Y. Chen, *Coord. Chem. Rev.*, 2023, **482**, 215078.
223 C. Teodosiu, R. Wenkert, L. Tofan and C. Paduraru, *Rev. Chem. Eng.*, 2014, **30**, 403–420.
224 R. Selvasembian, W. Gwenzi, N. Chaukura and S. Mthembu, *J. Hazard. Mater.*, 2021, **417**, 125960.
225 C. Freitas, M. I. Severino, A. Al Mohtar, O. Kolmykov, V. Pimenta, F. Nouar, C. Serre and M. Pinto, *ACS Mater. Lett.*, 2024, **6**, 174–181.
226 Y. Yu, J. Wang, J. Lian and X. Cheng, *RSC Adv.*, 2014, **4**, 18222–18228.
227 Z.-X. Fan, Q.-H. Zhao, S. Wang, Y. Bai, P.-P. Wang, J.-J. Li, Z.-W. Chu and G.-H. Chen, *RSC Adv.*, 2016, **6**, 26950–26953.
228 Z. Chu, Z. Fan, X. Zhang, X. Tan, D. Li, G. Chen and Q. Zhao, *Sensors*, 2018, **18**, 1565.
229 Z. Zhou, Q. Wang, Z. Zeng, L. Yang, X. Ding, N. Lin and Z. Cheng, *Anal. Methods*, 2013, **5**, 6045–6050.
230 Y. Su, D. Zhang, P. Jia, W. Gao, Y. Li, Z. Bai, X. Liu, Q. Deng, J. Xu and C. Yang, *Spectrochim. Acta, Part A*, 2019, **217**, 86–92.
231 Y. Chen, Y. Wu, Y. Zhu and S. Tian, *Polym. Int.*, 2022, **71**, 169–174.
232 M. Mahapatra, M. Bourguignon, B. Grignard, M. Vandevenne, M. Galleni and C. Detrembleur, *Angew. Chem., Int. Ed.*, 2024, **64**, e202413605.
233 M. Mahapatra, M. Bourguignon, P. Stiernet, S. Melo, B. Grignard, M. Vandevenne, M. Galleni and C. Detrembleur, *Adv. Funct. Mater.*, 2025, e23095.
234 C. Liang, Y. Jadidi, Y. Chen, U. Gracida-Alvarez, J. M. Torkelson, T. R. Hawkins and J. B. Dunn, *ACS Sustainable Chem. Eng.*, 2024, **12**, 12161–12170.
235 C. Pu, J. Yang, S. Jin, Y. Zhou and W. Gong, *ACS Appl. Polym. Mater.*, 2025, **7**, 7600–7611.

 